

**THE IMPACT OF ICELANDIC VOLCANIC ERUPTIONS
UPON THE ANCIENT SETTLEMENT AND ENVIRONMENT OF NORTHERN BRITAIN.**

VOLUME 2.

FIGURES.

John Patrick Grattan.

This work is submitted in fulfilment of the requirements for a Doctor of Philosophy in the Faculty of
Pure Science at the University of Sheffield.



IMAGING SERVICES NORTH

Boston Spa, Wetherby
West Yorkshire, LS23 7BQ
www.bl.uk

BEST COPY AVAILABLE.

	Page.
Figure 1.1. Ten year cycles in northern Fennoscandian summer temperature anomalies.	1
Figure 1.2. The location and genera of 37 chronologies used to reconstruct summer temperatures. across Europe.	2
Figure 1.3. Location map for tree-ring chronologies.	3
Figure 1.4. Temperature reconstructions from North American chronologies.	4
Figure 1.5. Location of tree-ring chronologies in Maine.	5
Figure 1.6. Average reconstructed temperature differences.	6
Figure 2.1. Evolution of eruption chronologies 1970-1982.	7
Figure 2.2. Eruption chronology 0 - 1970 A.D.	8
Figure 3.1. The latitudinal band cooled by the eruption of El Chichón.	9
Figure 3.2. The distribution of the El Chichón aerosol cloud relative to time and latitude.	10
Figure 3.3. The influence of the Southern Oscillation on global air pressure.	11
Figure 3.4. Composite sea surface temperature anomaly.	12
Figure 3.5. Composite sea surface temperature anomaly.	13
Figure 3.6. Superposed epoch analysis of Darwin surface pressure.	14
Figure 4.1. Total acids output of selected major volcanic eruptions.	15
Figure 4.2. Total sulphuric acid output of selected major volcanic eruptions.	16
Figure 4.3. Total erupted mass of selected major volcanic eruptions.	17
Figure 4.4. Summer mean temperatures at Brunswick, New Jersey.	18
Figure 4.5. Summer mean temperatures at New Haven, Connecticut.	19
Figure 4.6 Summer and June mean temperatures at New Haven, Connecticut.	20
Figure 4.7. Summer mean temperatures at Stockholm and Voyri.	21
Figure 4.8. Summer mean temperatures at Trondheim, Copenhagen, Gothenburg.	22
Figure 4.9. Summer mean temperatures at Uppsala & St. Petersburg.	23
Figure 4.10. Summer mean temperatures in Central England.	24
Figure 4.11. Summer mean temperatures in Edinburgh.	25
Figure 4.12. Summer position of the "Icelandic Low" in 1816.	26
Figure 4.13. European rainfall anomalies % in the Summer of 1816.	27
Figure 5.1. Acid volatile emission of selected volcanoes.	28

	Page
Figure 5.2. July temperatures in Central England 1770-1790.	29
Figure 5.3. June temperatures in Central England 1770-1790.	30
Figure 5.4. August temperatures in Central England 1770-1790.	31
Figure 5.5. Variance of Central England July temperatures from the mean of 1770-1790.	32
Figure 5.6. Edinburgh summer temperatures 1775-1790.	33
Figure 5.7. Synoptic maps and temperature records: June and July 1783.	34
Figure 5.8. Schematic model of the transport of volcanic material 1783.	35
Figure 5.9. Winter temperatures in Edinburgh 1764-1830.	36
Figure 5.10. Variation of Edinburgh winter temperatures.	37
Figure 5.11. Variation of Edinburgh winter temperatures from the Sixty-six year mean.	38
Figure 5.12. Winter temperatures in Central England, 1771-1791.	39
Figure 5.13. Variation of winter temperatures from the (1733-1833) 100 year mean.	40
Figure 6.1. Cattle mortality in Iceland	41
Figure 6.2. Sheep mortality in Iceland.	42
Figure 6.3. Transport of volcanic material from Iceland.	43
Figure 6.4a. Ash fall from the eruptions of the volcano Katla.	44
Figure 6.4b. Ash fall from the Askja eruption 1875.	45
Figure 6.5. Tephra fall locations in Britain.	46
Figure 6.6. Locations Mentioned in the text.	47
Figure 6.7 Fluorine concentrations in the River Ytri-Raga.	48
. Figure 6.8. Synoptic map June 23rd 1783.	49
Figure 6.9. The association between atmospheric circulation and volcanic pollution.	50
Figure 7.1. Theoretical framework for the interpretation of EDMA results.	51
Figure 7.2. Location map. Loch Hellisdale.	52
Figure 7.3. Palnology of the Loch Hellisdale.	53
Figure 7.4. Correlation between radiocarbon dates and palaeoenvironmental zones.	54
Figure 7.5. Sediment geochemistry Loch Hellisdale.	55
Figure 7.6. Diatom assemblage and Silicon in Loch Hellisdale.	56
Figure 8.1. Sample locations.	57

	Page
Figure 8.2a. Sediment geochemistry Loch A'Barpa.	58
Figure 8.2b. Sediment geochemistry Loch A'Barpa.	59
Figure 8.3. Tephra distribution, Loch Obisary.	60
Figure 8.4a. Sediment geochemistry Loch Obisary.	61
Figure 8.4b. Sediment geochemistry Loch Obisary.	62
Figure 8.5. Tephra distribution, Loch Druidibeg.	63
Figure 8.6a. Sediment geochemistry Loch Druidibeg.	64
Figure 8.6b. Sediment geochemistry Loch Druidibeg.	65
Figure 9.1. Location map, Borve bog.	66
Figure 9.2. Tephra distribution in Borve Bog.	67
Figure 9.3a. Sediment geochemistry Borve Bog.	68
Figure 9.3b. Sediment geochemistry Borve Bog.	69
Figure 9.4a. Sediment geochemistry Borve Bog. Chemizone BV1.	70
Figure 9.4b. Sediment geochemistry Borve Bog. Chemizone BV1.	71
Figure 9.5a. Sediment geochemistry Borve Bog. Chemizone BV2.	72
Figure 9.5b. Sediment geochemistry Borve Bog. Chemizone BV2.	73
Figure 9.6a. Sediment geochemistry Borve Bog. Chemizone BV3.	74
Figure 9.6b. Sediment geochemistry Borve Bog. Chemizone BV3.	75
Figure 9.7. Organic content Borve Bog.	76
Figure 9.8a. Sediment geochemistry Borve Bog. Chemizone BV4.	77
Figure 9.8b. Sediment geochemistry Borve Bog. Chemizone BV4.	78
Figure 9.9a. Sediment geochemistry Borve Bog. Chemizone BV5.	79
Figure 9.9b. Sediment geochemistry Borve Bog. Chemizone BV5.	80
Figure 9.10. Summary pollen diagram Borve Bog.	81
Figure 10.1. Site location Strath of Kildonan.	82
Figure 10.2. General tephra distribution, Strath of Kildonan.	83
Figure 10.3. Detailed tephra distribution, Strath of Kildonan.	84
Figure 10.4a. Sediment Geochemistry, Strath of Kildonan.	85
Figure 10.4b. Sediment Geochemistry, Strath of Kildonan.	86

	Page
Figure 10.5a. Sediment Geochemistry. Chemizone KL1, Strath of Kildonan.	87
Figure 10.5b. Sediment Geochemistry Chemizone KL1, Strath of Kildonan.	88
Figure 10.6a. Sediment Geochemistry Chemizone KL1a, Strath of Kildonan.	89
Figure 10.6b. Sediment Geochemistry Chemizone KL1a, Strath of Kildonan.	90
Figure 10.7a. Sediment Geochemistry Chemizone KL1b, Strath of Kildonan.	91
Figure 10.7b. Sediment Geochemistry Chemizone KL1b, Strath of Kildonan.	92
Figure 10.8a. Sediment Geochemistry Chemizone KL2, Strath of Kildonan.	93
Figure 10.8b. Sediment Geochemistry Chemizone KL2, Strath of Kildonan.	94
Figure 10.9a. Sediment Geochemistry Chemizone KL3, Strath of Kildonan.	95
Figure 10.9b. Sediment Geochemistry Chemizone KL3 Strath of Kildonan.	96
Figure 10.10a. Sediment Geochemistry Chemizone KL4, Strath of Kildonan.	97
Figure 10.10b. Sediment Geochemistry Chemizone KL4, Strath of Kildonan.	98
Figure 10.11. Tephra distribution in Chemizone KL4.	99
Figure 10.12a. Sediment Geochemistry Chemizone KL5, Strath of Kildonan.	100
Figure 10.12b. Sediment Geochemistry Chemizone KL5, Strath of Kildonan.	101
Figure 10.13a. Sediment Geochemistry Chemizone KL6, Strath of Kildonan.	102
Figure 10.13b. Sediment Geochemistry Chemizone KL6, Strath of Kildonan.	103
Figure 10.14a. Sediment Geochemistry Chemizone KL7, Strath of Kildonan.	104
Figure 10.14b. Sediment Geochemistry Chemizone KL7, Strath of Kildonan.	105

Figures

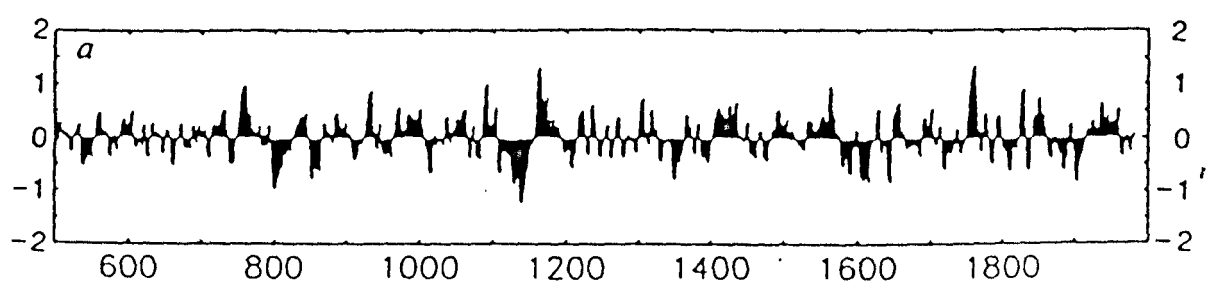


Figure 1.1. Ten year cycles in reconstructed northern Fennoscandian summer temperature anomalies relative to 1951-1970 mean. From Briffa *et al.* 1990.

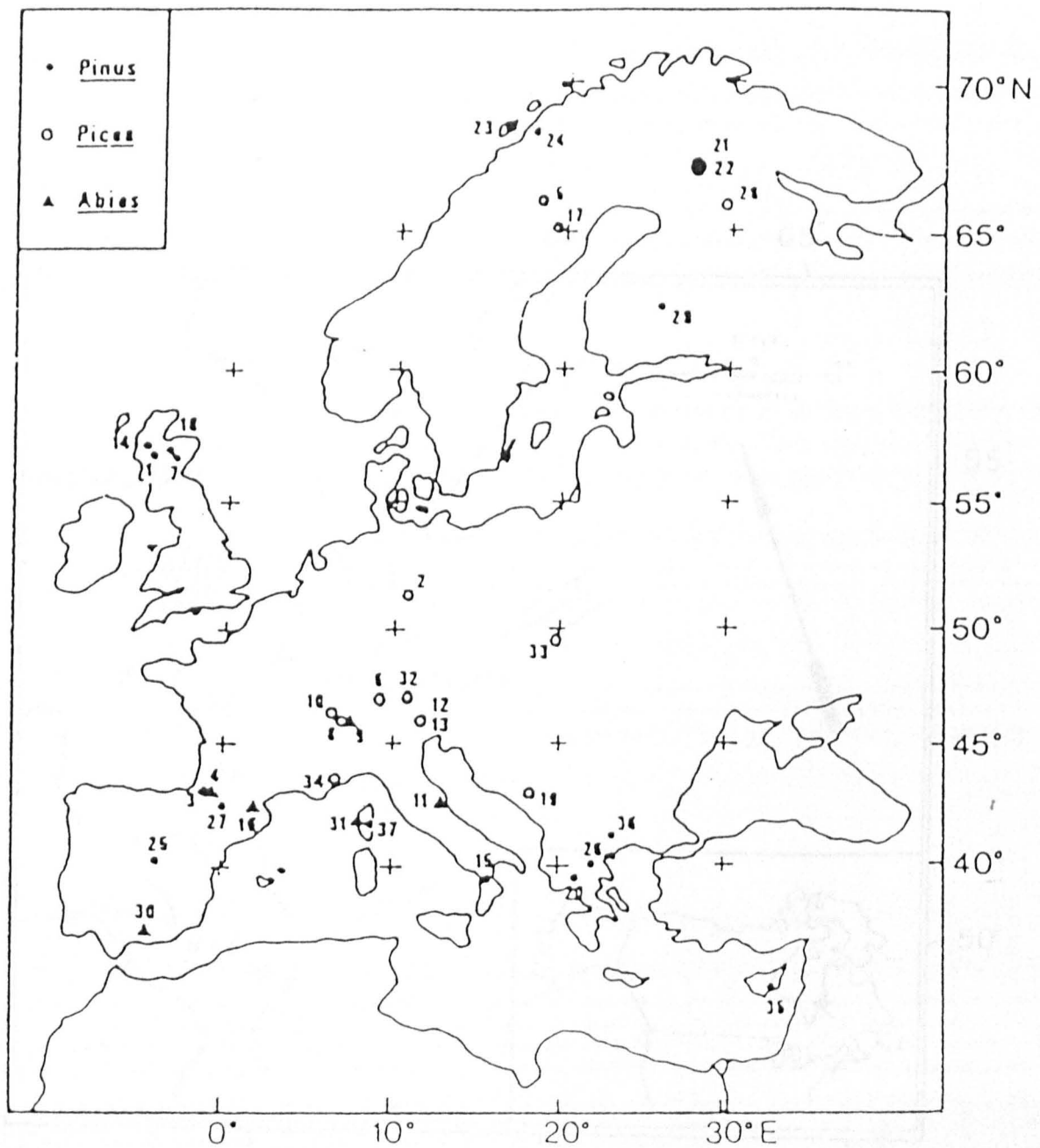


Figure 1.2. The location and genera of 37 chronologies used to reconstruct summer temperatures across Europe. From Briffa *et al.* 1988.

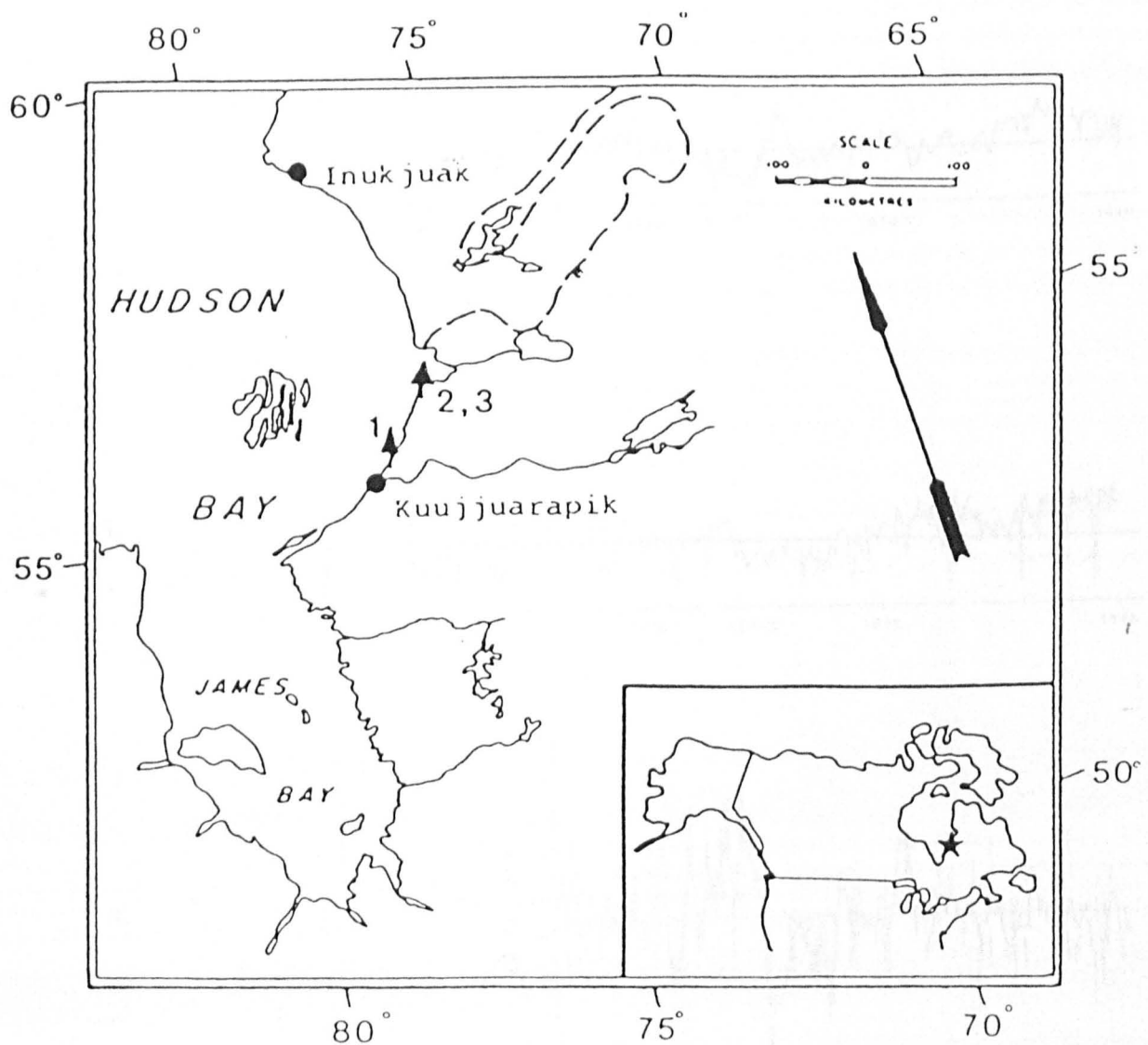
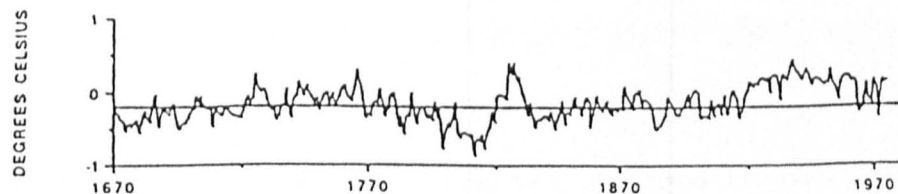


Figure 1.3. Location map for tree-ring chronologies. 1 = Kuujjuarapik, 2 = Richmond Gulf, 3 = Castle Peninsula. From Jacoby *et al.* 1988.

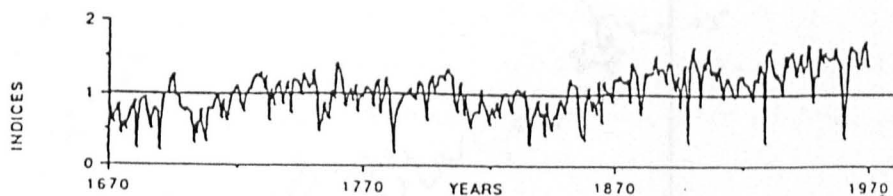
1.



2.



3.



4.

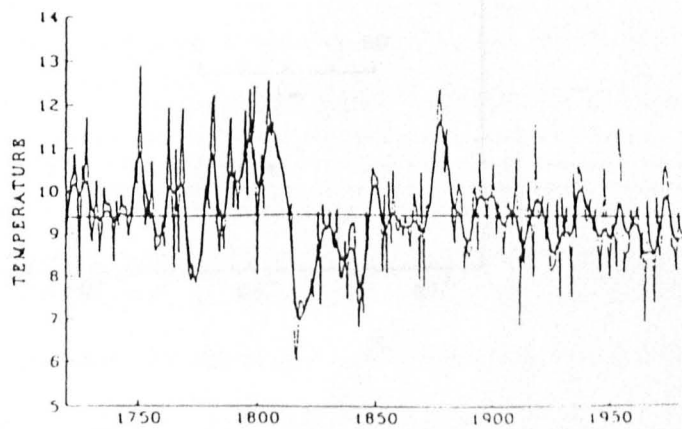


Figure 1.4. Comparisons between temperature reconstructions from North American chronologies. 1: Northern Hemisphere, Jacoby *et al.* 1989. 2: Northern Hemisphere, Groveman & Landsberg 1979. 3: Temperature indices California, LaMarche & Stockton 1974. 4: Local temperatures at Kuujjuarapik, Jacoby *et al.* 1988.

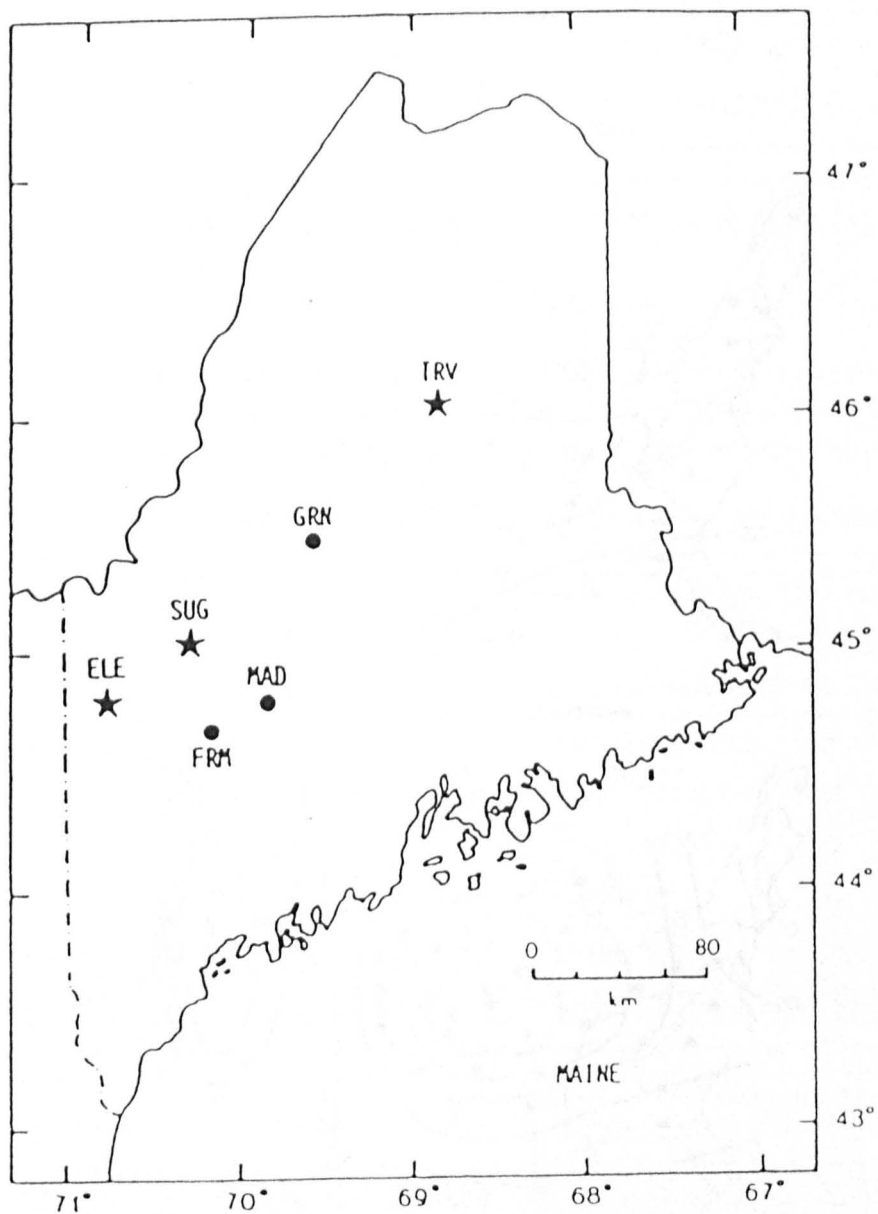
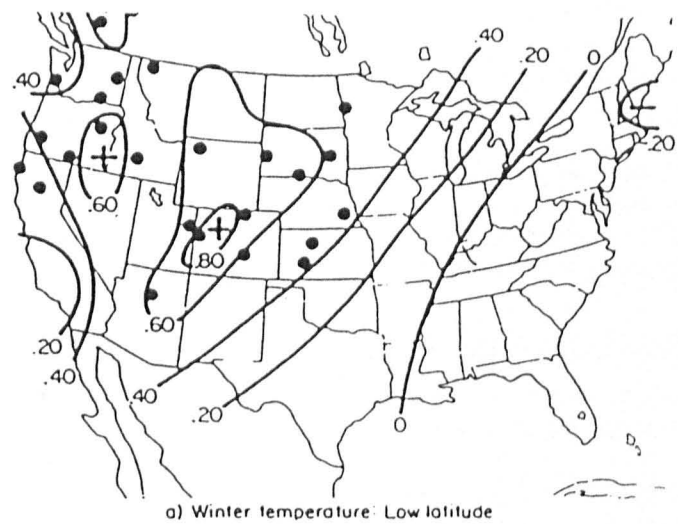
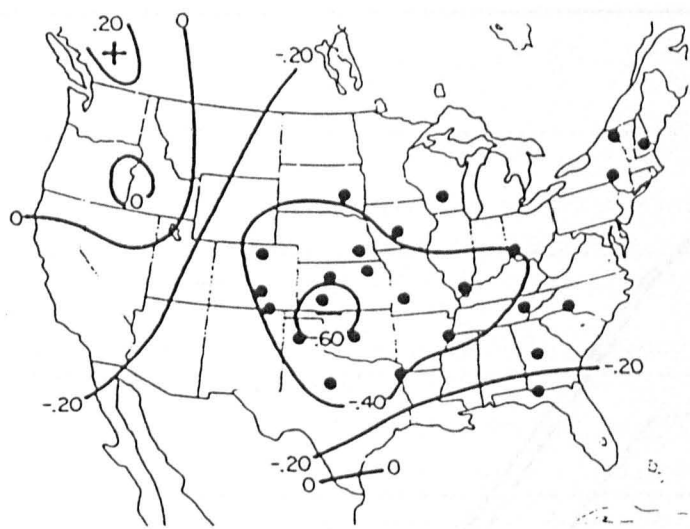


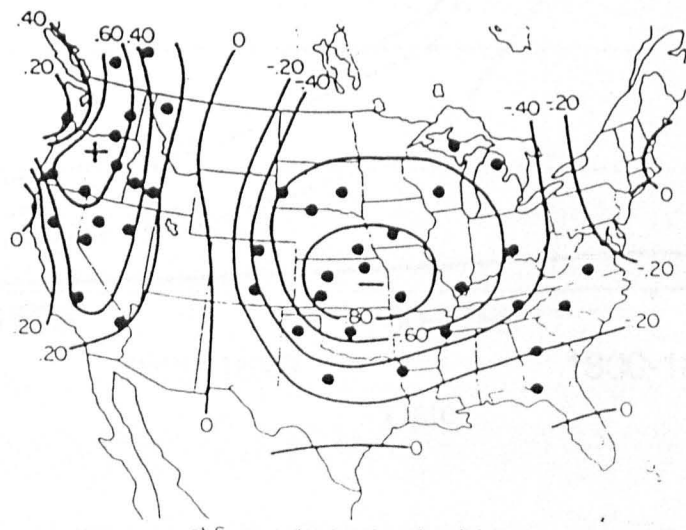
Figure 1.5. Location of tree-ring chronologies in Maine. Tree-ring sites (Stars) TRV = Traveler Mt., SUG = Sugarloaf Mt., ELE = Elephant Mt. Comparative climatic stations (Filled circles) GRN = Greenville, MAD = Madison, FRM = Farmington. From Conkey 1986.



a) Winter temperature: Low latitude



b) Spring temperature: Low latitude



1900-1980

c) Summer temperature: Low latitude

Figure 1.6. Average reconstructed temperature differences (degrees centigrade) between the average of years 0 to 2 after eruption dates minus the average of years 1 to 5 prior to key dates for low-latitude eruptions. A: Winter. B: Spring. C: Summer. Heavy dots indicate temperature departures significant at the 95% level. From Lough & Fritts 1987.

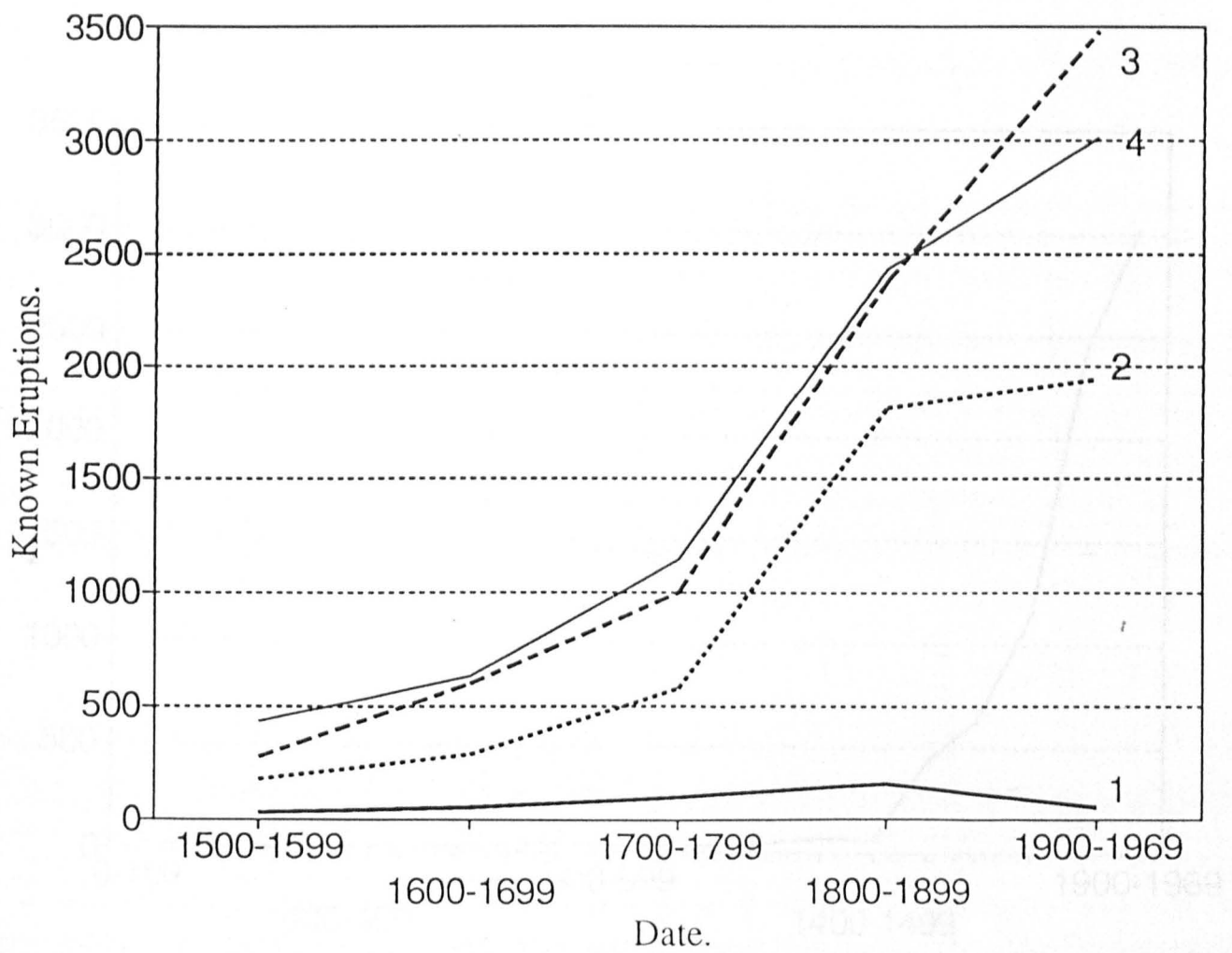


Figure 2.1. Evolution of eruption chronologies 1970-1982.

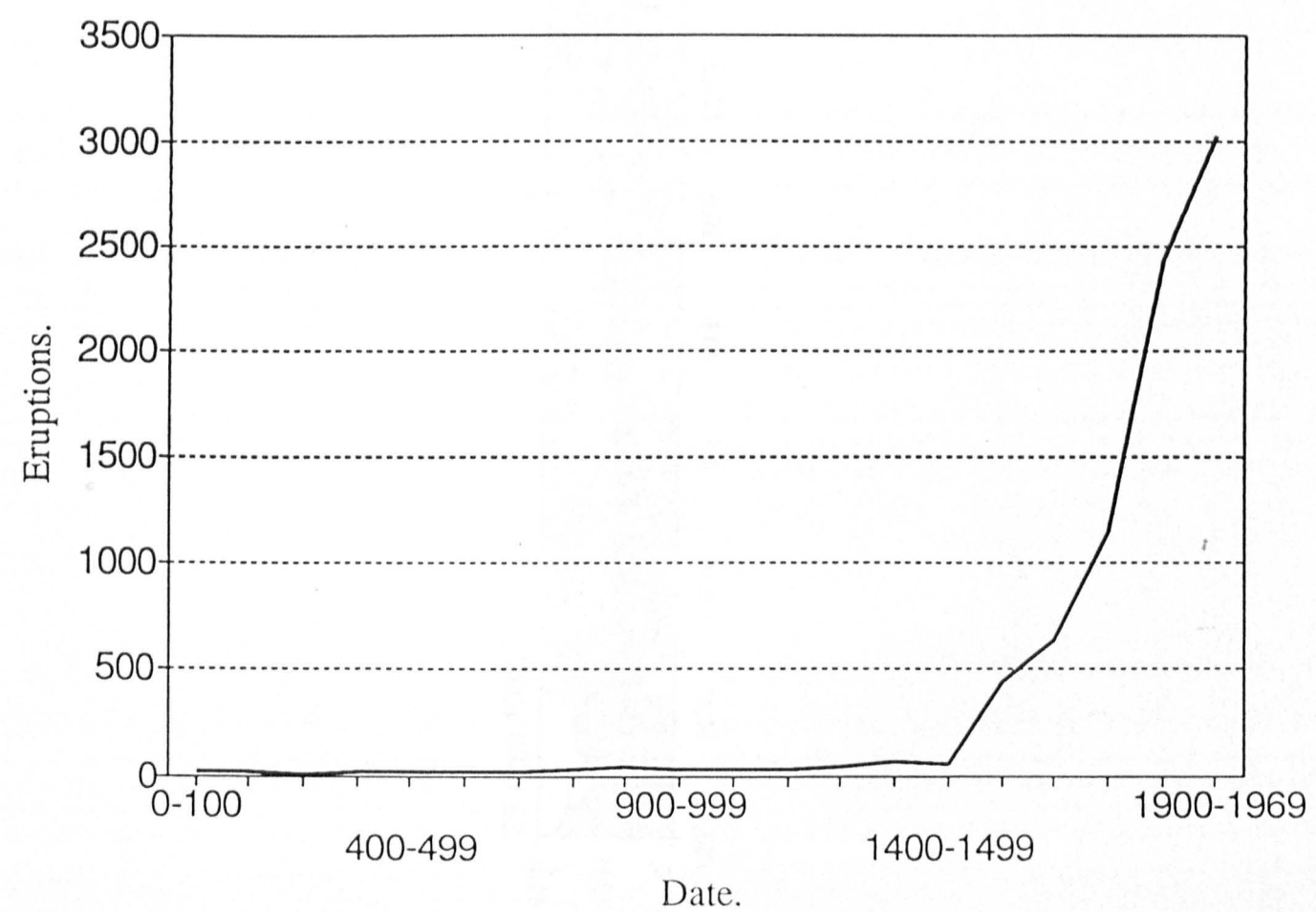


Figure 1. The eruption of Mount St. Helens, April 18, 1980. Figure 2.2. Eruption chronology 0 - 1970 A.D. (Based on the data of the April 4, 1962 eruption of El Chichón, from Gómez & Wilson 1988.)

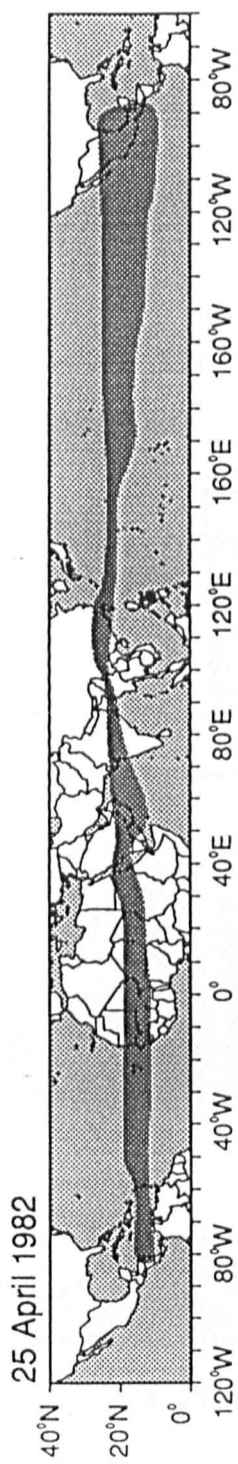


Figure 3.1. The narrow latitudinal band initially cooled by the stratospheric aerosol cloud of the April 4, 1982 eruption of El Chichón. From Robock & Matson 1983.

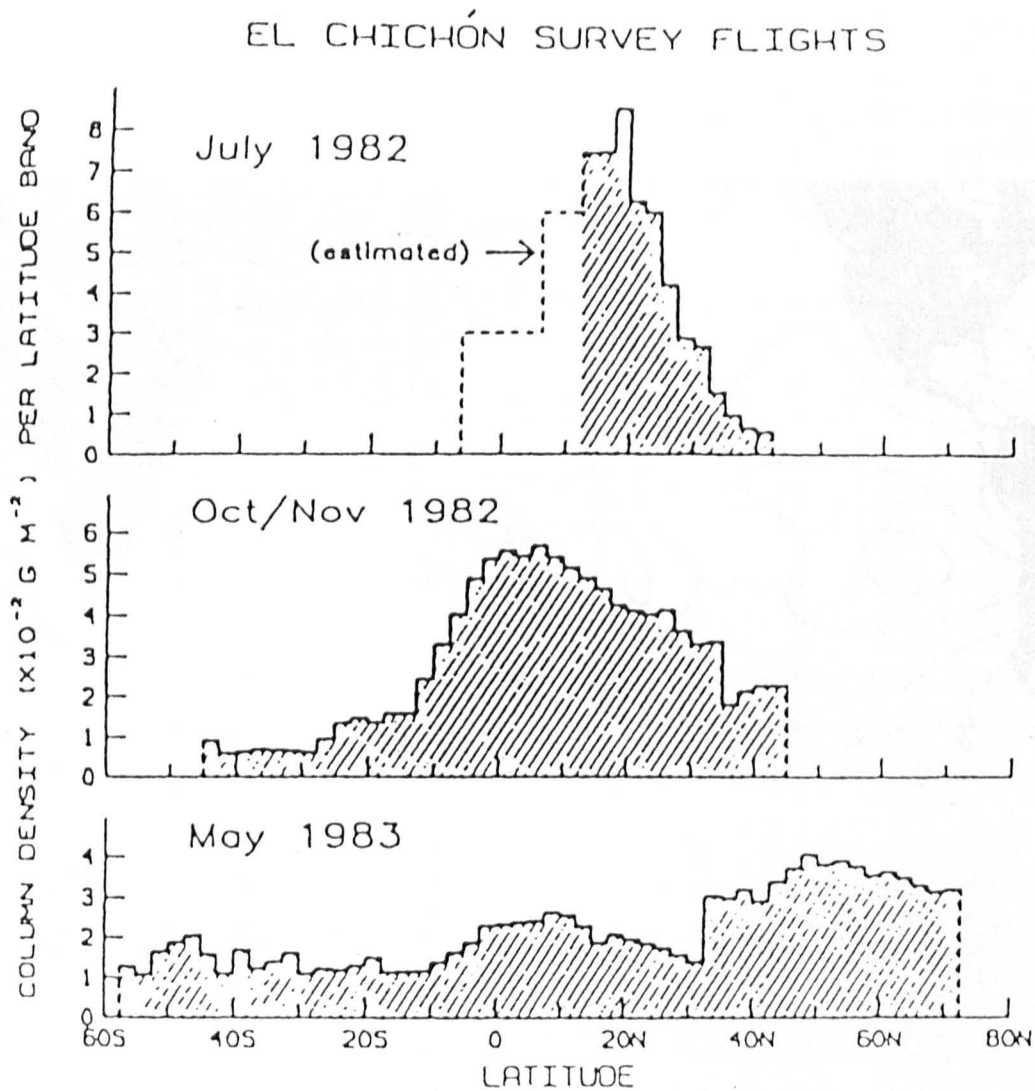


Figure 3.2. The distribution of the El Chichón aerosol cloud relative to time and latitude. From McCormick *et al.* 1984.

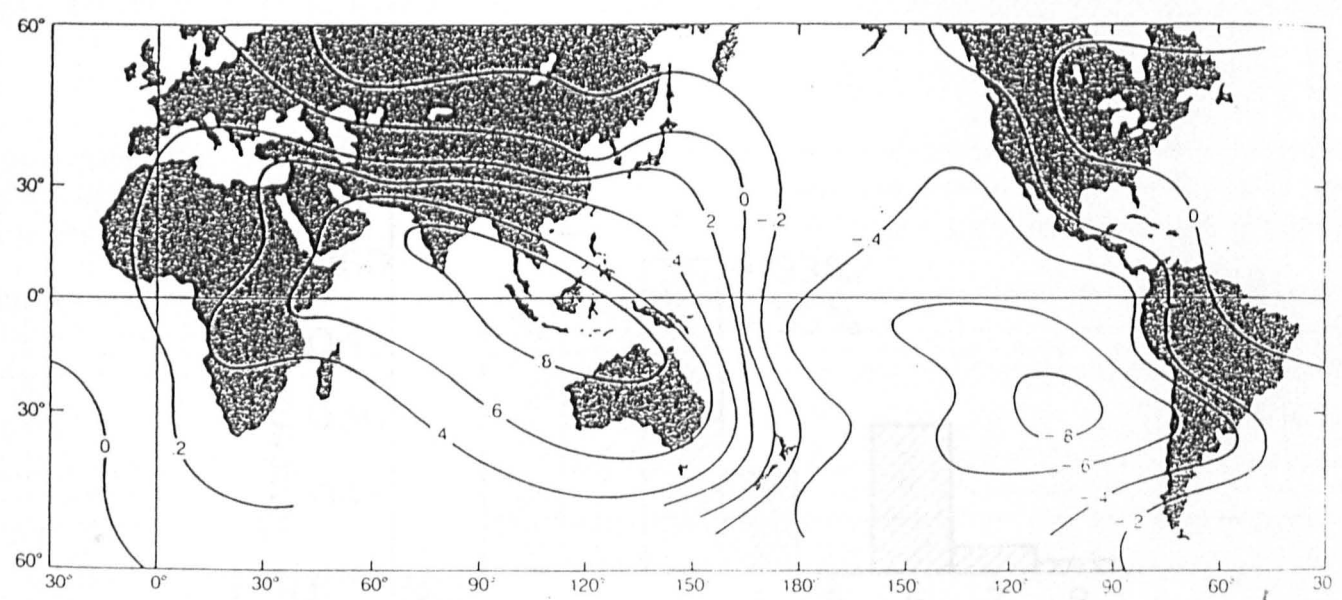


Figure 3.3. The influence of the Southern Oscillation on global air pressure. From Ramage 1986.

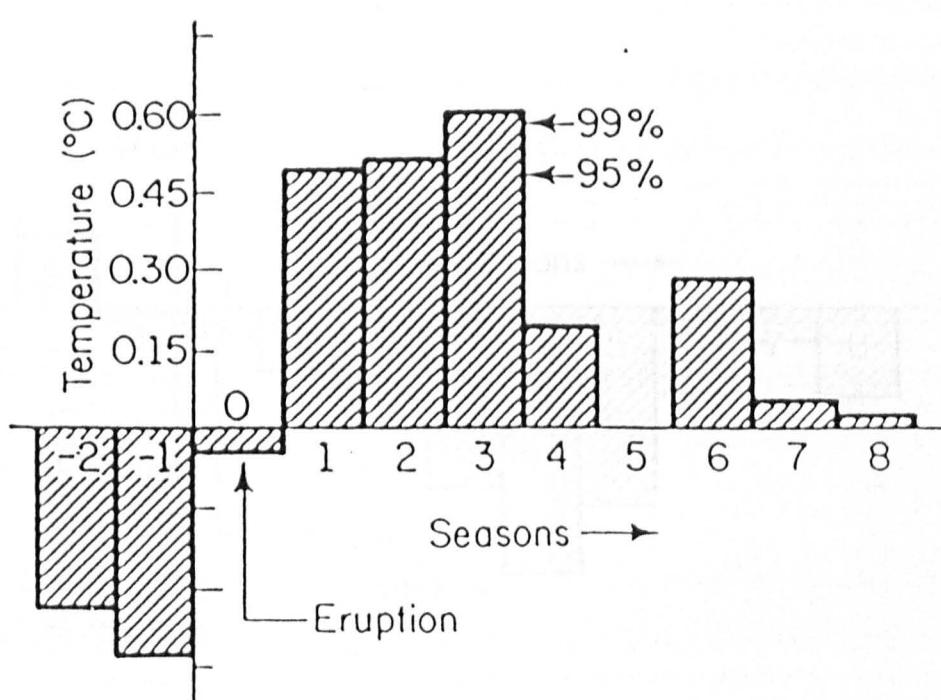


Figure 3.4. Composite sea surface temperature anomaly for twelve low-latitude stratospheric aerosols, from 2 seasons before and 8 seasons after the eruption. From Handler 1986.

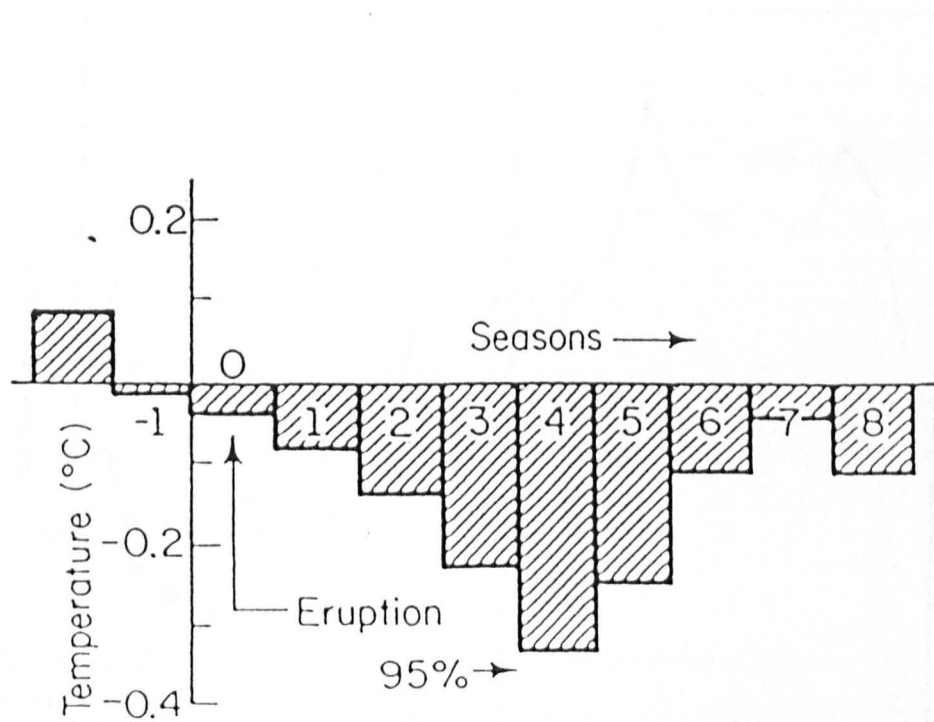


Figure 3.5. Composite sea surface temperature anomaly for twenty-one high latitude stratospheric aerosols, from 2 seasons before and 8 seasons after the eruption. From Handler 1986.

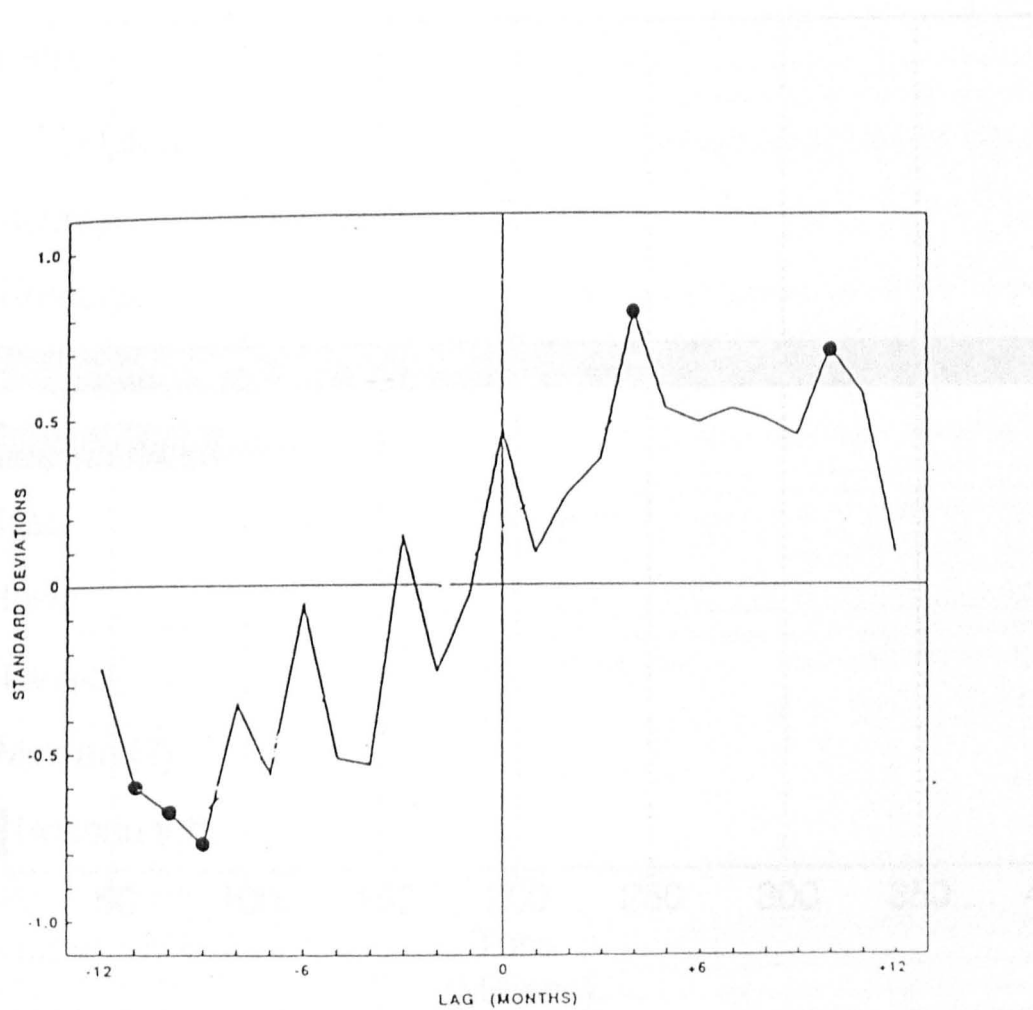


Figure 3.6. Superposed epoch analysis of Darwin surface pressure. Before and after key low-latitude eruptions. After Nicholls 1988.

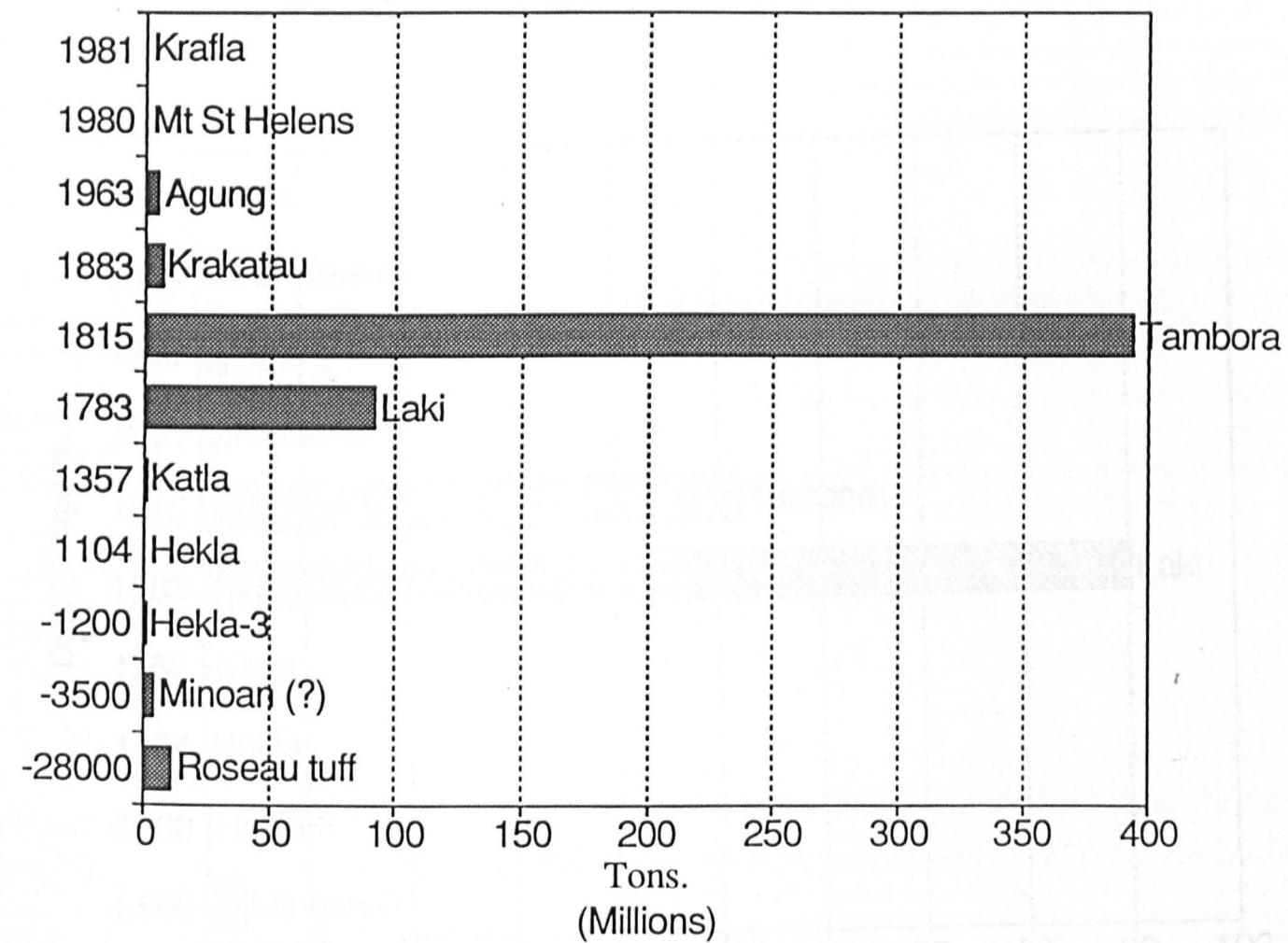


Figure 4.1. Total acids output of selected major volcanic eruptions. Data from Devine *et al.* [1984].

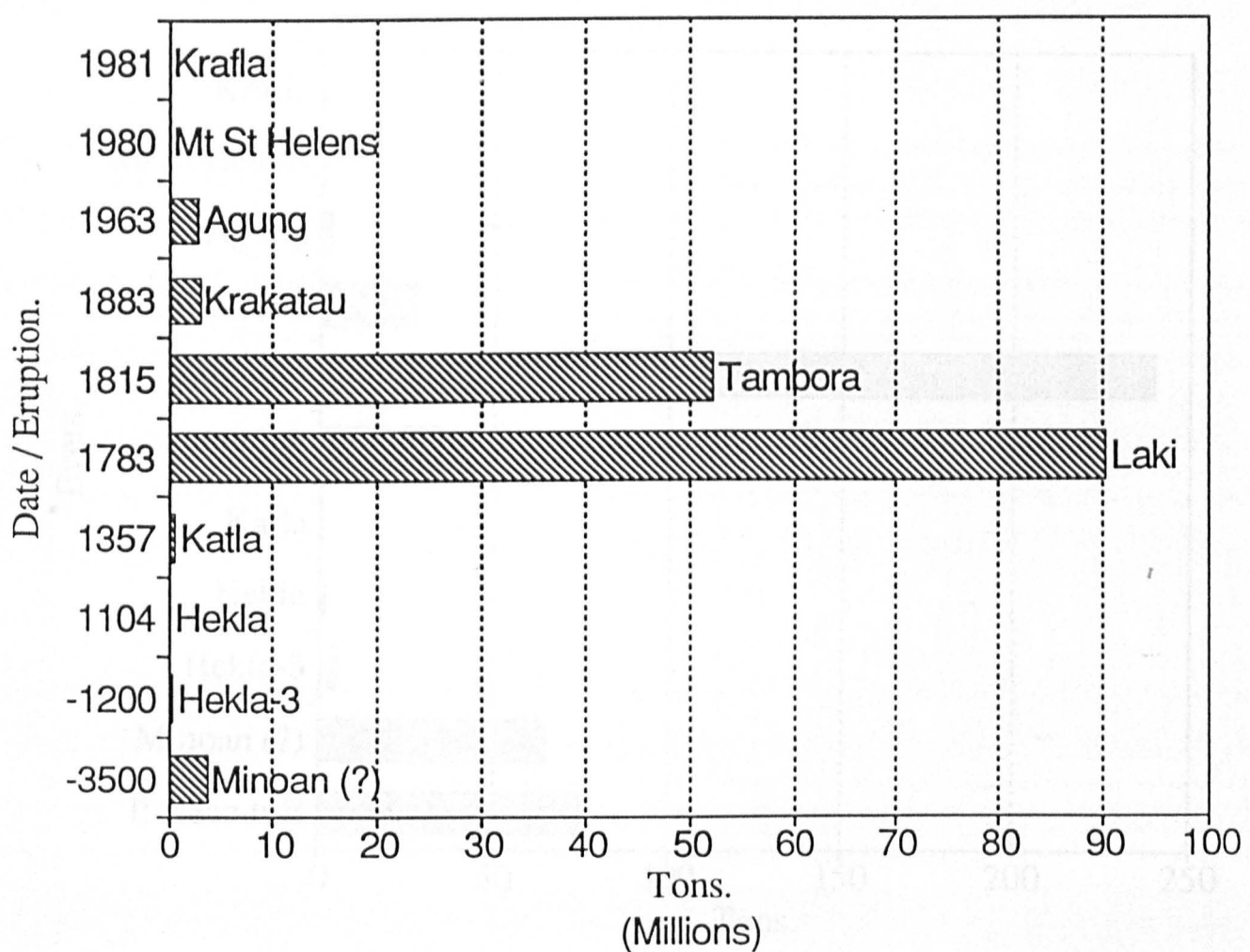


Figure 4.2. Total sulphuric acid output of selected major volcanic eruptions. Data from Palais & Sigurdsson [1989] and Sigurdsson & Carey [1992].

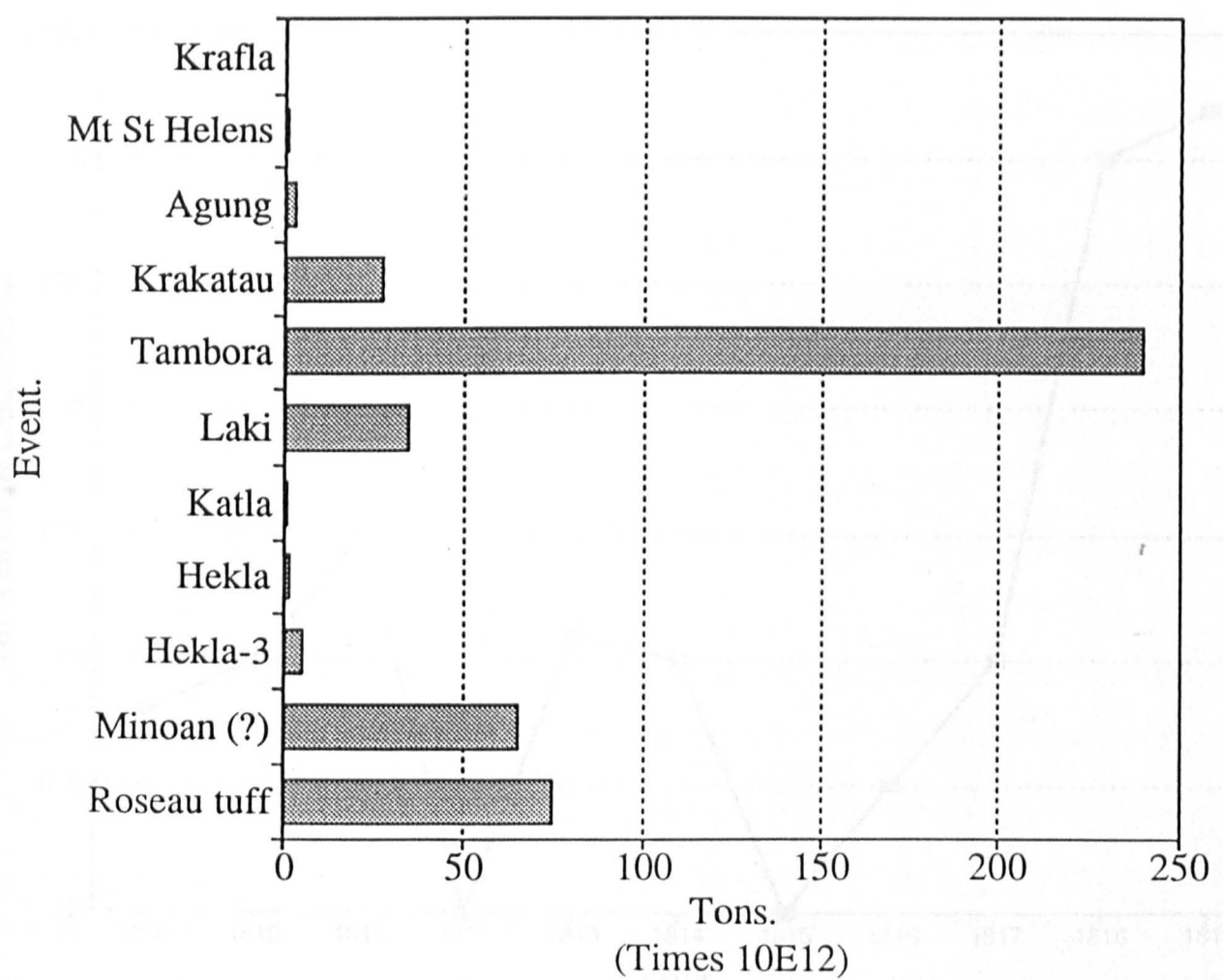


Figure 4.3. Total erupted mass of selected major volcanic eruptions. Data from Stothers [1984b].

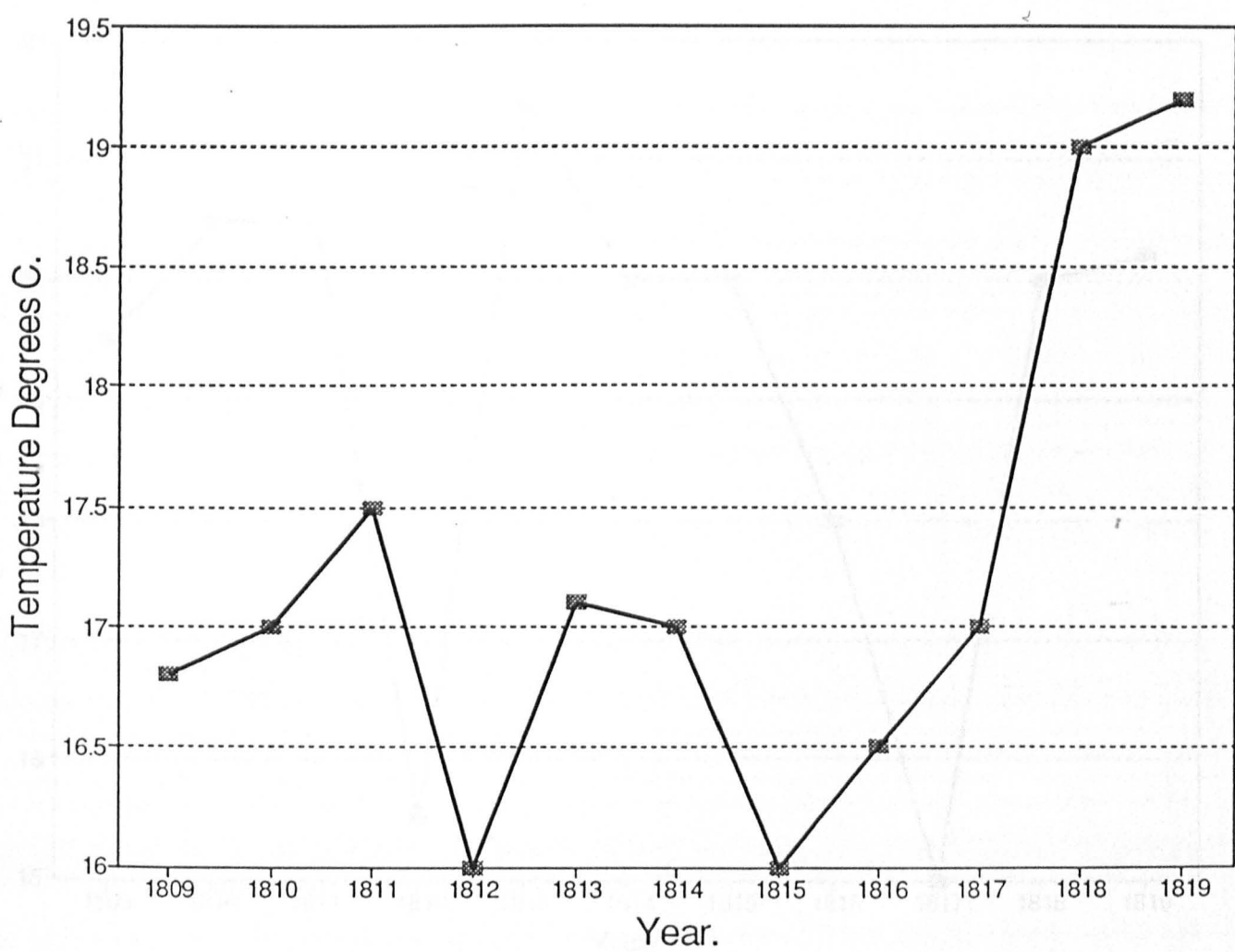


Figure 4.4. Summer mean temperatures at Brunswick, New Jersey. Data from Baron [1992].

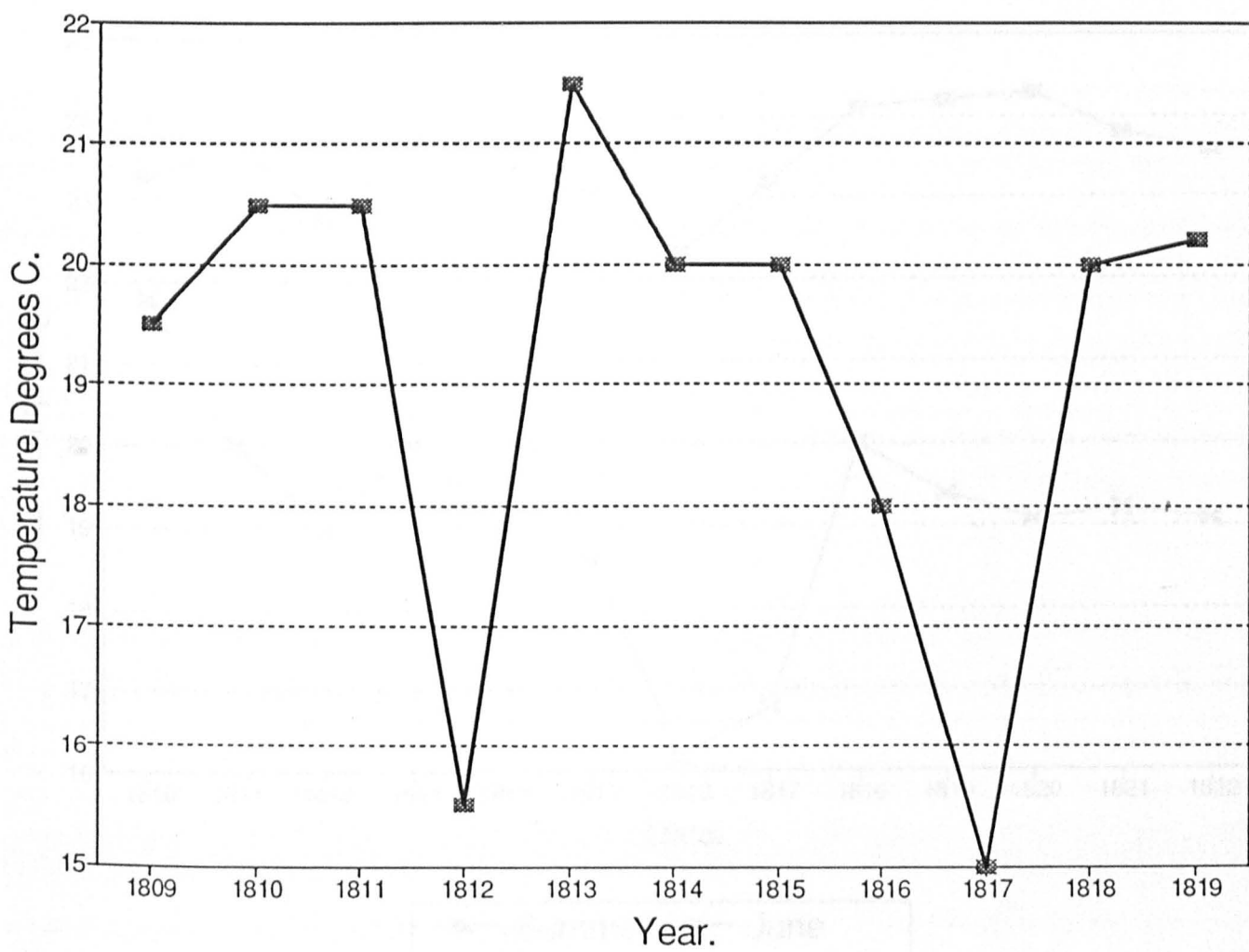


Figure 4.5. Summer mean temperatures at New Haven, Connecticut. Data from Baron [1992].

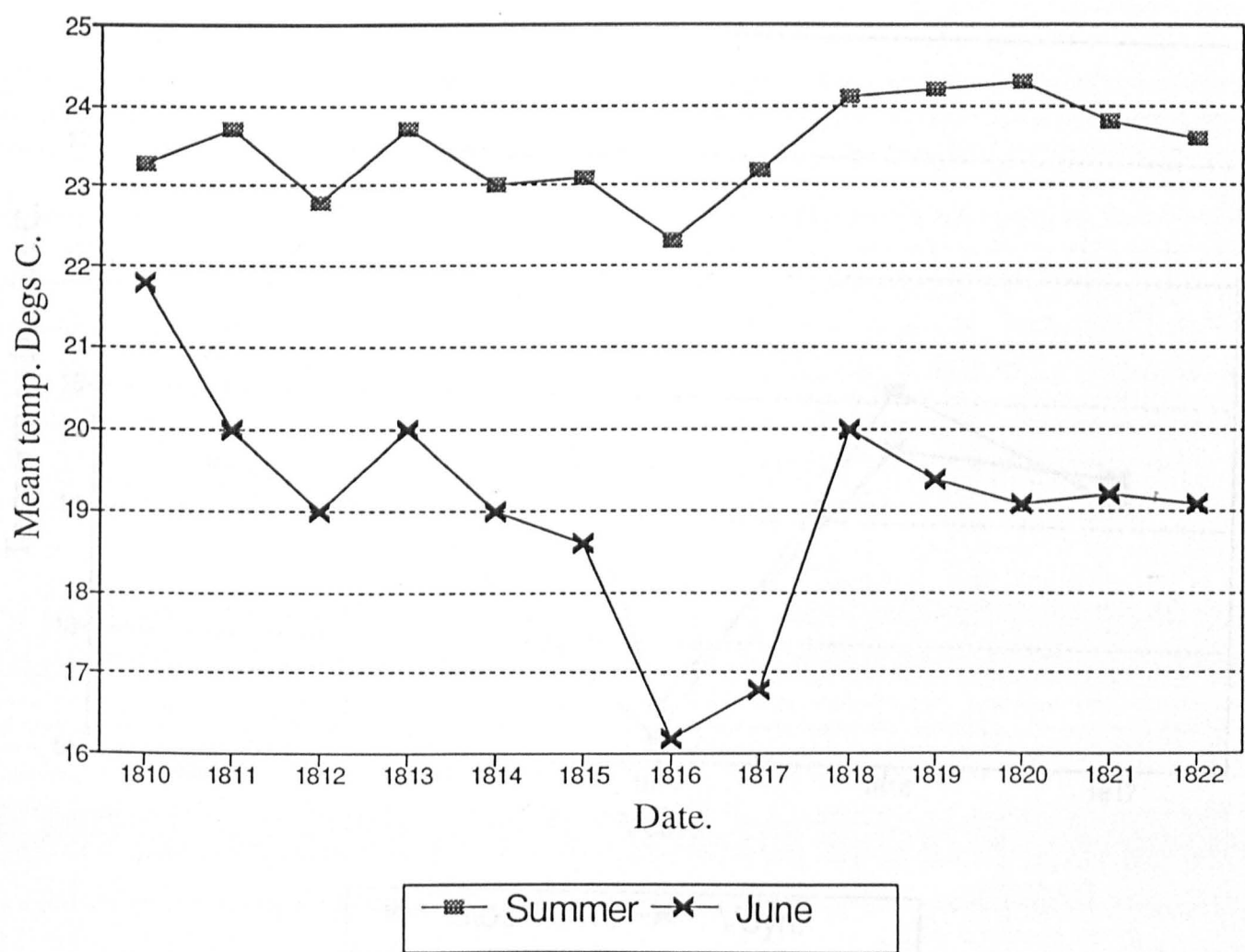


Figure 4.6 Summer and June mean temperatures at New Haven, Connecticut. Data from Sigurdsson [1982].

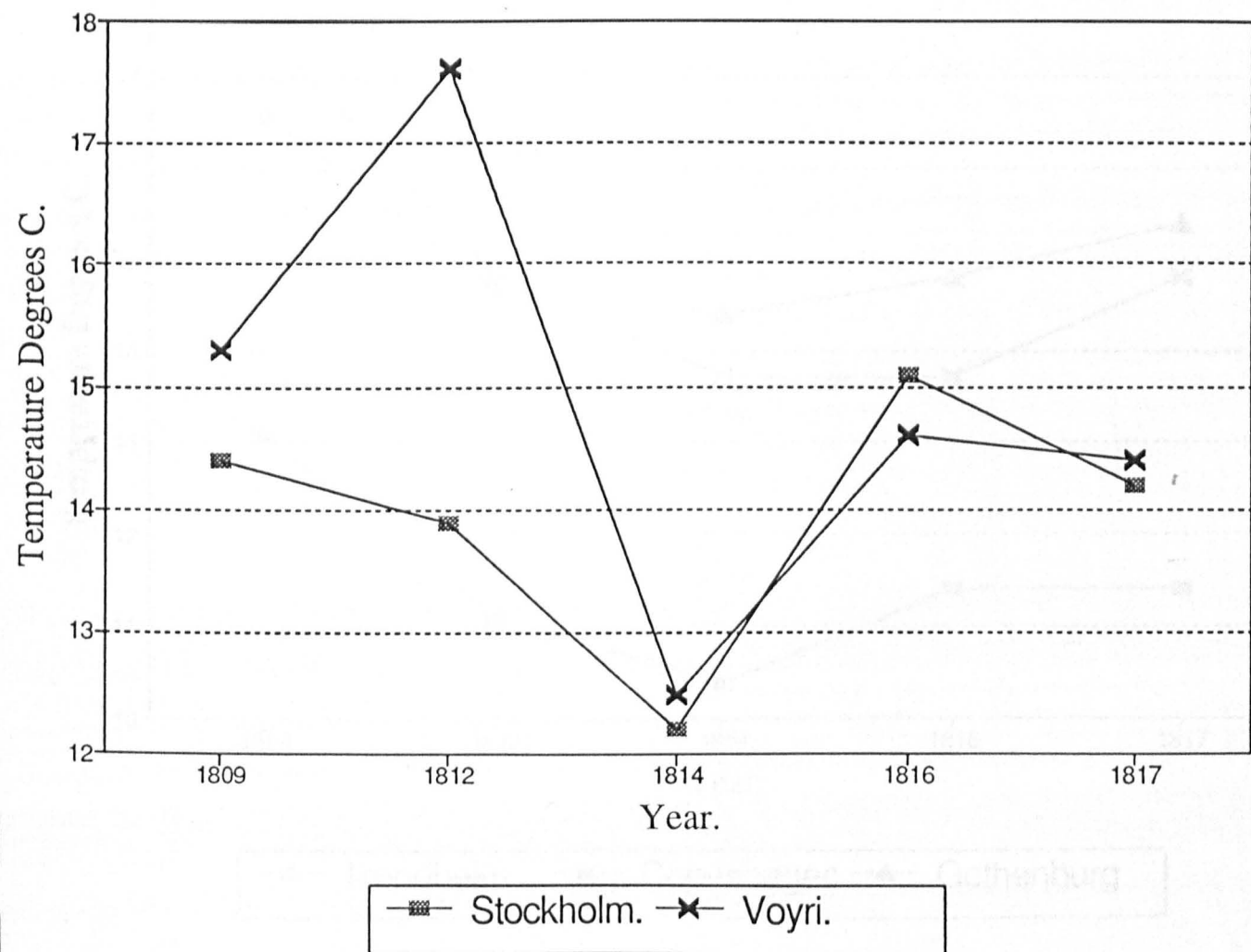


Figure 4.7. Summer mean temperatures at Stockholm and Voyri. Data from Neumann [1990].

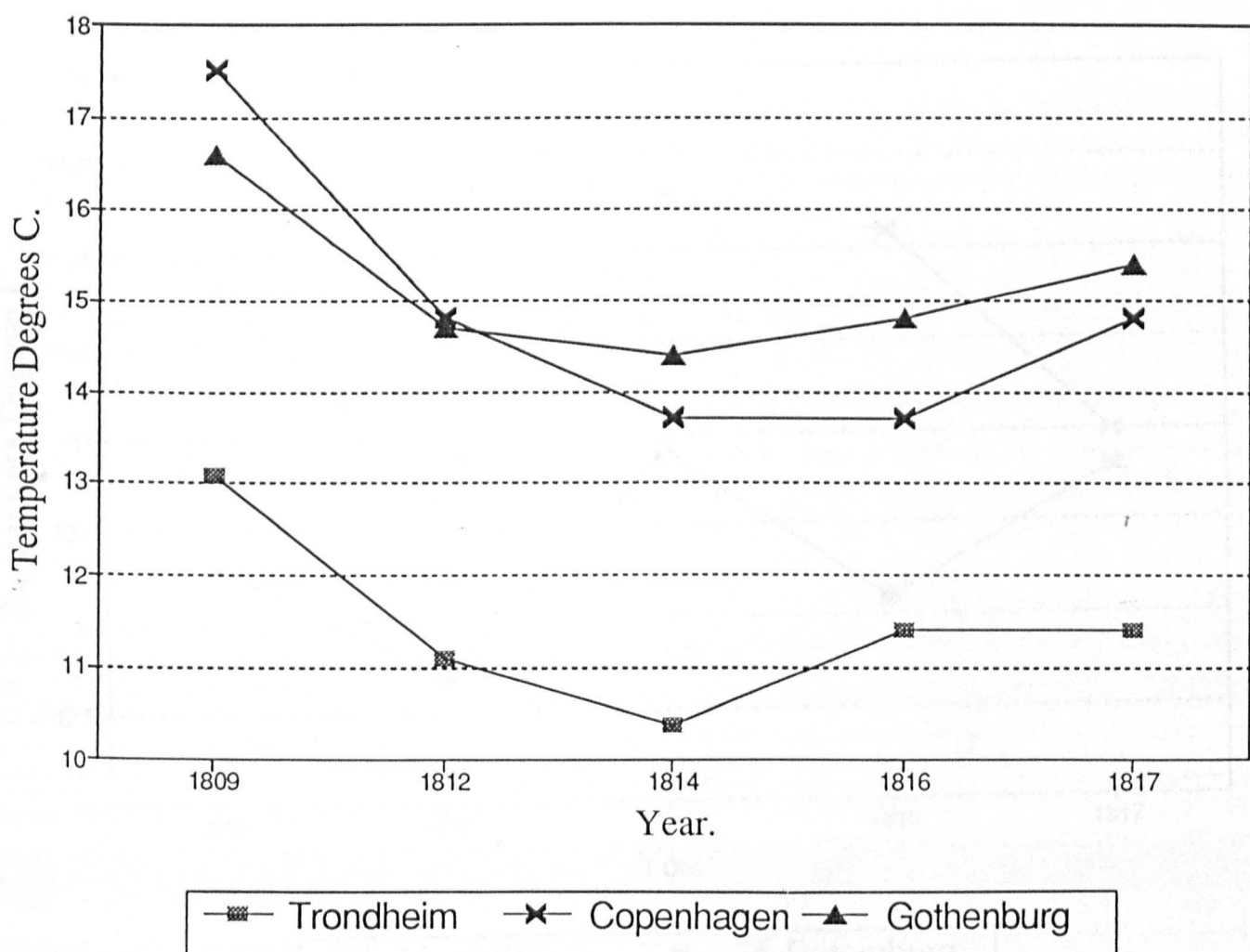


Figure 4.8. Summer mean temperatures at Trondheim, Copenhagen, Gothenburg.

Data from Neumann [1990].

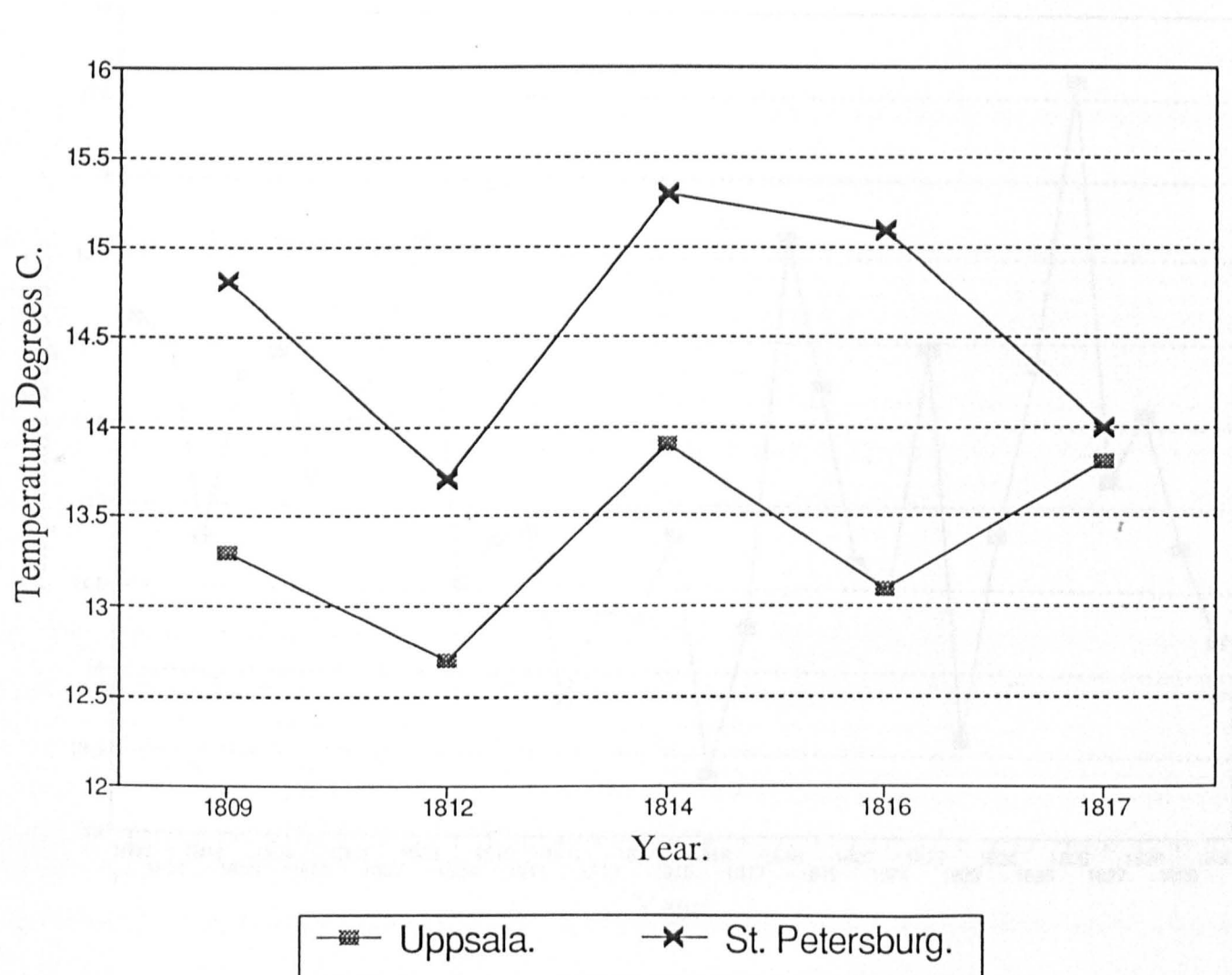


Figure 4.9. Summer mean temperatures at Uppsala & St. Petersburg.

Data from Neumann [1990].

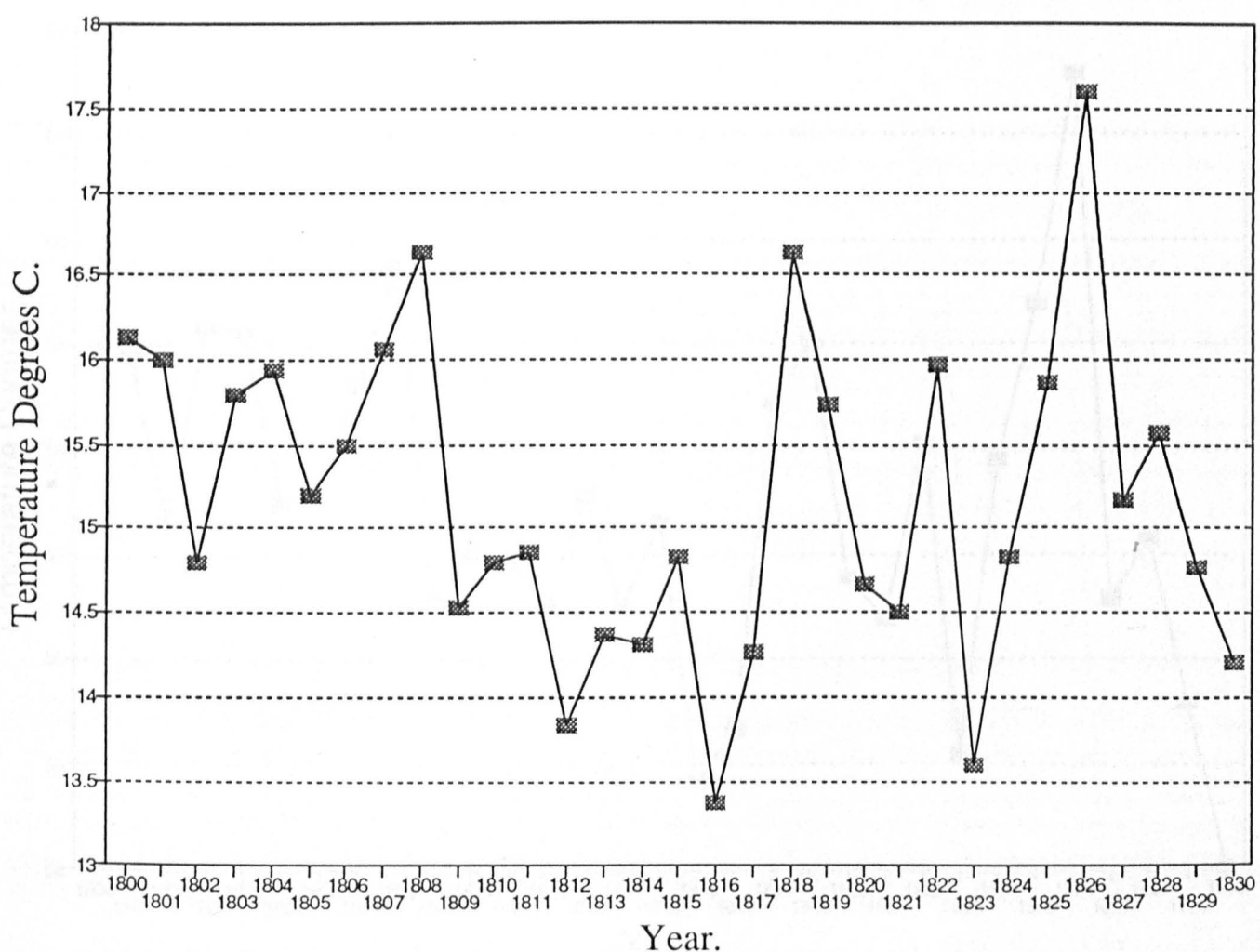


Figure 4.10. Summer mean temperatures in Central England. Data from Manley [1974].

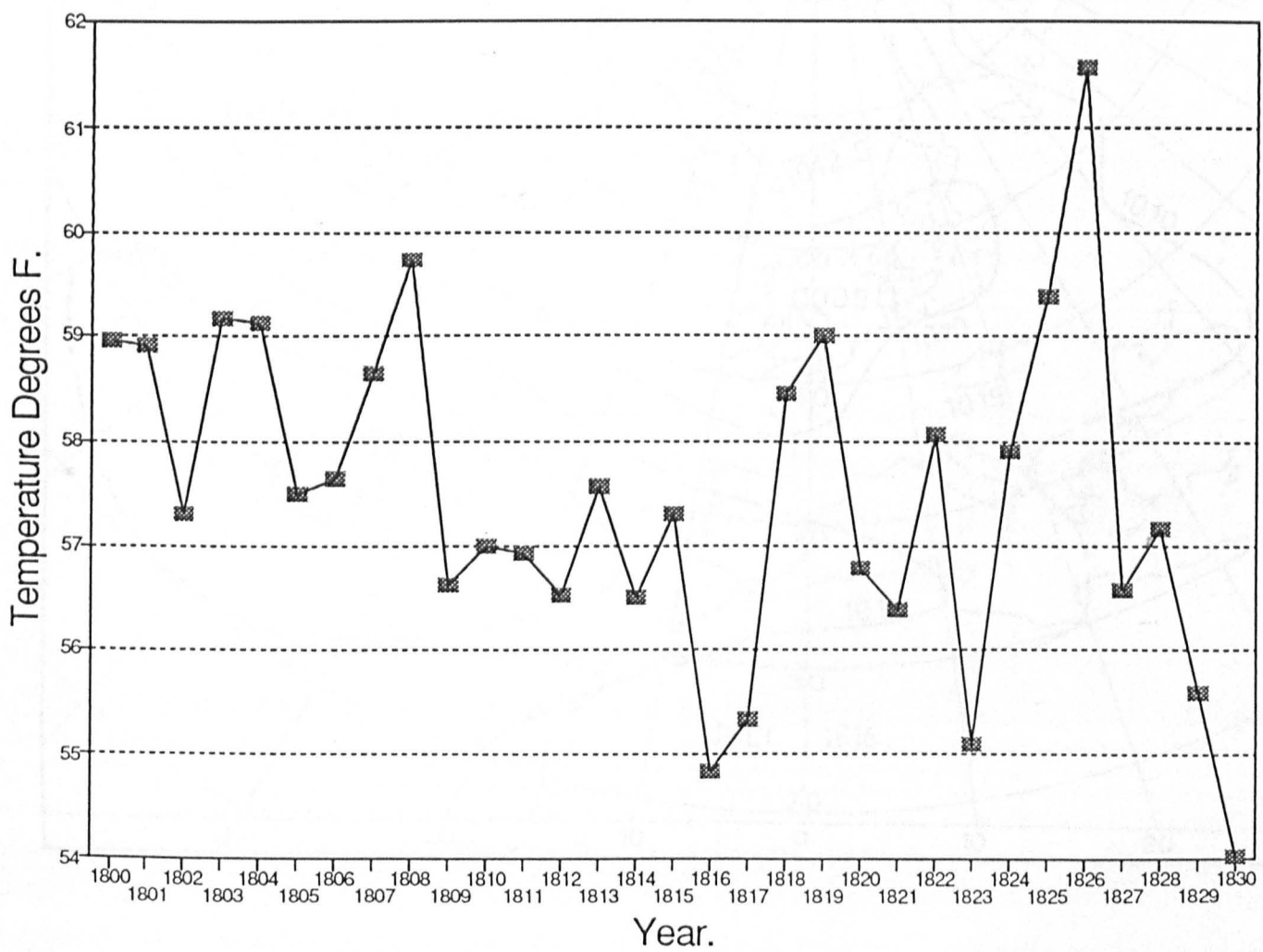


Figure 4.11. Summer mean temperatures in Edinburgh. Data from Mossman [1896].

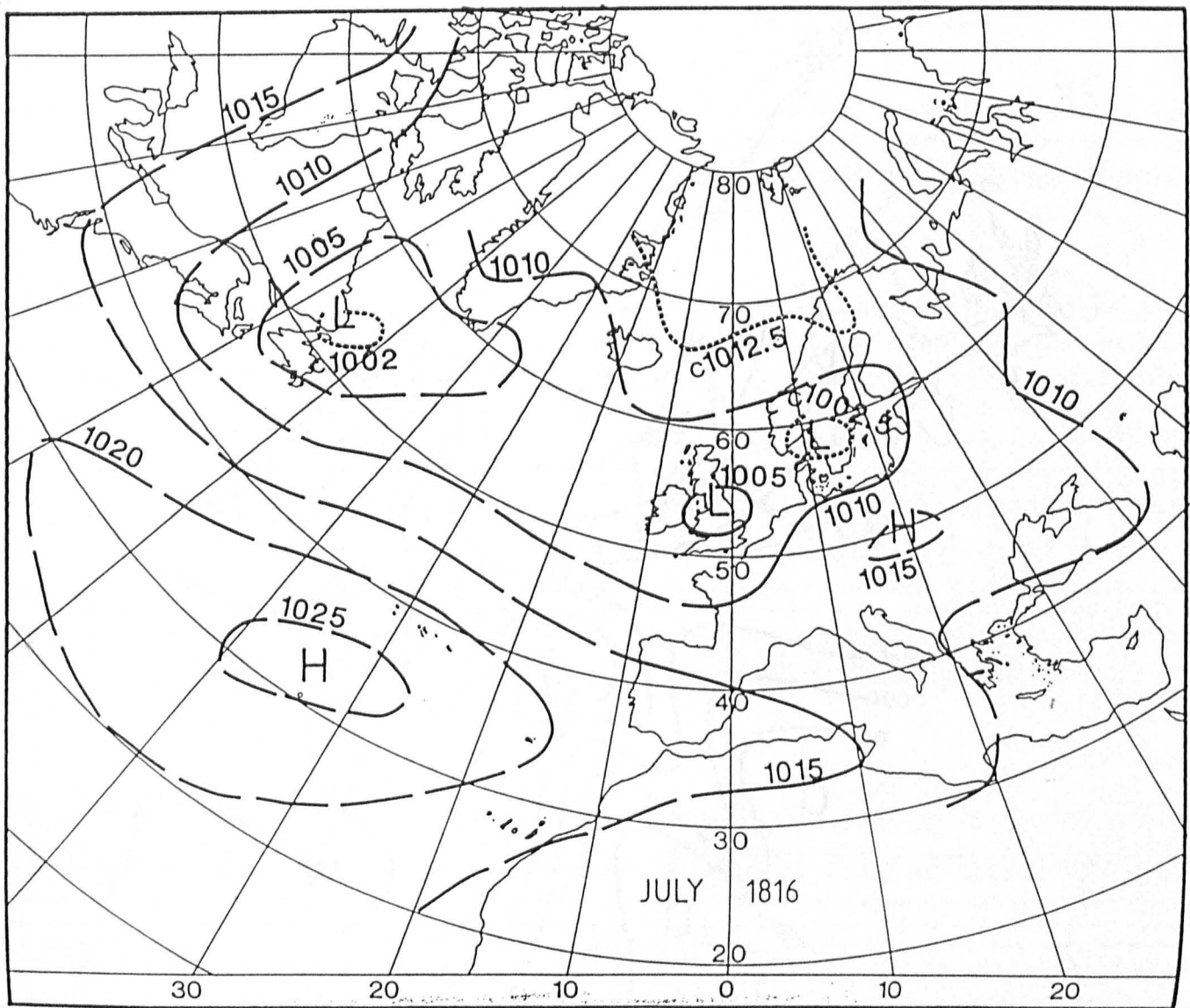


Figure 4.12. Summer position of the "Icelandic Low" in 1816. From Lamb [1992].

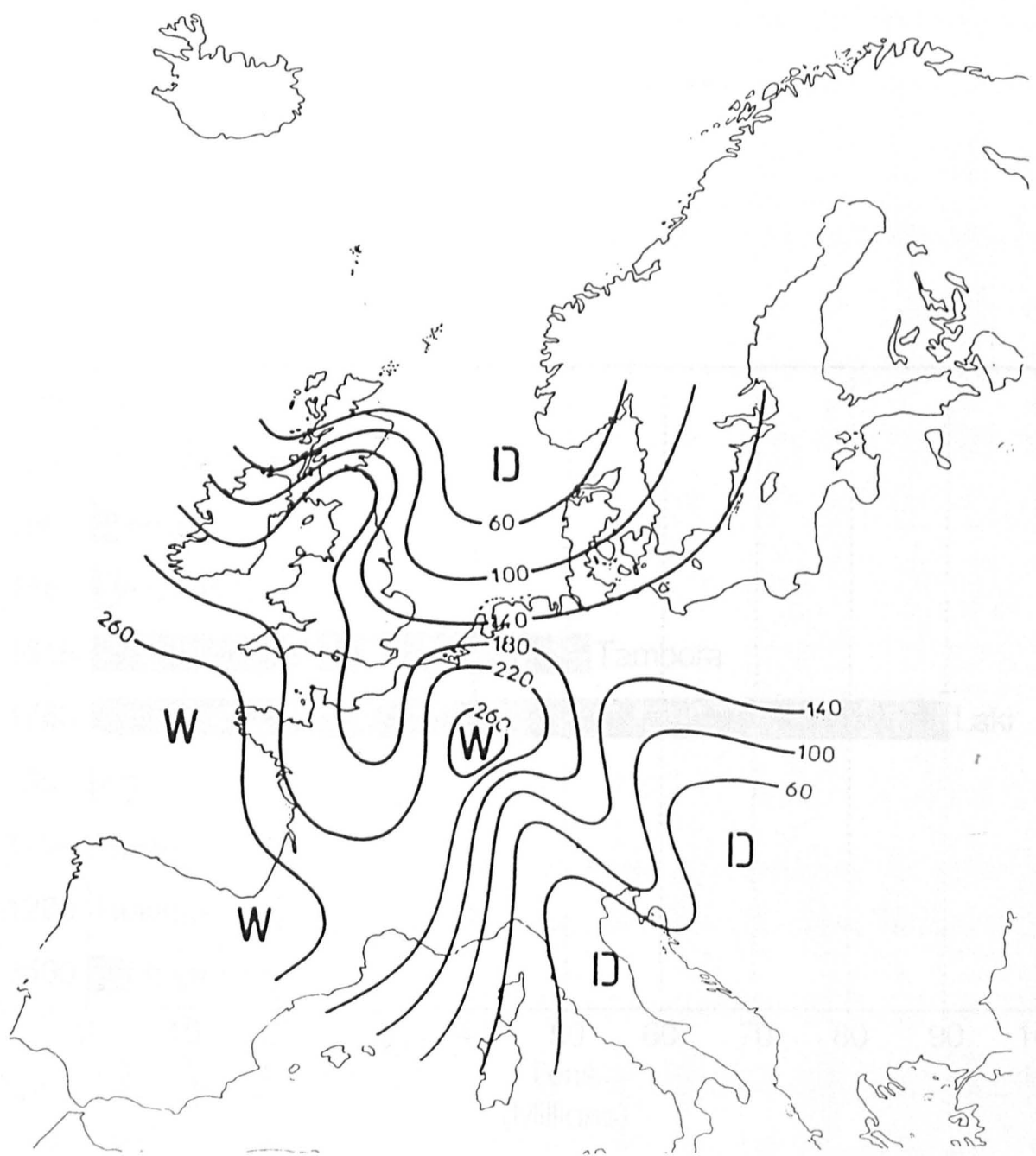


Figure 4.13. European rainfall anomalies % in the Summer of 1816. From Kington [1992].

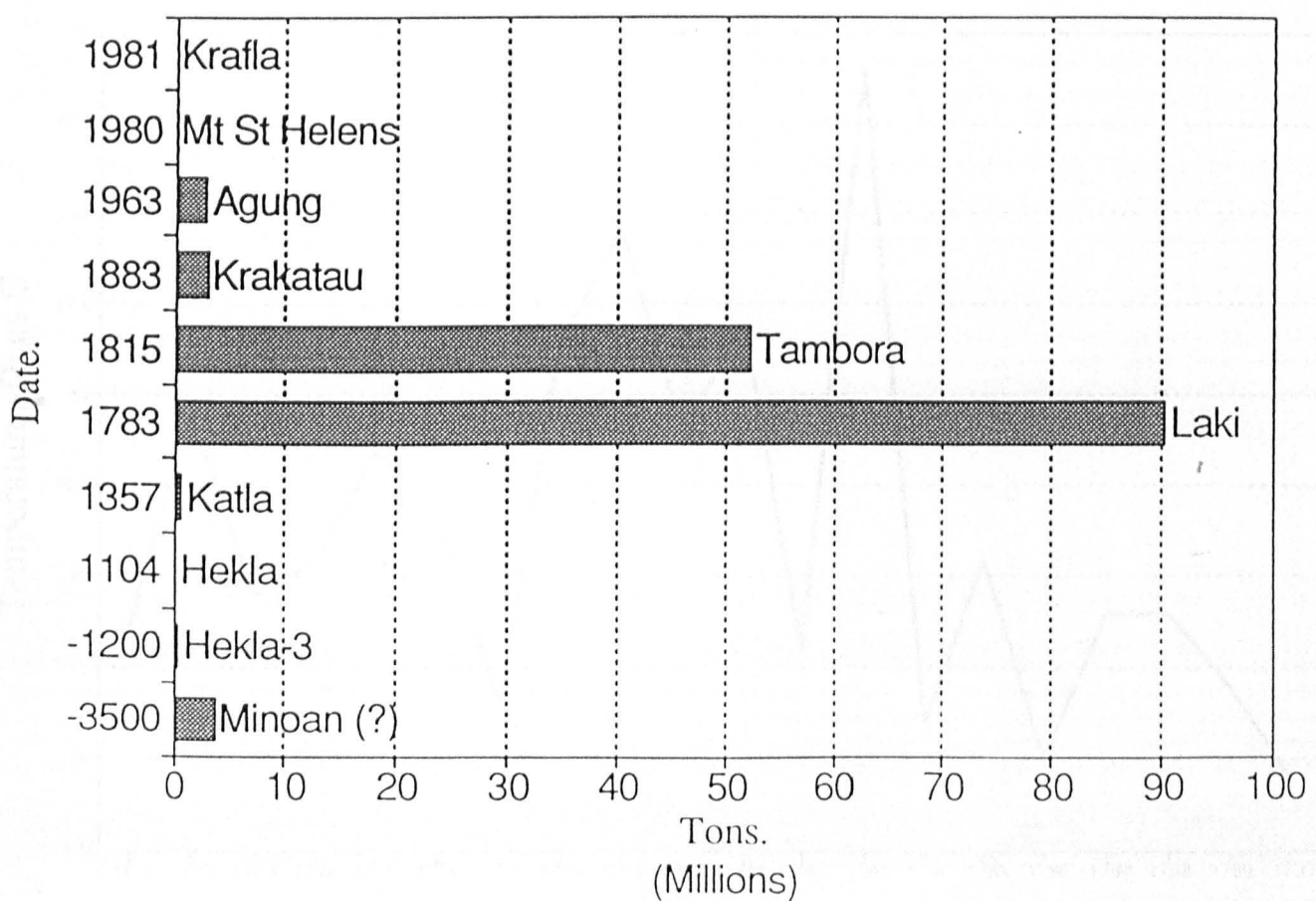


Figure 5.1. Acid volatile emission of selected volcanoes. [Data from Devine *et al.* 1984; & Sigurdsson *et al.* 1985].

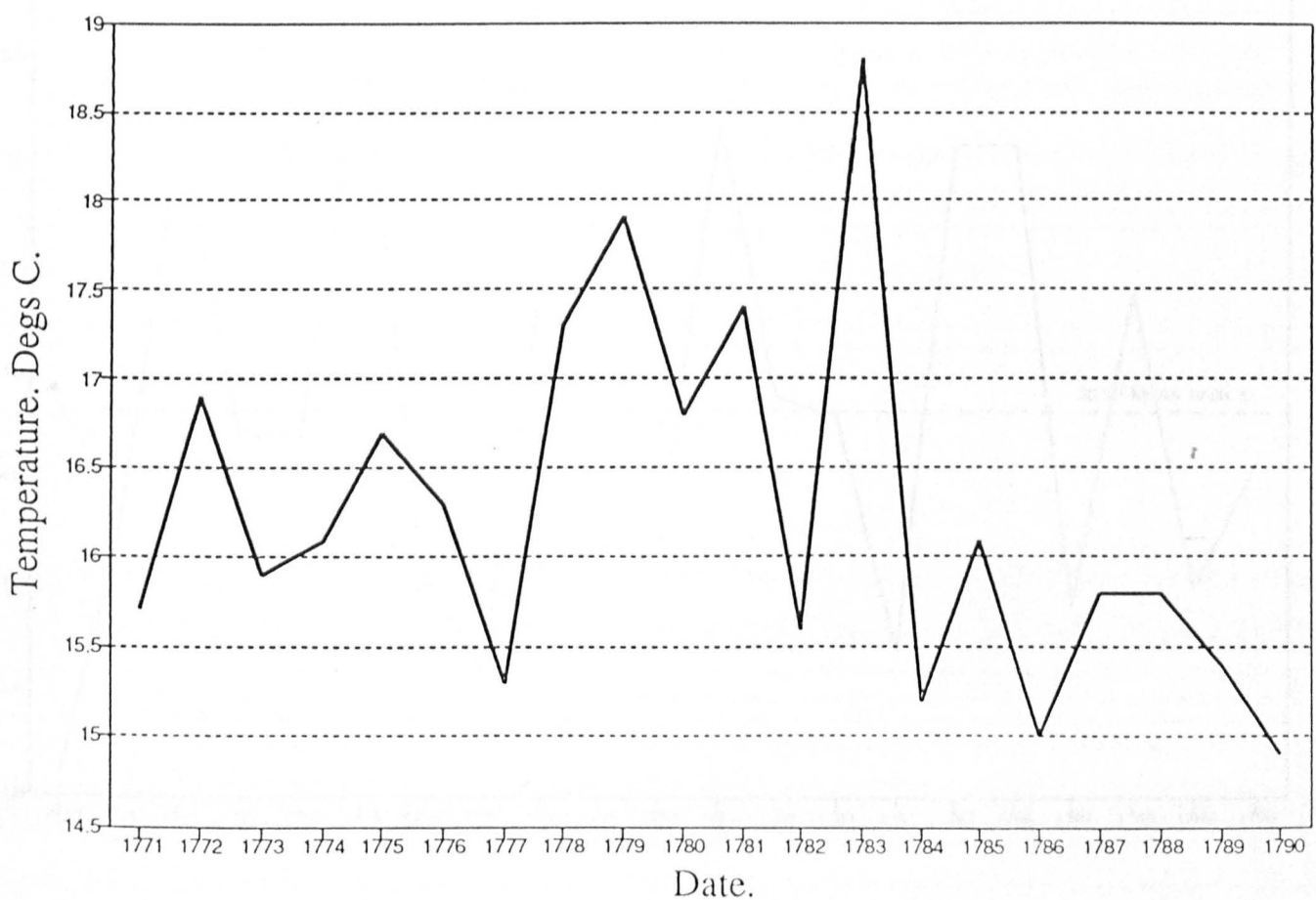


Figure 5.2. July temperatures in Central England 1770-1790.

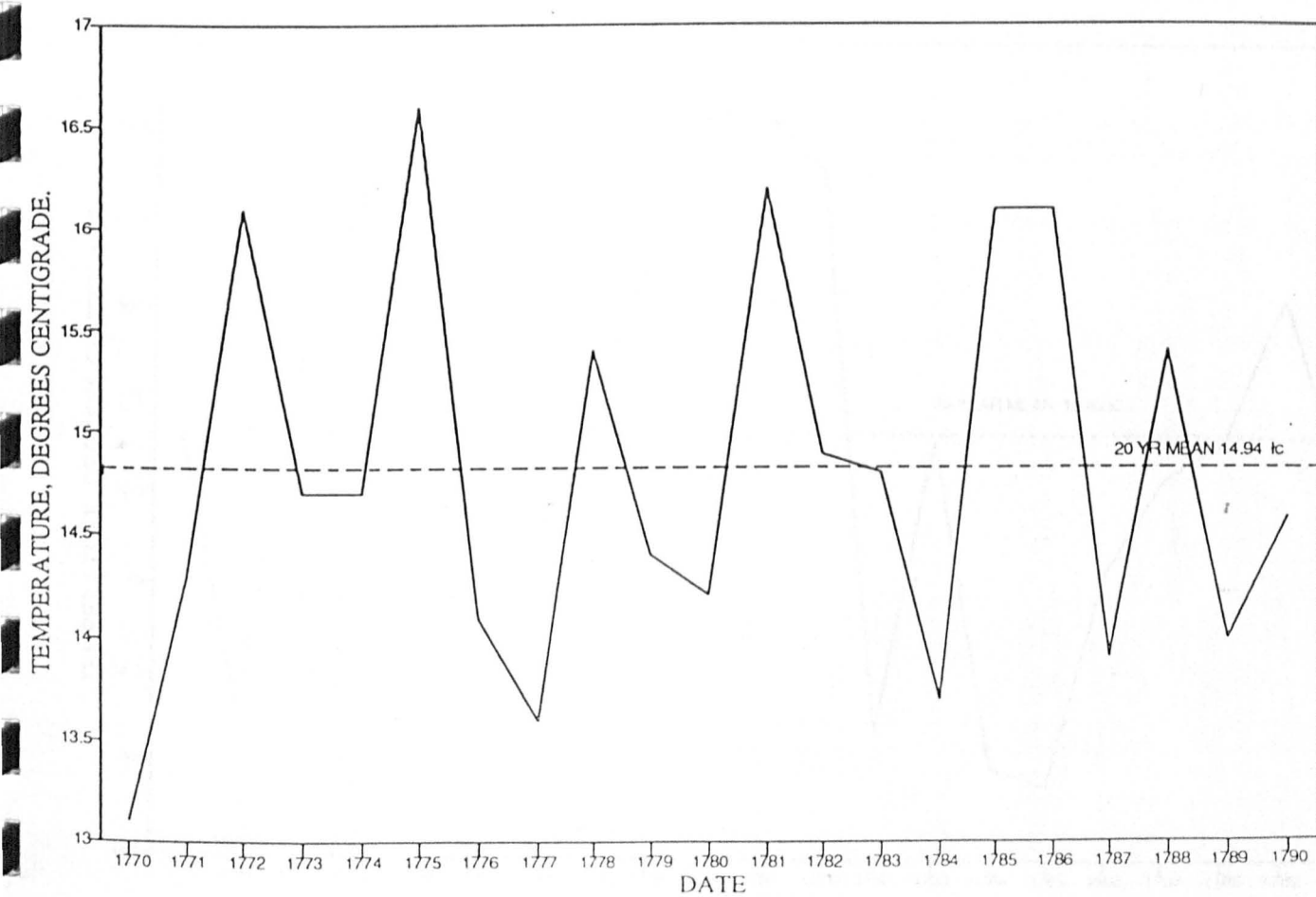


Figure 5.3. June temperatures in Central England 1770-1790.

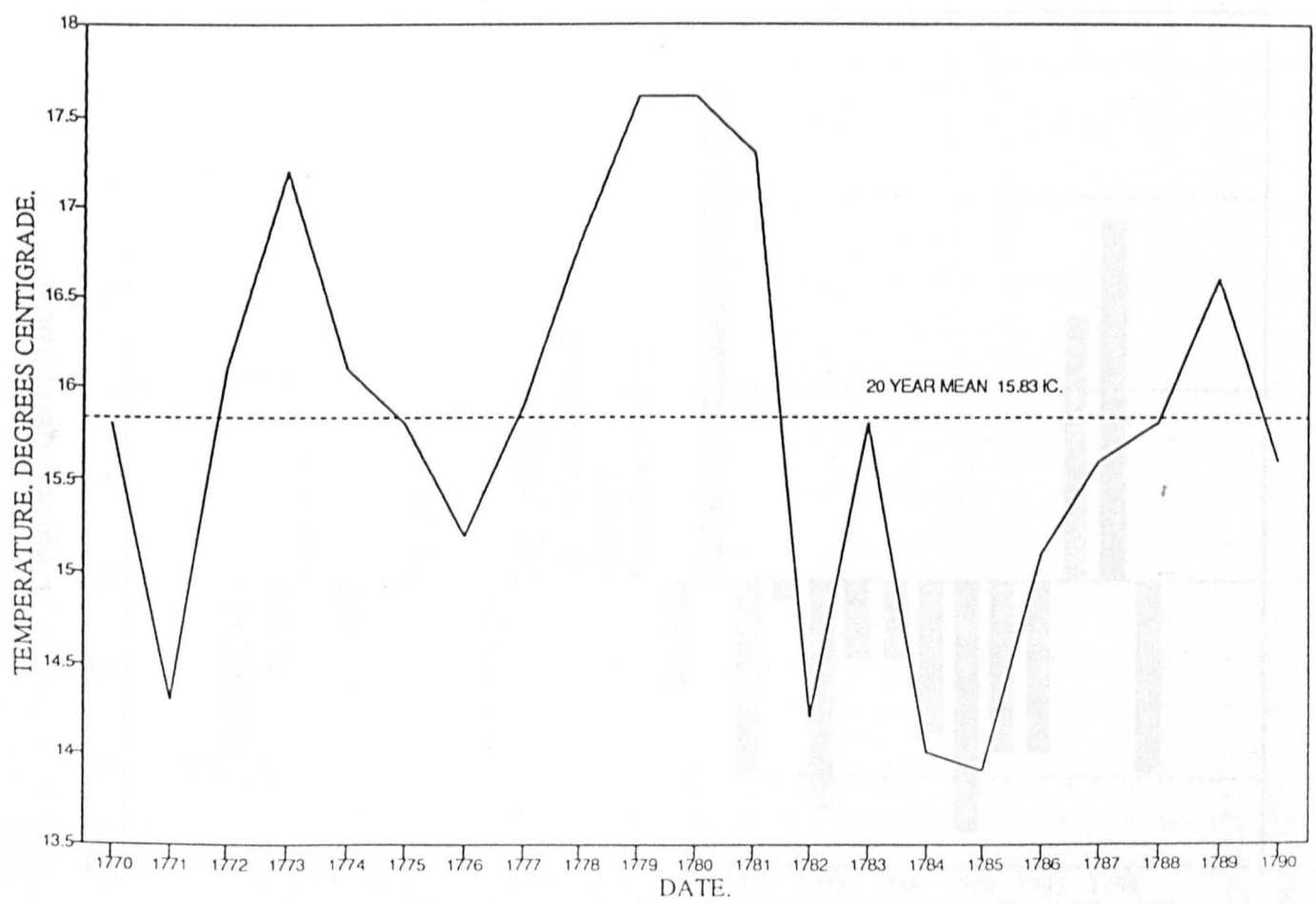


Figure 5.4. August temperatures in Central England 1770-1790.

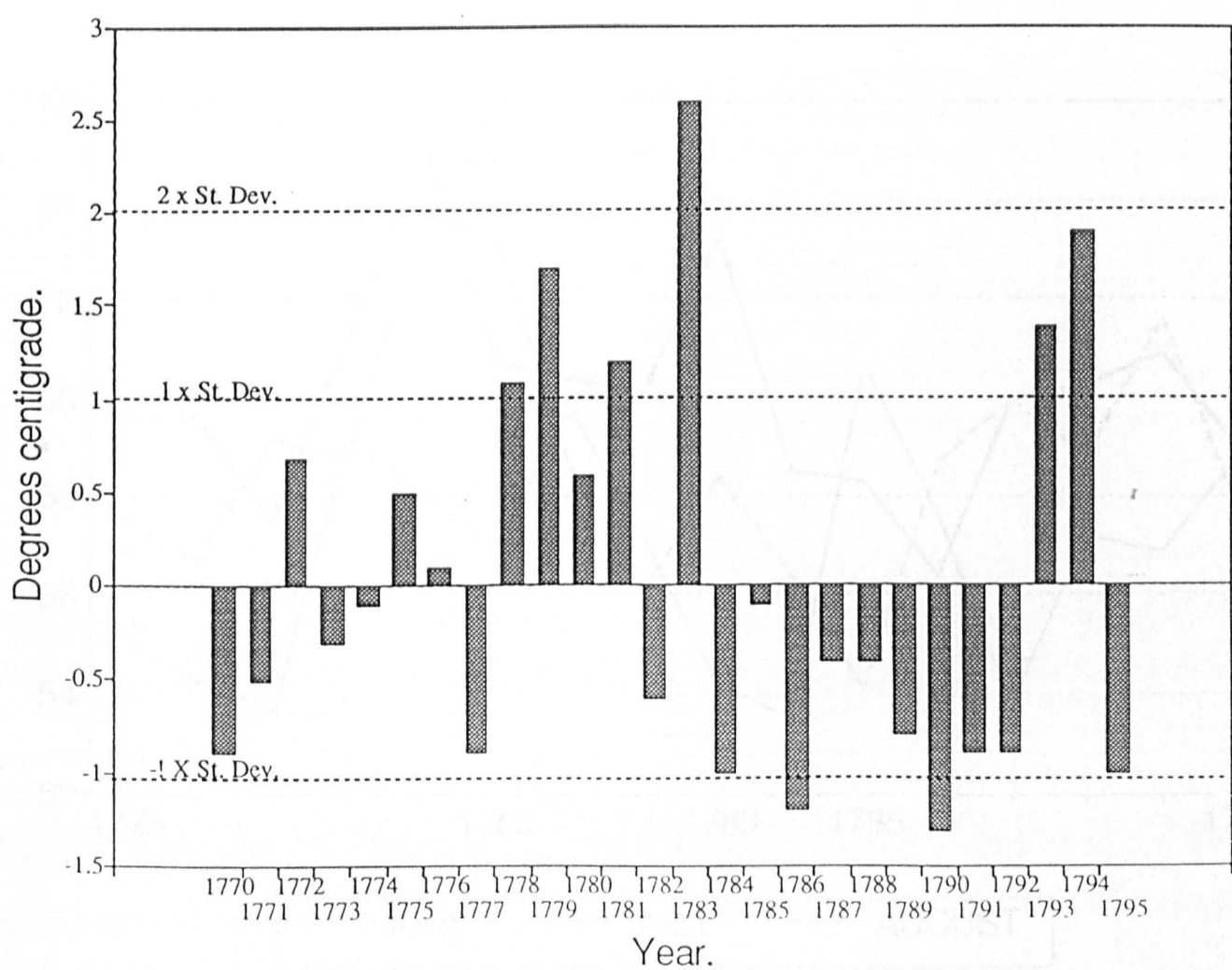


Figure 5.5. Variance of Central England July temperatures in Central England from the mean of 1770-1790.

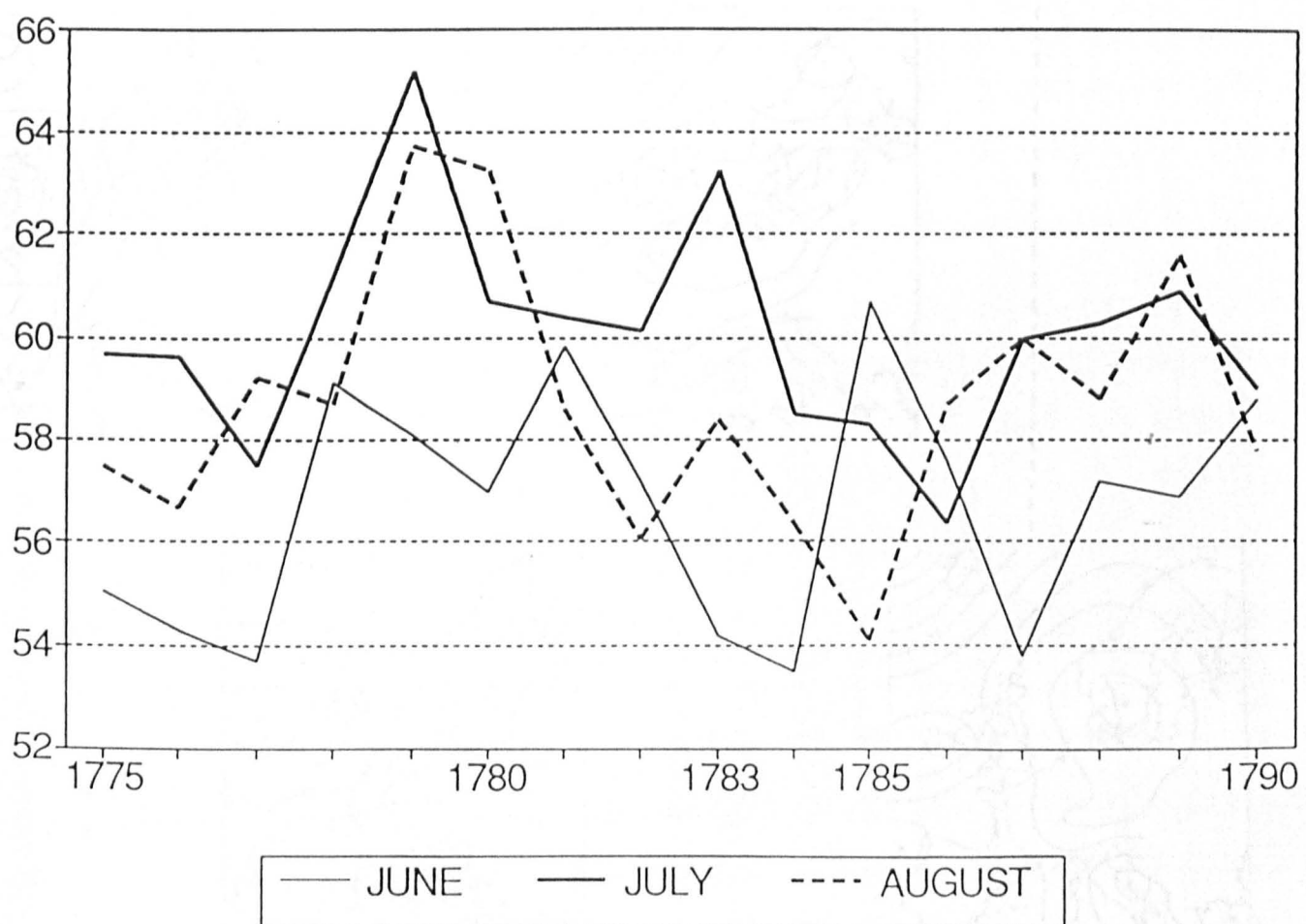


Figure 5.6. Edinburgh summer temperatures 1775-1790.

Mean Temperature 13 June to 5 July 1783
Lydon Hall Meteorological Register

34

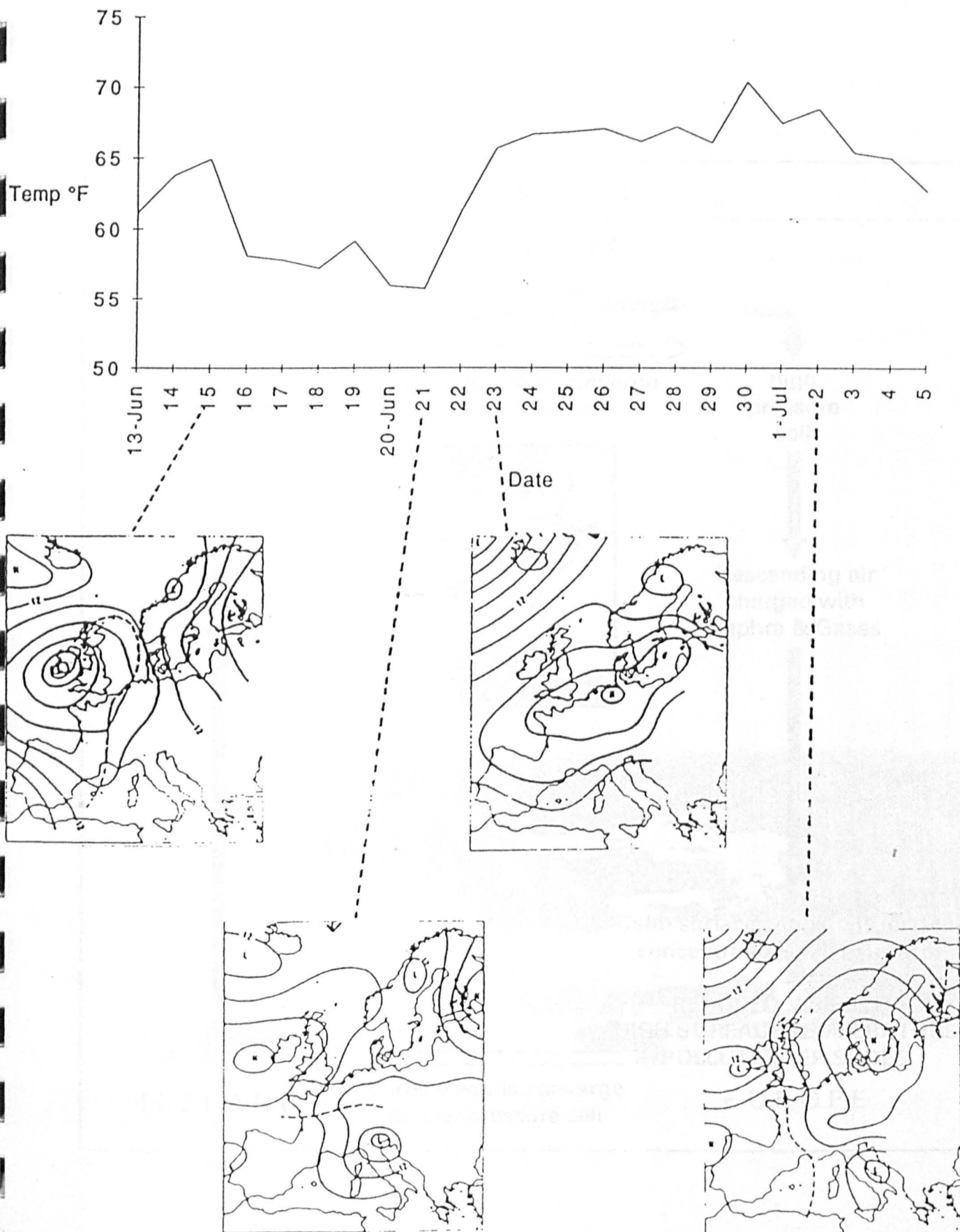


Figure 5.7. Synoptic maps and temperature records: June and July 1783.

Synoptic maps from Kington 1988; temperature from Barker 1783.

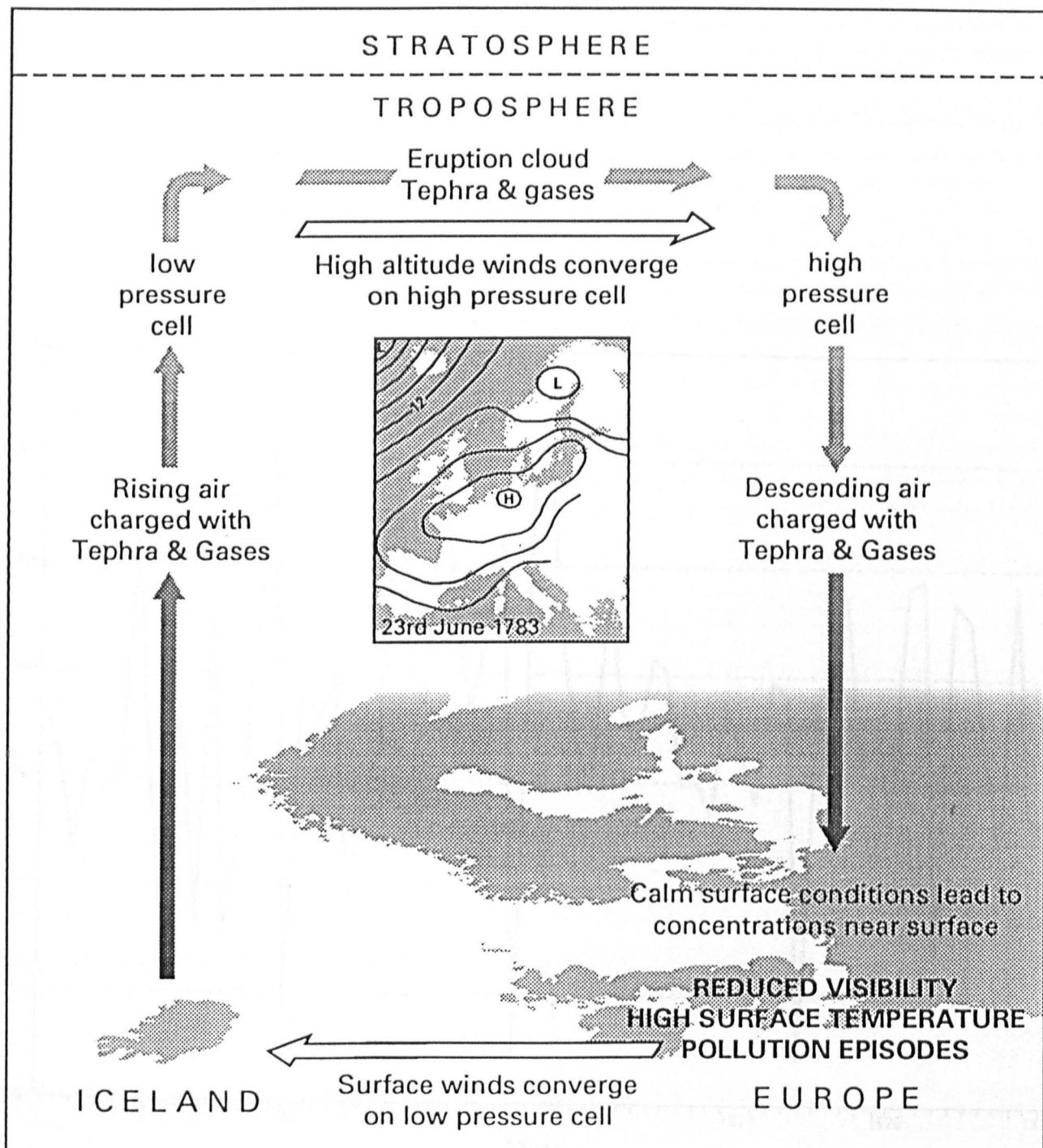


Figure 5.8. Schematic model of the transport of volcanic material to north west Europe in 1783.

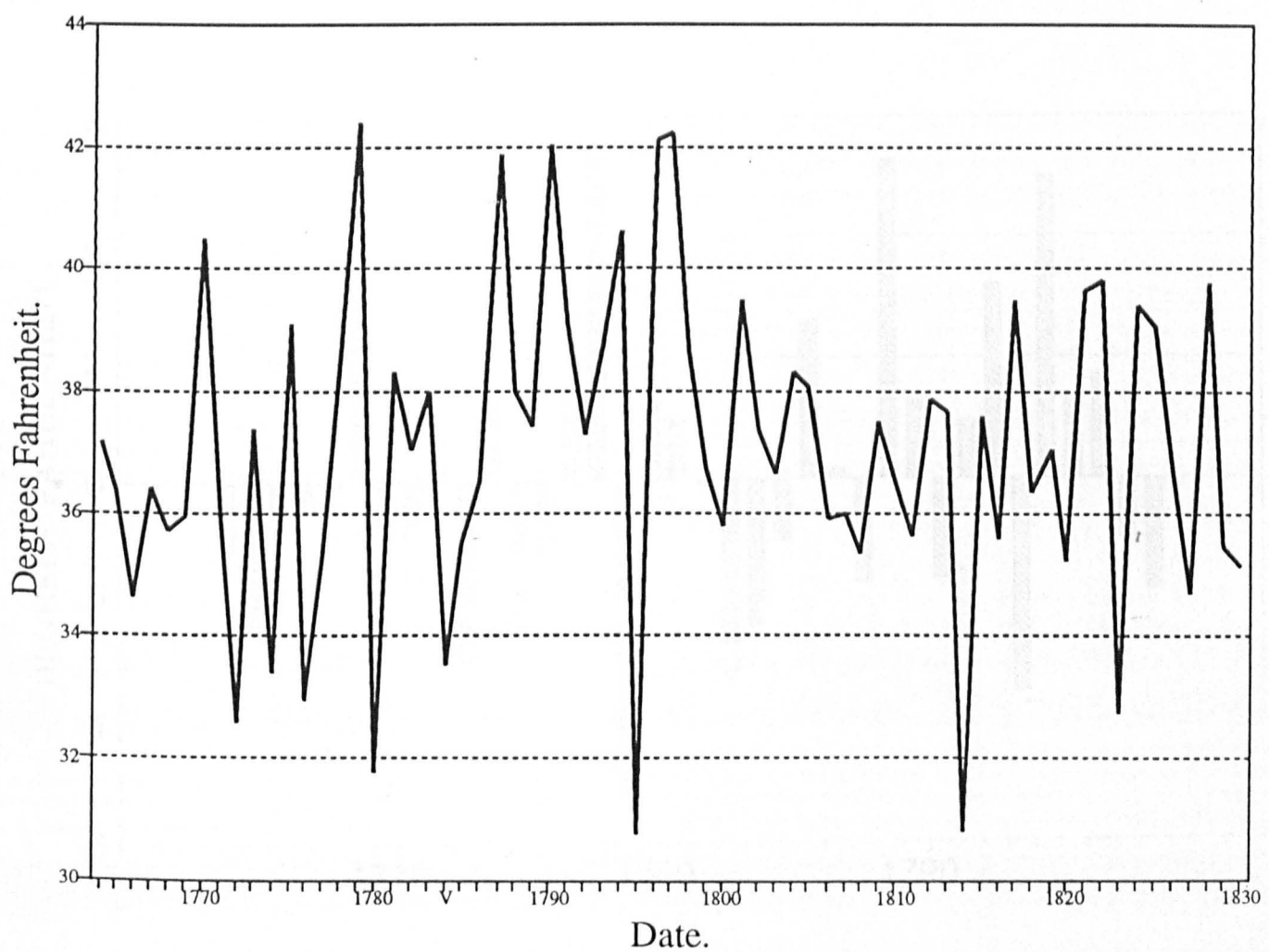


Figure 5.9. Winter temperatures in Edinburgh 1764-1830.

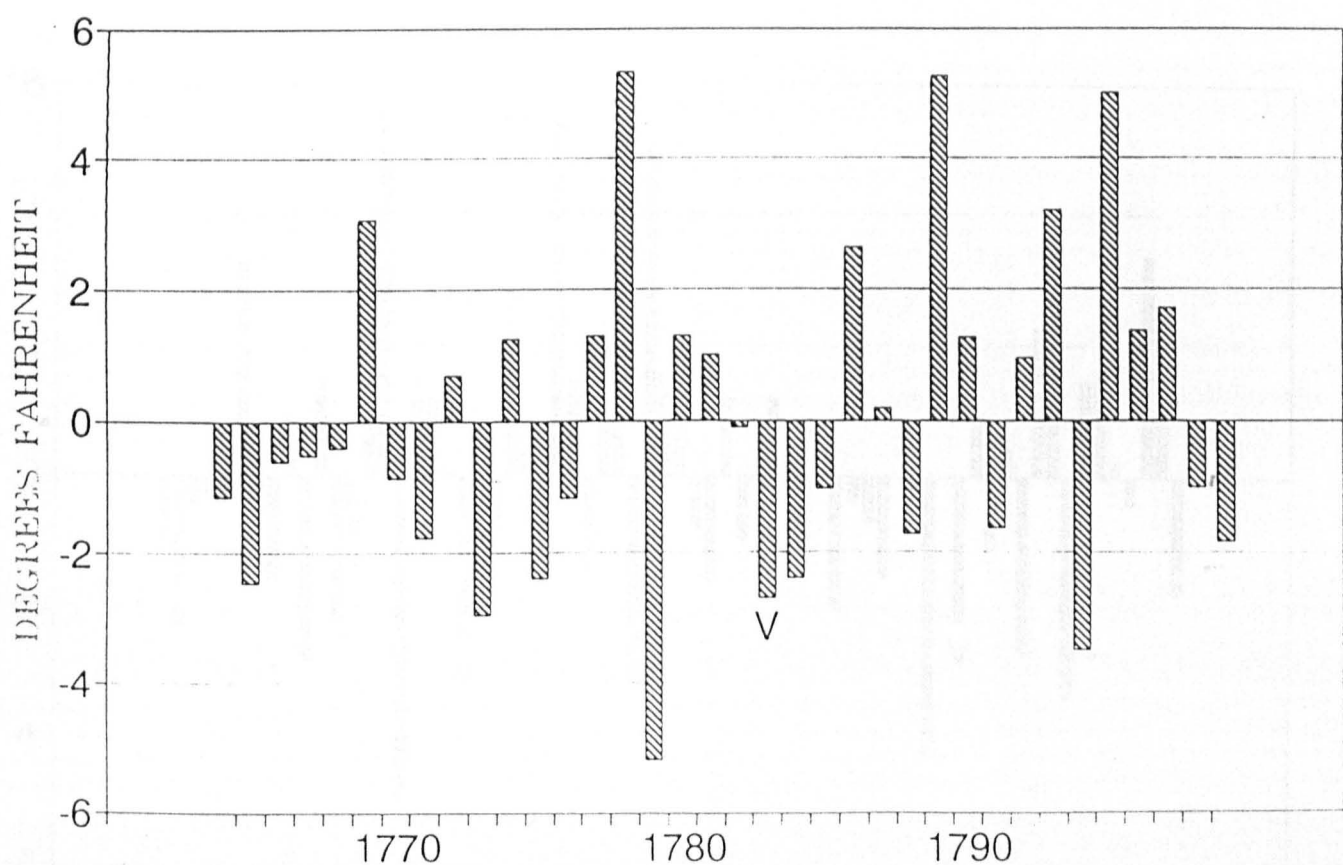


Figure 5.10. Variation of Edinburgh winter temperatures from the thirty four year mean, 1764-1800.

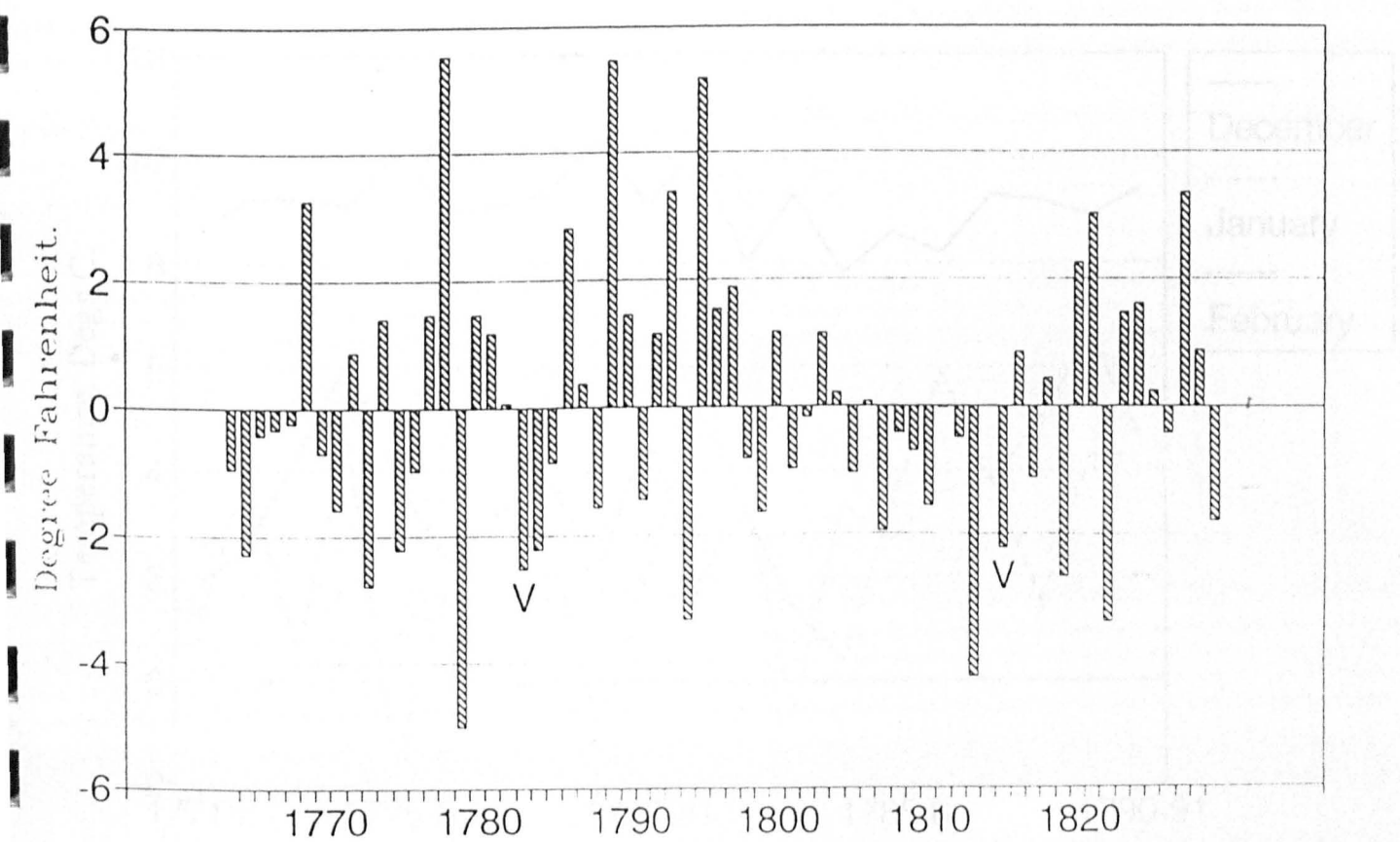


Figure 5.11. Variation of Edinburgh winter temperatures from the Sixty-six year mean,
1764-1830.

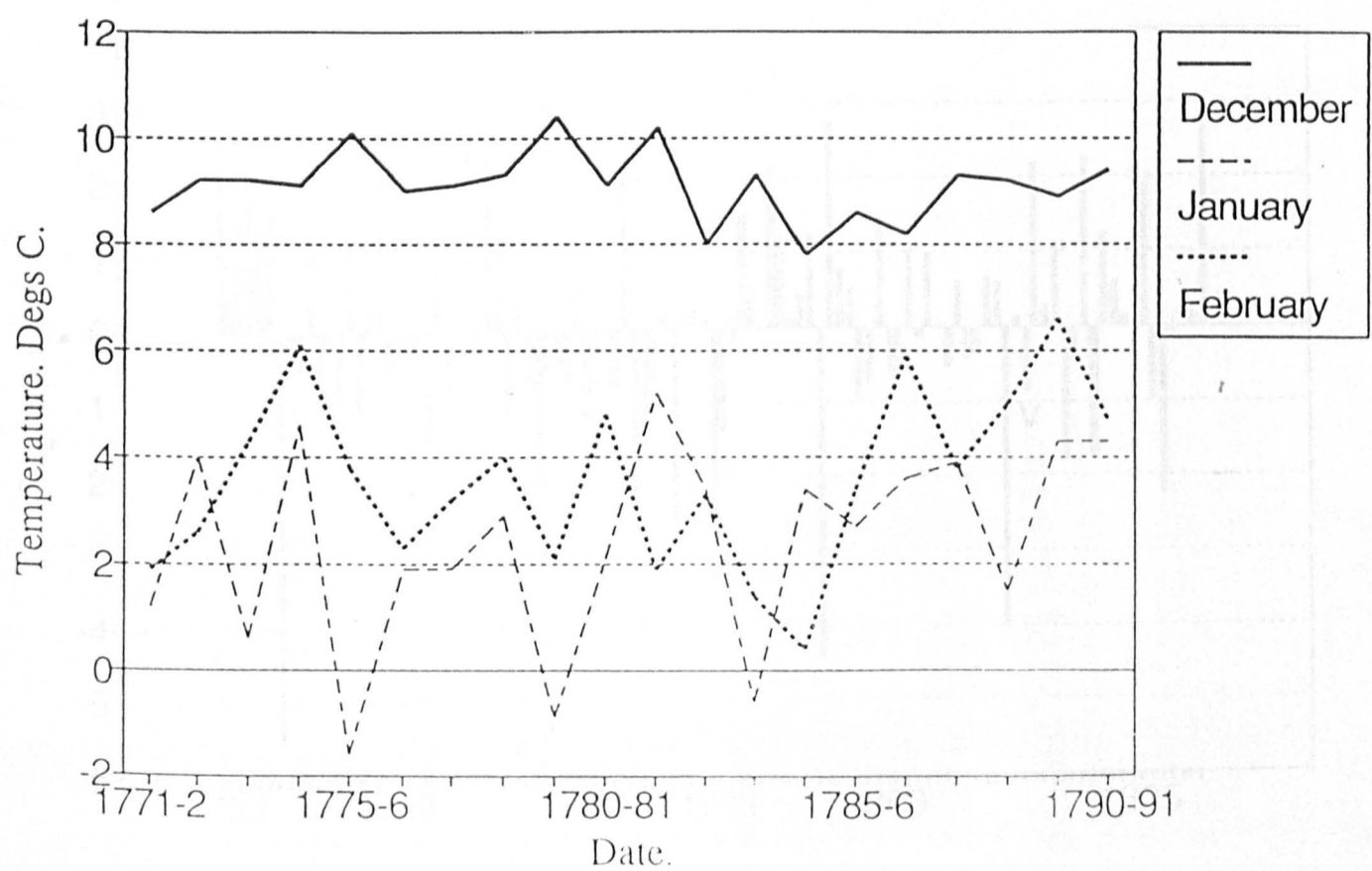


Figure 5.12. Winter temperatures in Central England, 1771-1791.

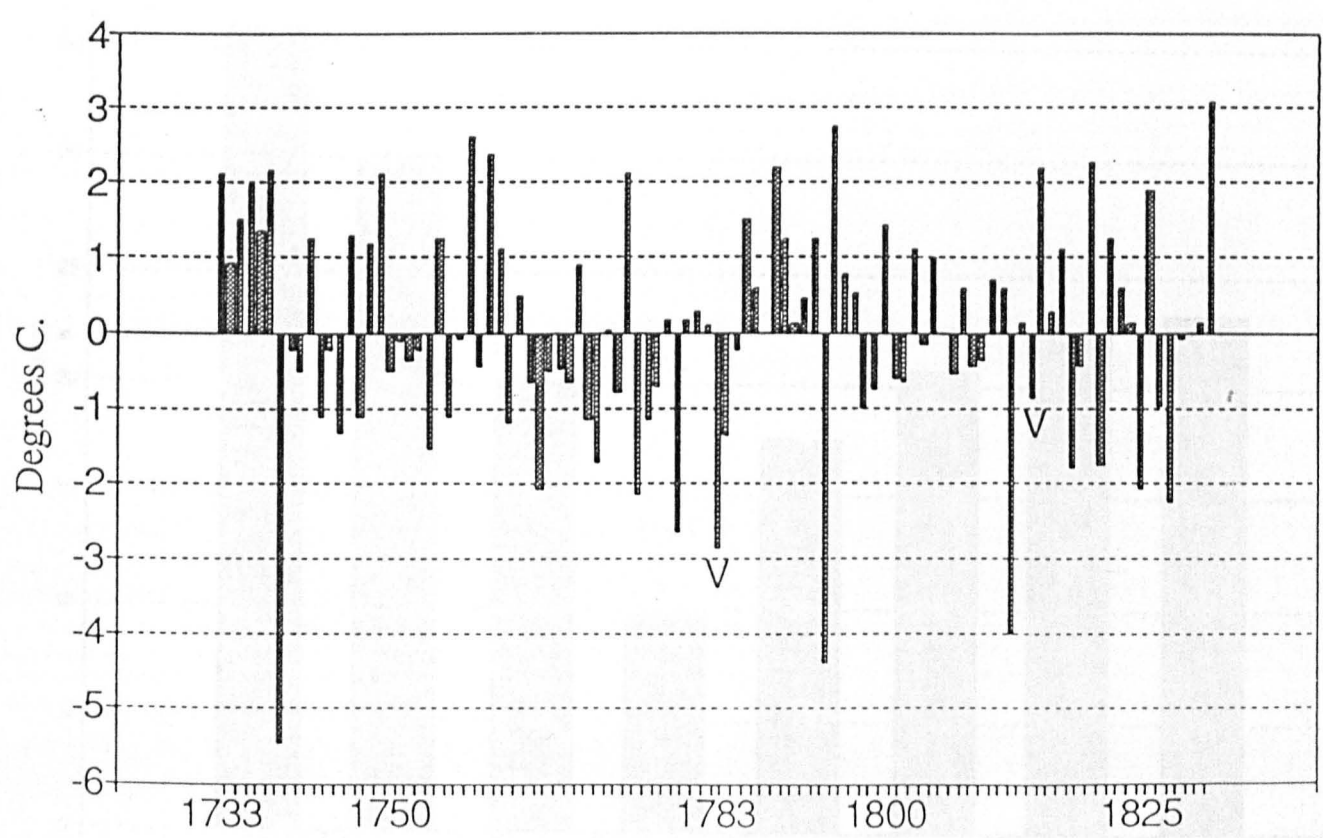


Figure 5.13. Variation of winter temperatures from the (1733-1833) 100 year mean.

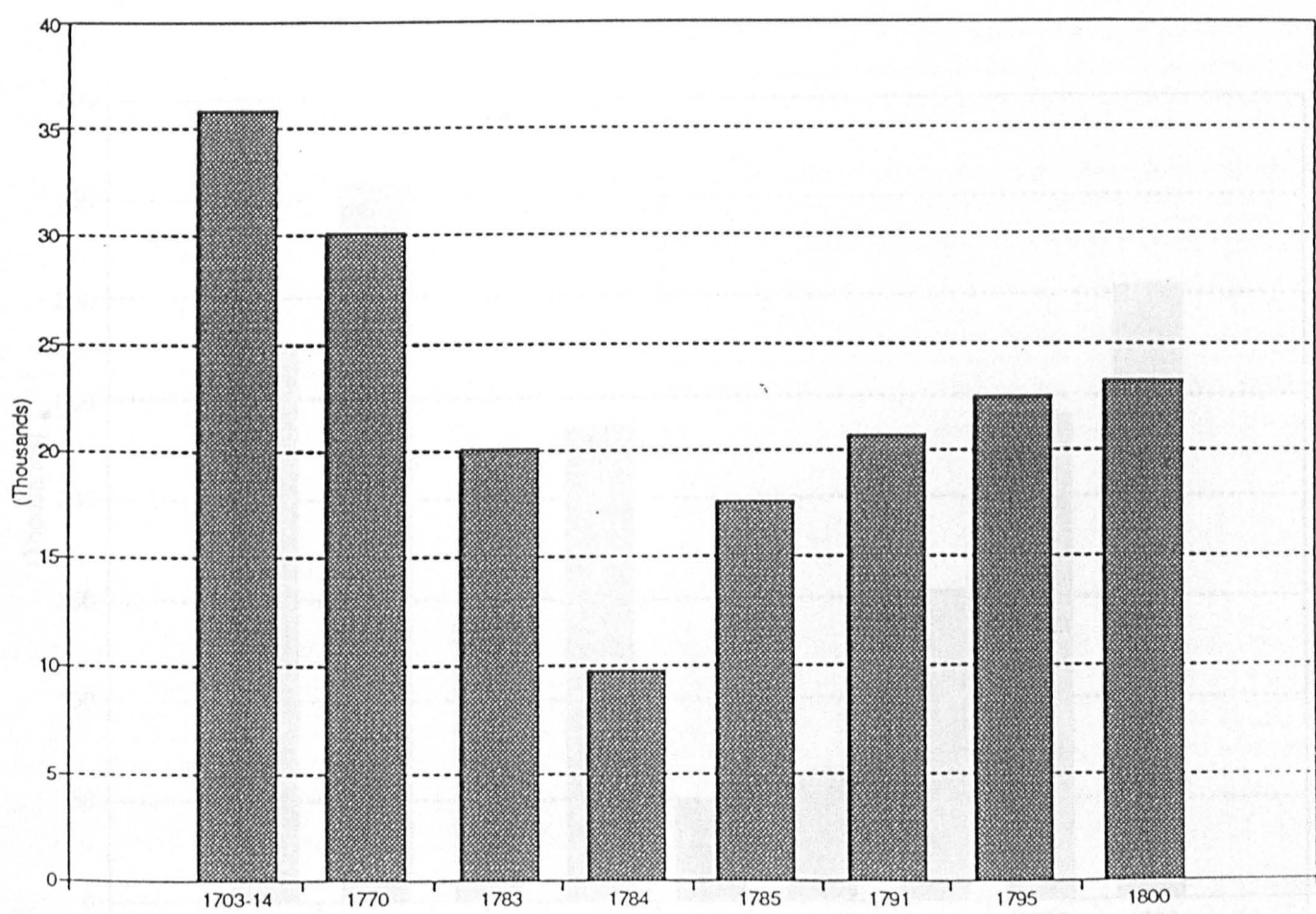


Figure 6.1. Cattle mortality in Iceland. Data from Gerrard [1991]

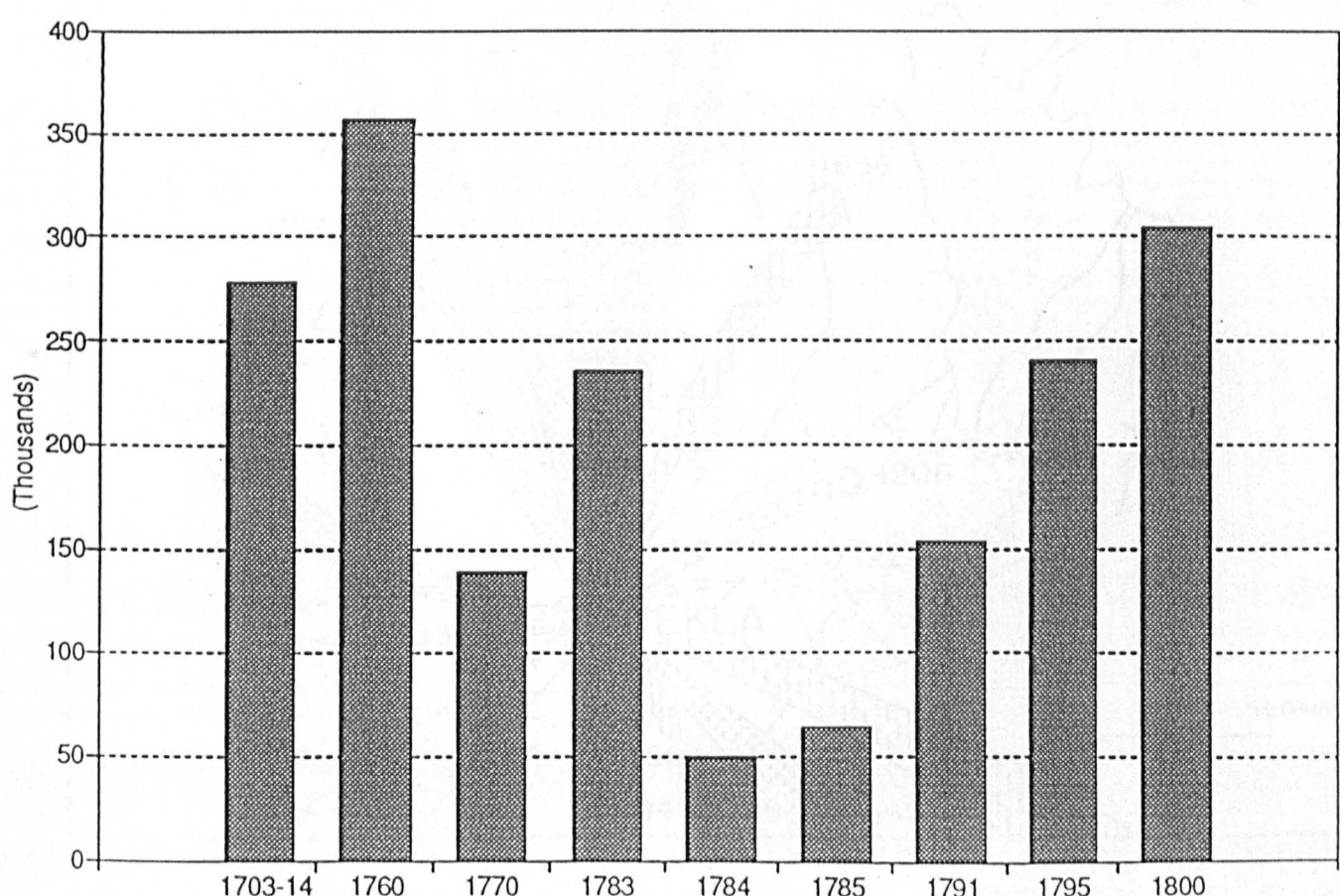


Figure 6.2. Sheep mortality in Iceland. Data from Gerrard [1991]

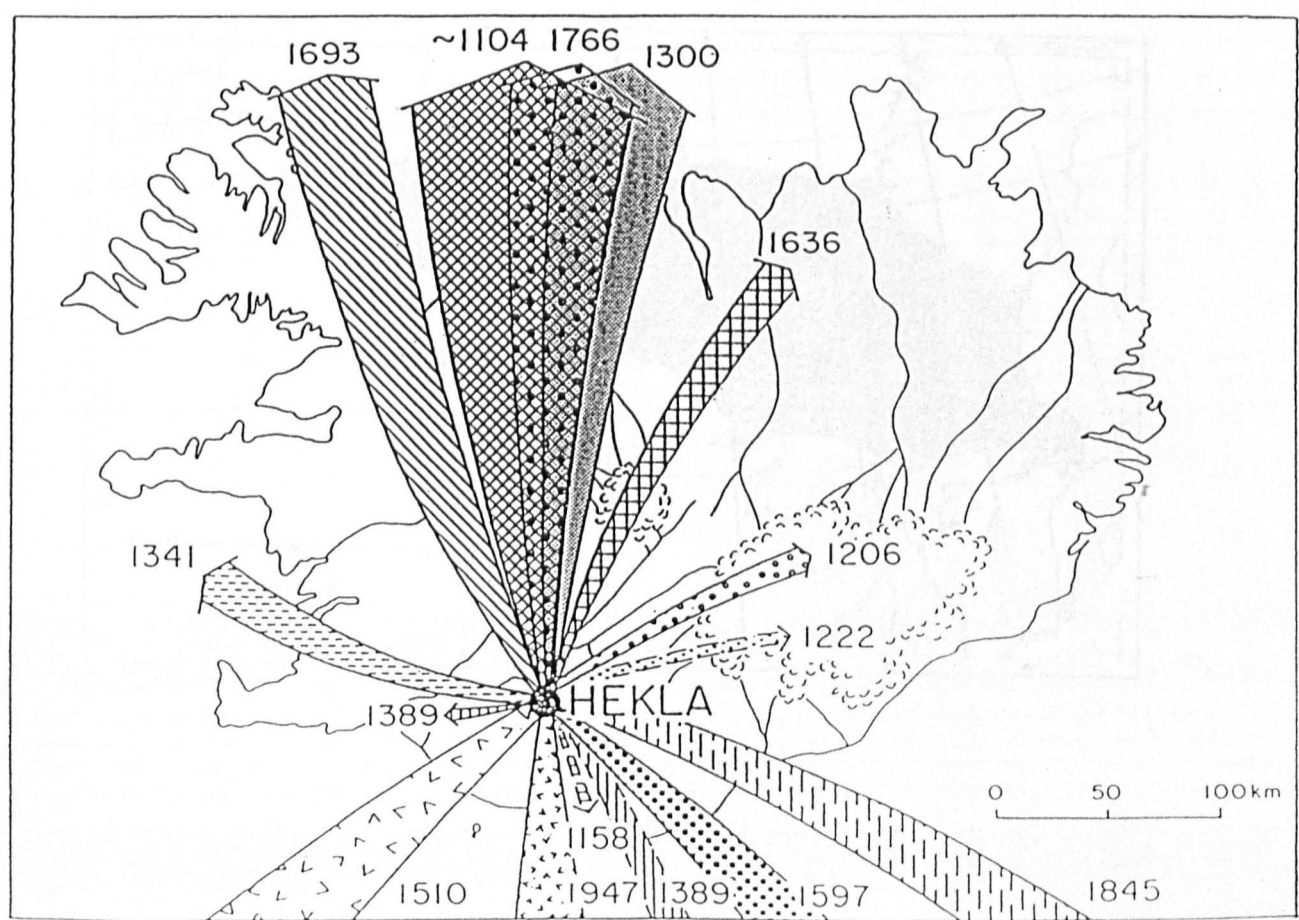


Figure 6.3. Transport of volcanic material from Iceland. From Thórarinsson [1967].



IMAGING SERVICES NORTH

Boston Spa, Wetherby
West Yorkshire, LS23 7BQ
www.bl.uk

PAGE NUMBERING AS
ORIGINAL

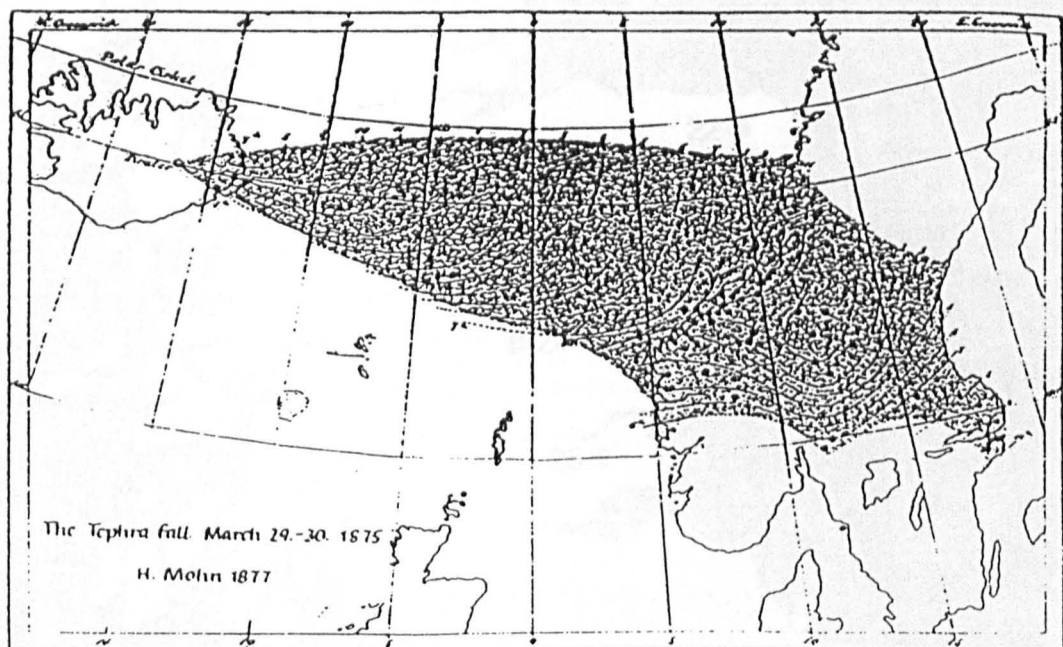


Figure 6.4b. Ash fall from the Askja eruption 1875. From Persson [1971].

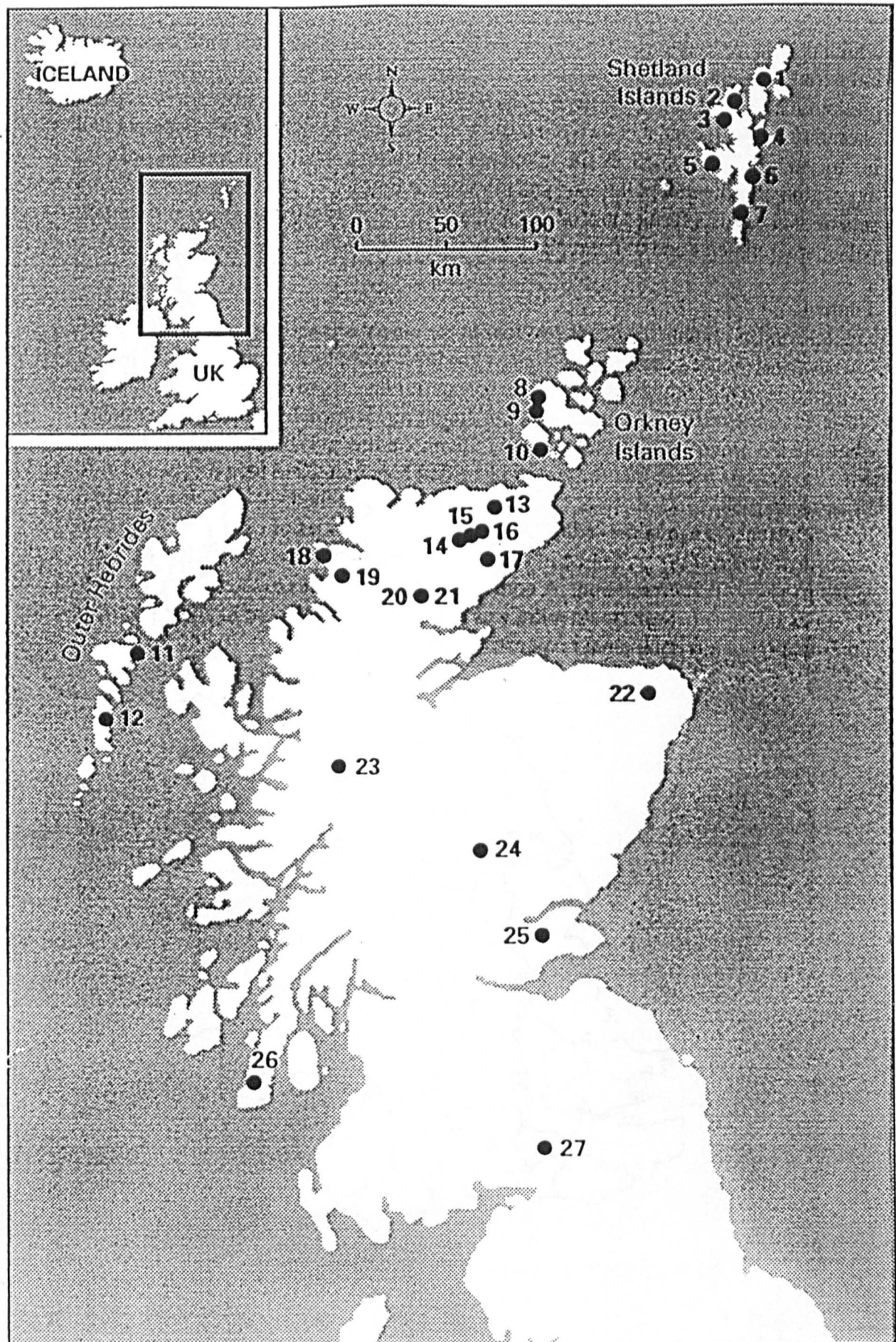


Figure 6.5. Tephra fall locations in Britain. Various sources.



Figure 6.6 Locations Mentioned in the text. © Department of History.

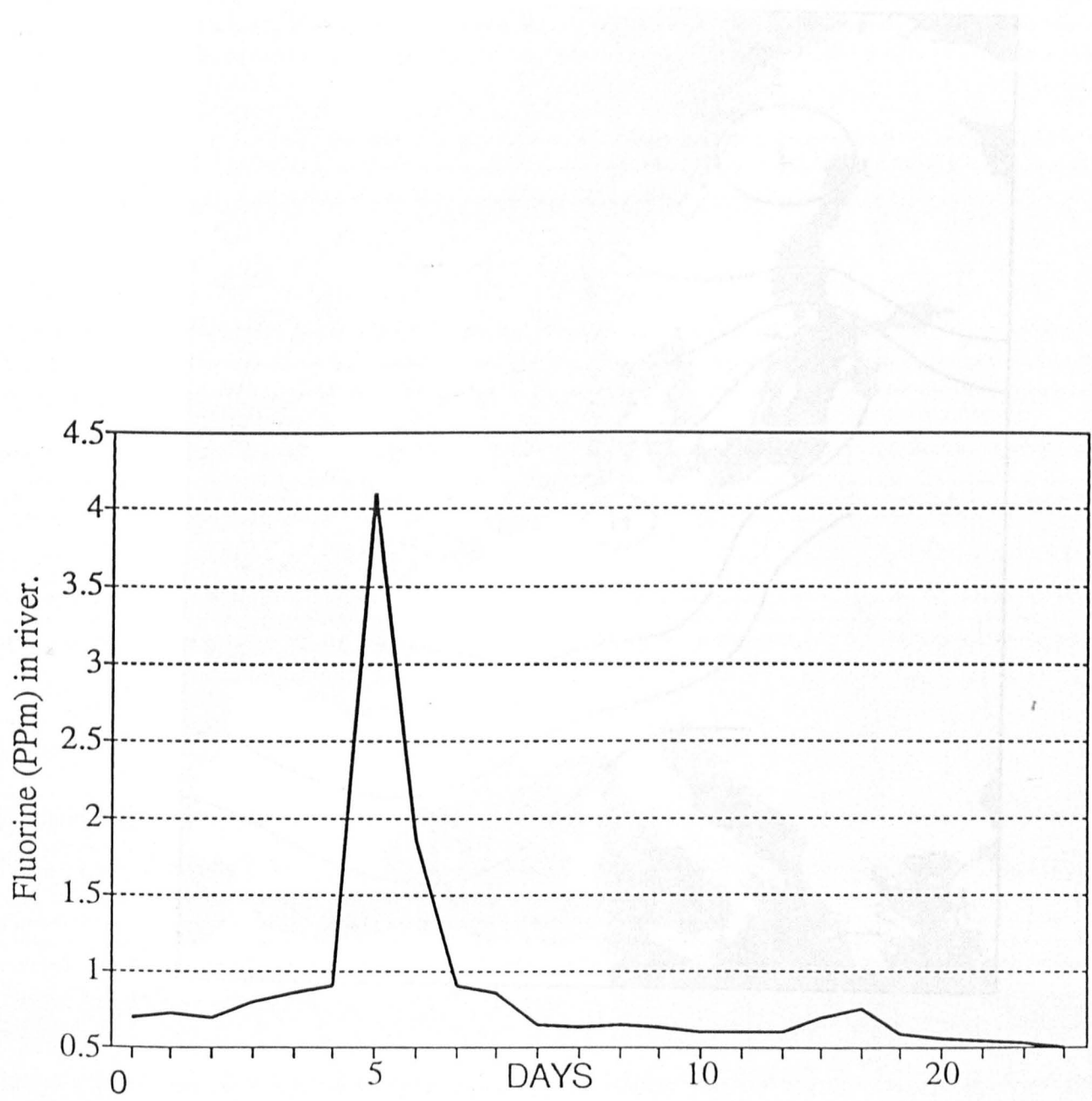


Figure 6.7 Fluorine concentrations in the River Ytri-Raga following the 1991 eruption of Hekla.

Data from Gudmundsson *et al.* [1992].

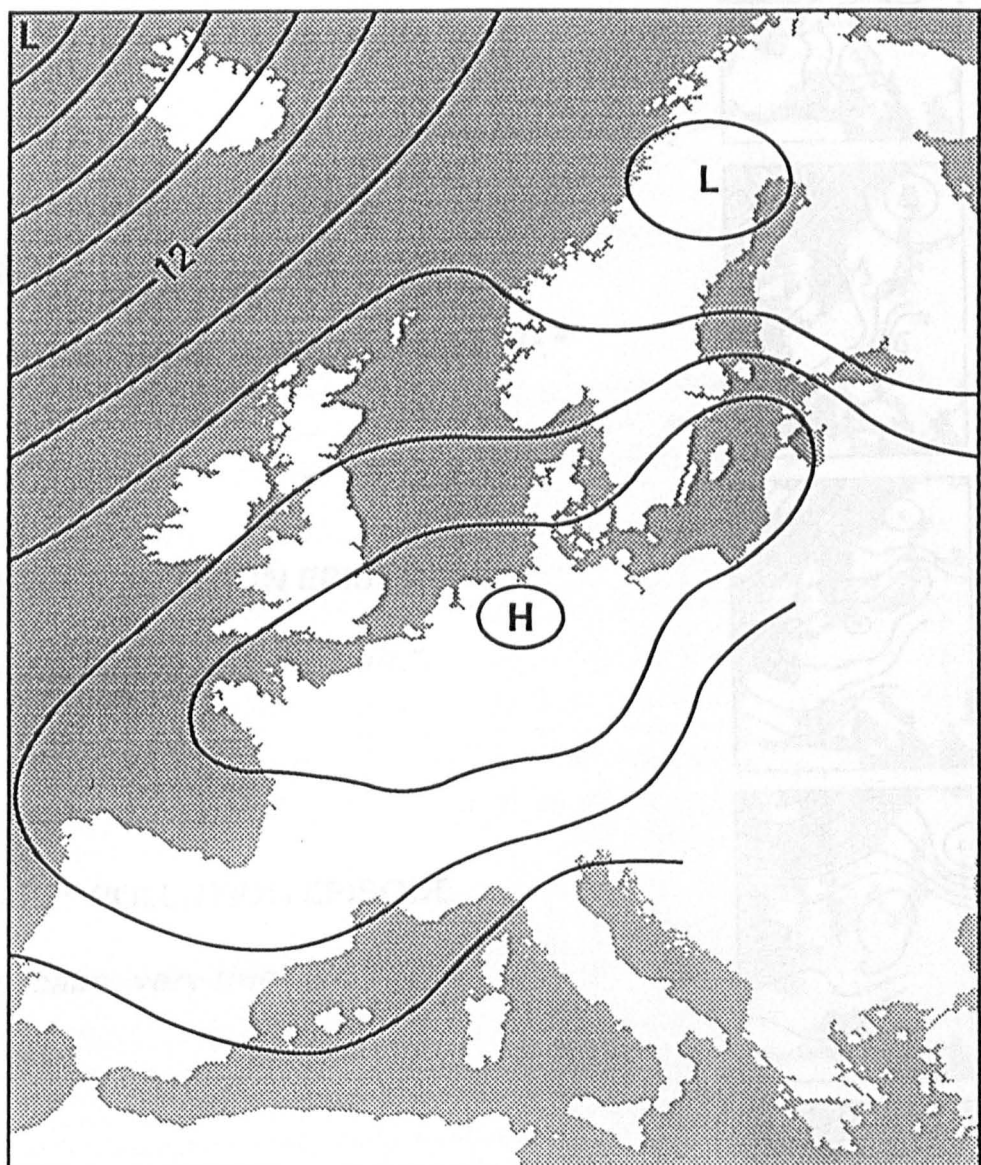


Figure 6.8. Synoptic map June 23rd 1783. From Kington [1988].

June 20th :

"Chiefly cloudy, calm and sometimes wetting."



June 21st :

"Cloudy and calm, thick moist air."



June 22nd :

"Hot, some sunshine, calm and thick air."



June 23rd : POLLUTION EPISODE

"Hot, calm. Sunny and thick air."



June 24th : POLLUTION EPISODE

"Sunny, calm, very thick air."



June 25th : POLLUTION EPISODE

"Hot, calm, very thick smokey air."



Figure 6.9. The association between atmospheric circulation and volcanic pollution.

Weather Observations From Barker 1783. Synoptic maps from Kington 1988.

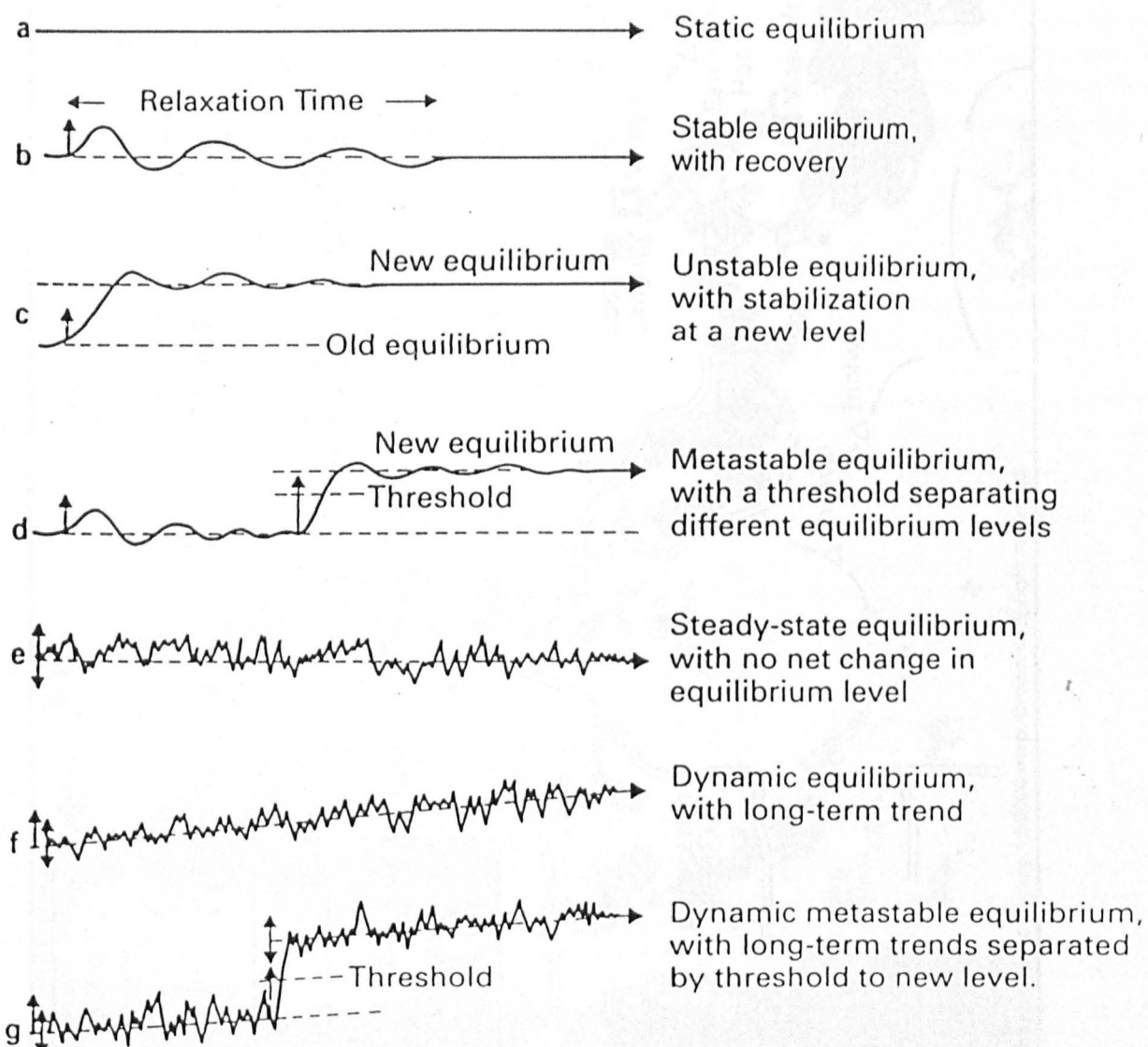
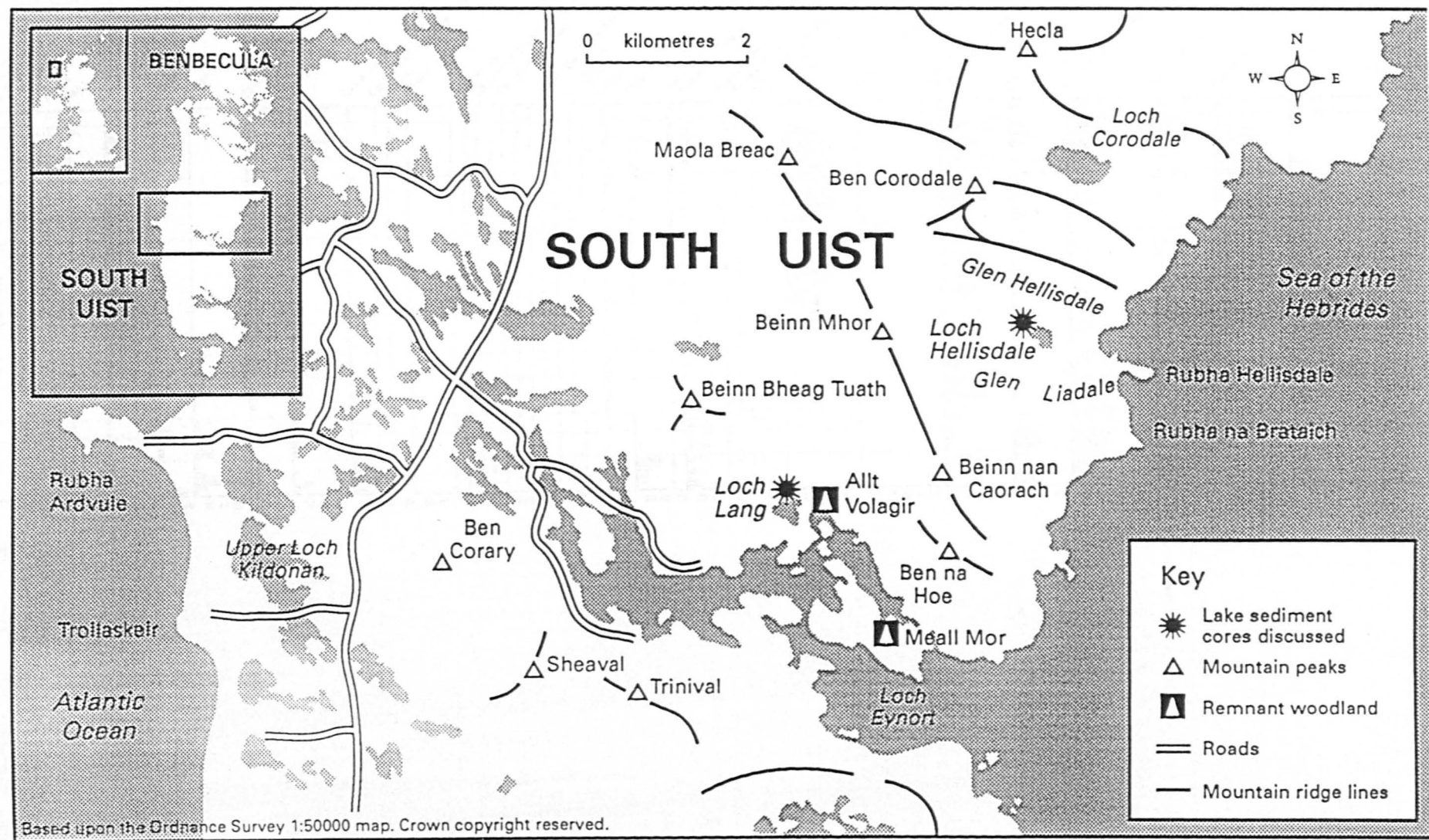


Figure 7.1. Theoretical framework for the interpretation of EDMA results. After Butzer [1982].

Figure 7.2. Location map. Loch Hellisdale.



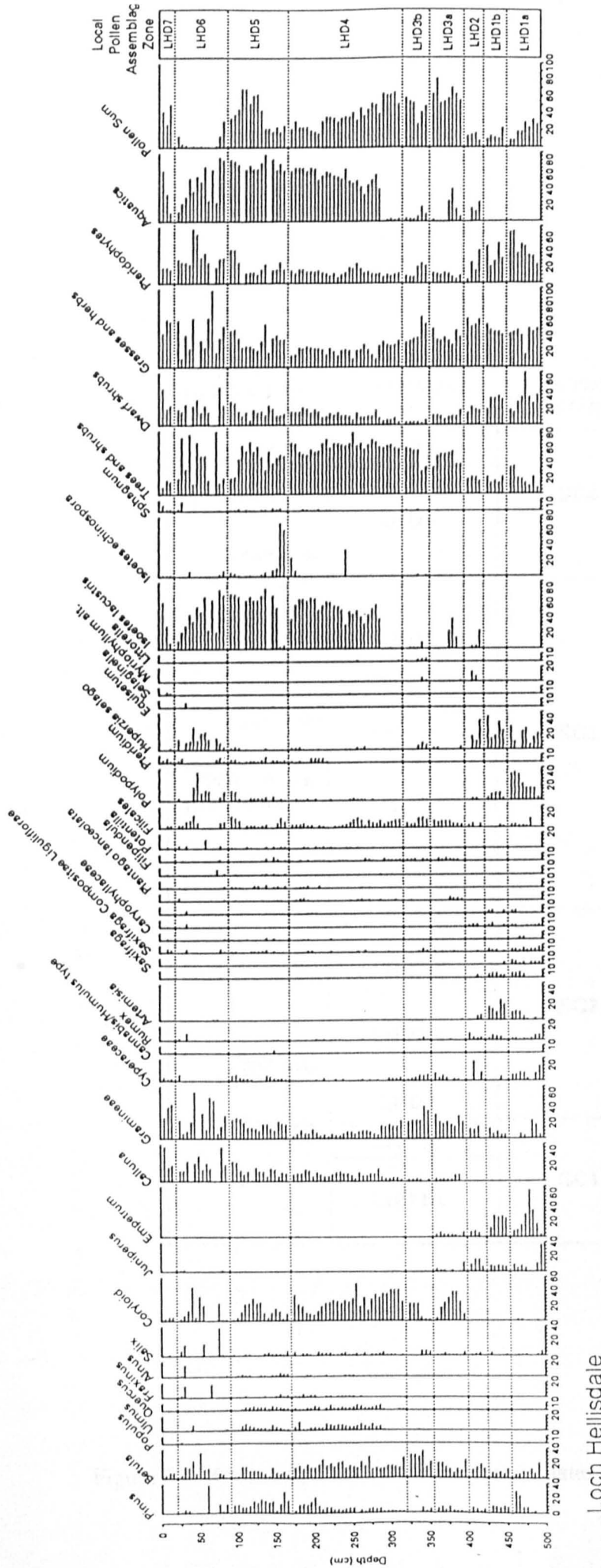


Figure 7.3. Palnology of the Loch Hellisdale. After Brayshaw [1992] and Kent *et al.* [in press].

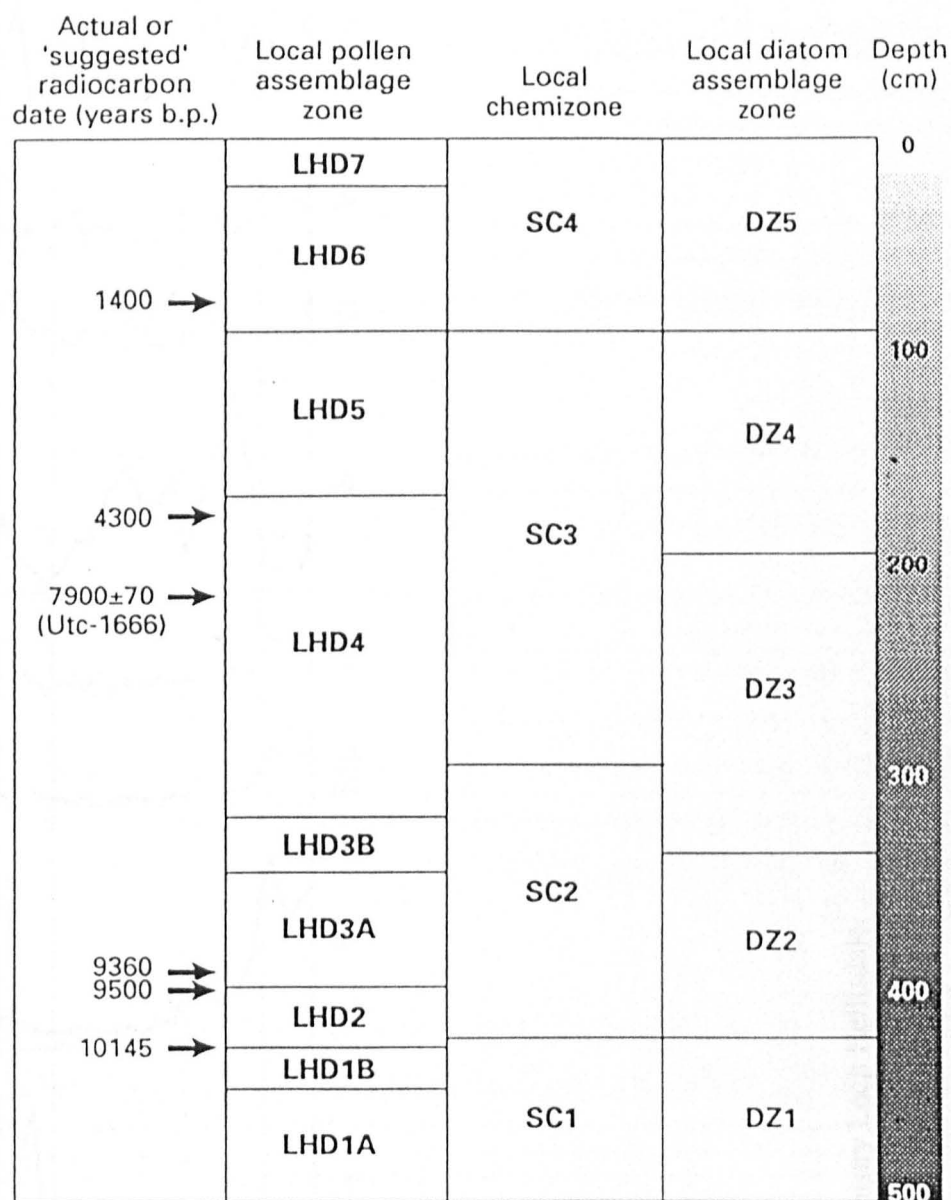
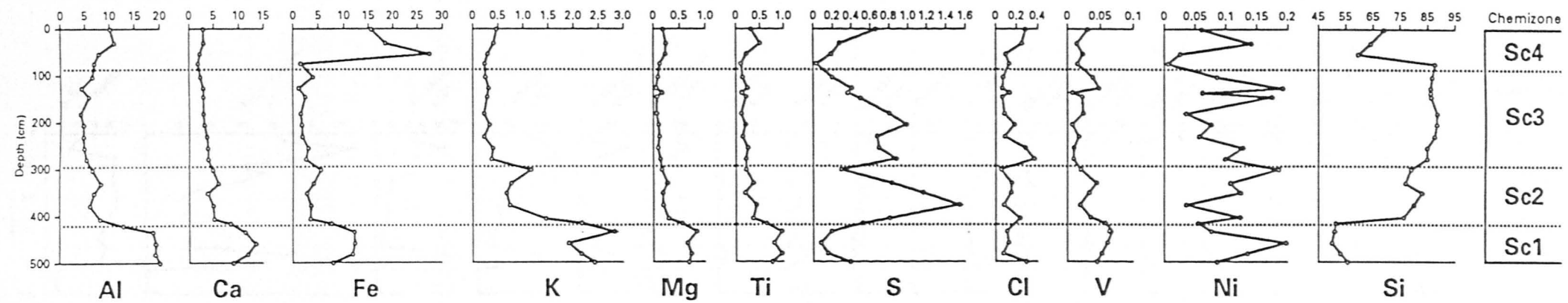


Figure 7.4. Correlation between radiocarbon dates and palaeoenvironmental zones.



Loch Hellisdale

Figure 7.5. Sediment geochemistry Loch Hellisdale.

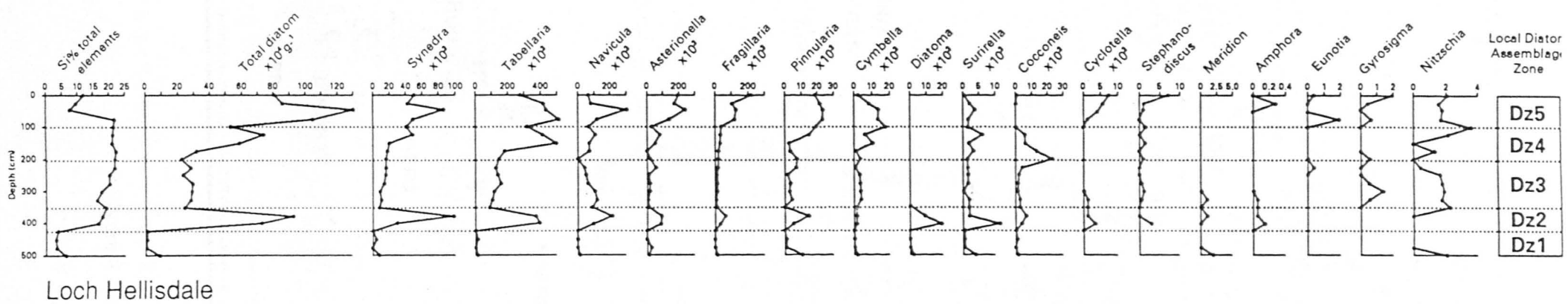


Figure 7.6. Diatom assemblage and Silicon in Loch Hellisdale.

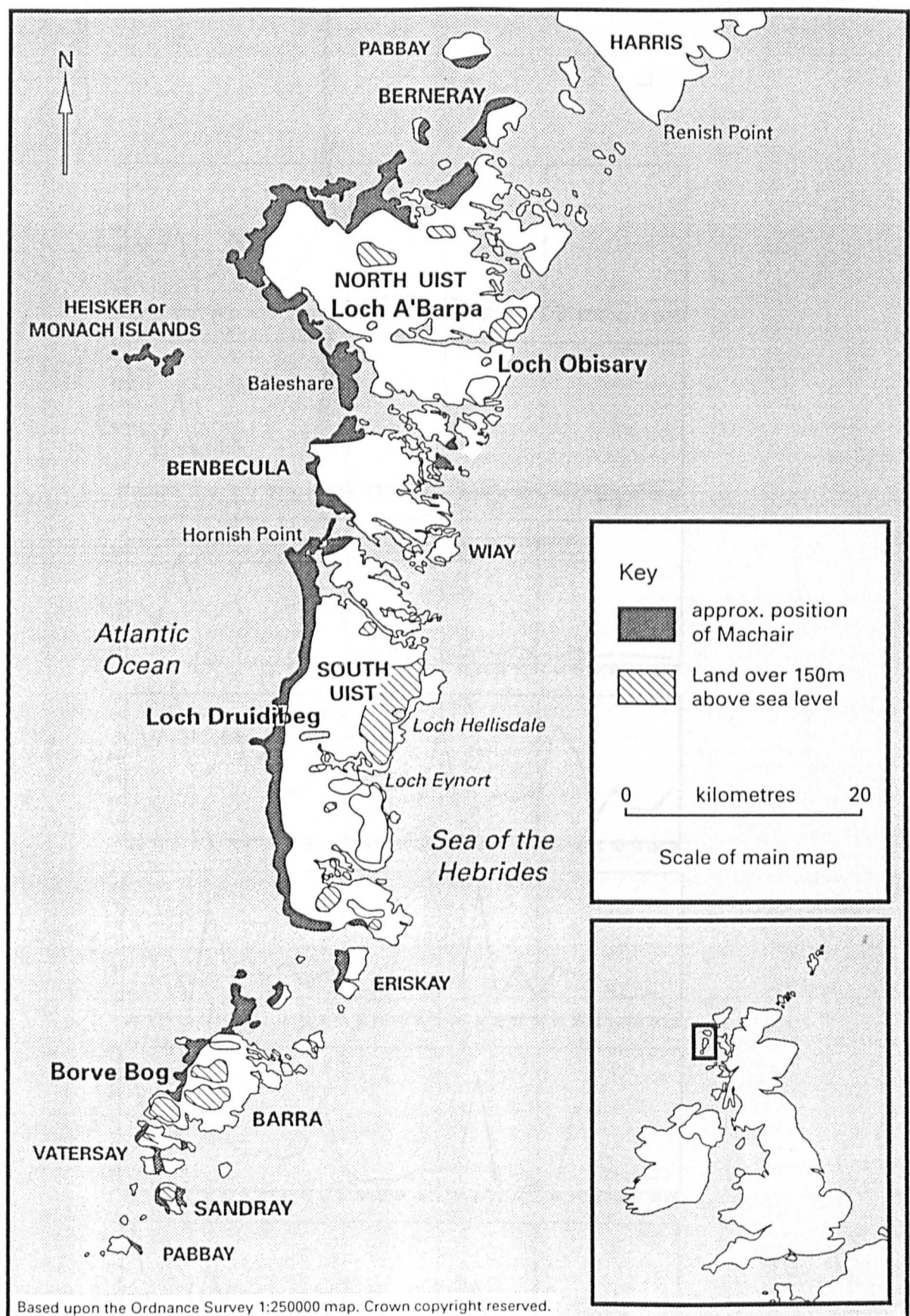


Figure 8.1. Sample locations

Chemizone.

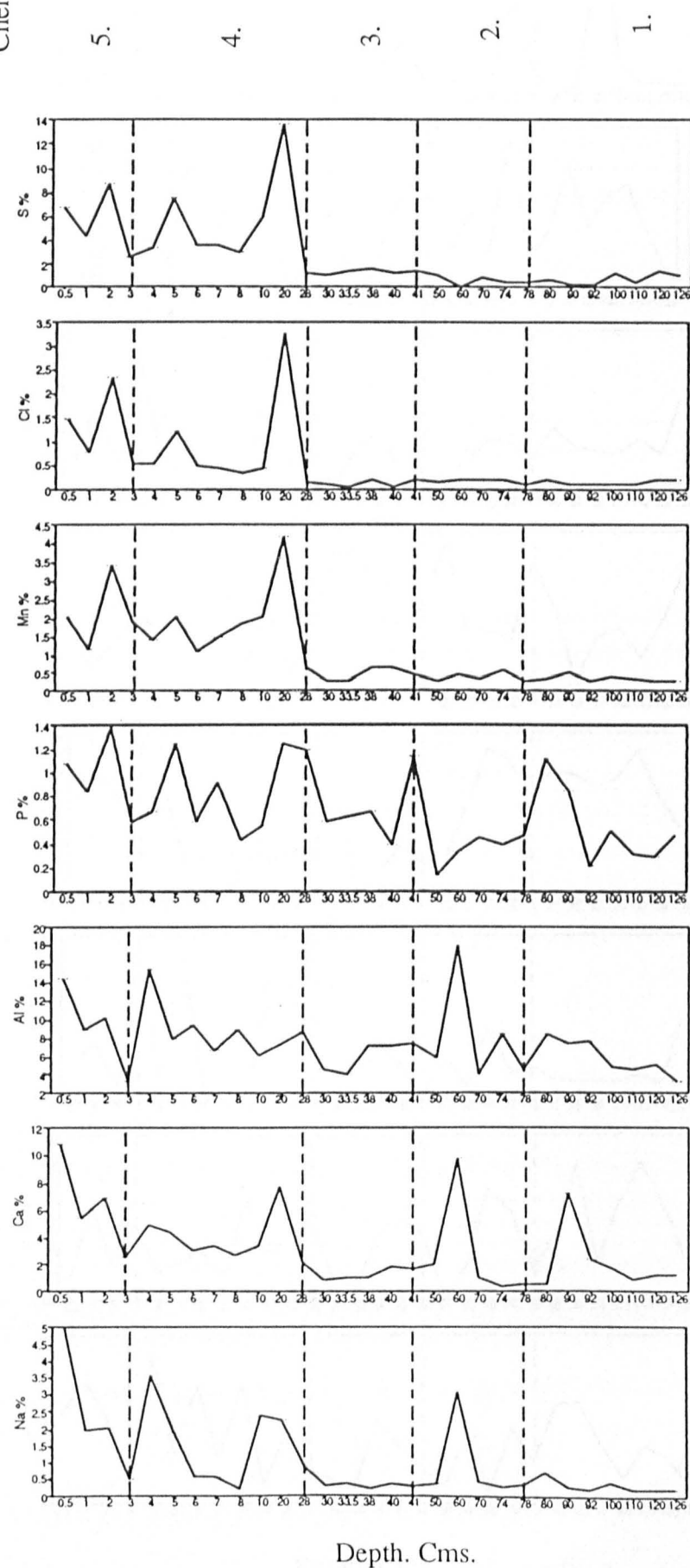
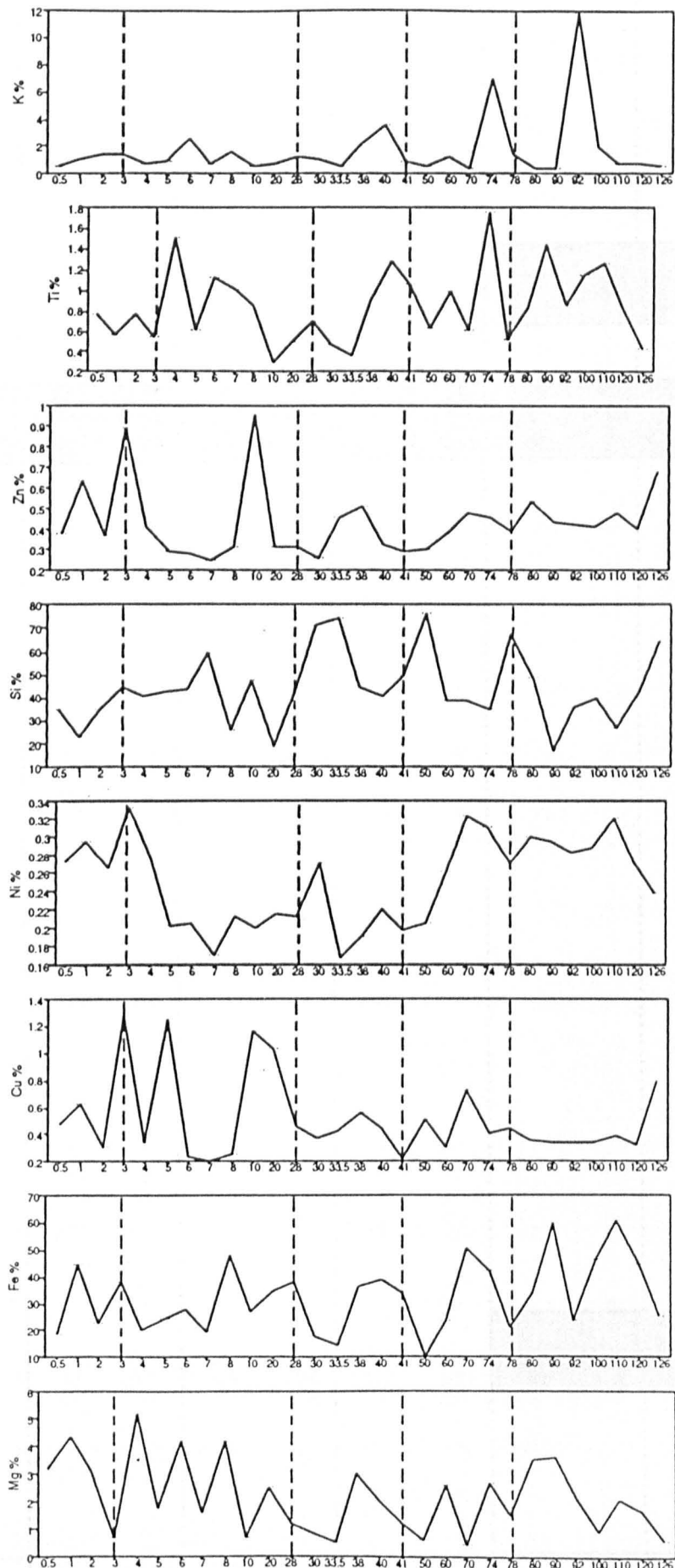


Figure 8.2a. Sediment geochemistry Loch A'Barpa.



Depth. Cms.

Figure 8.2b. Sediment geochemistry Loch A'Barpa.

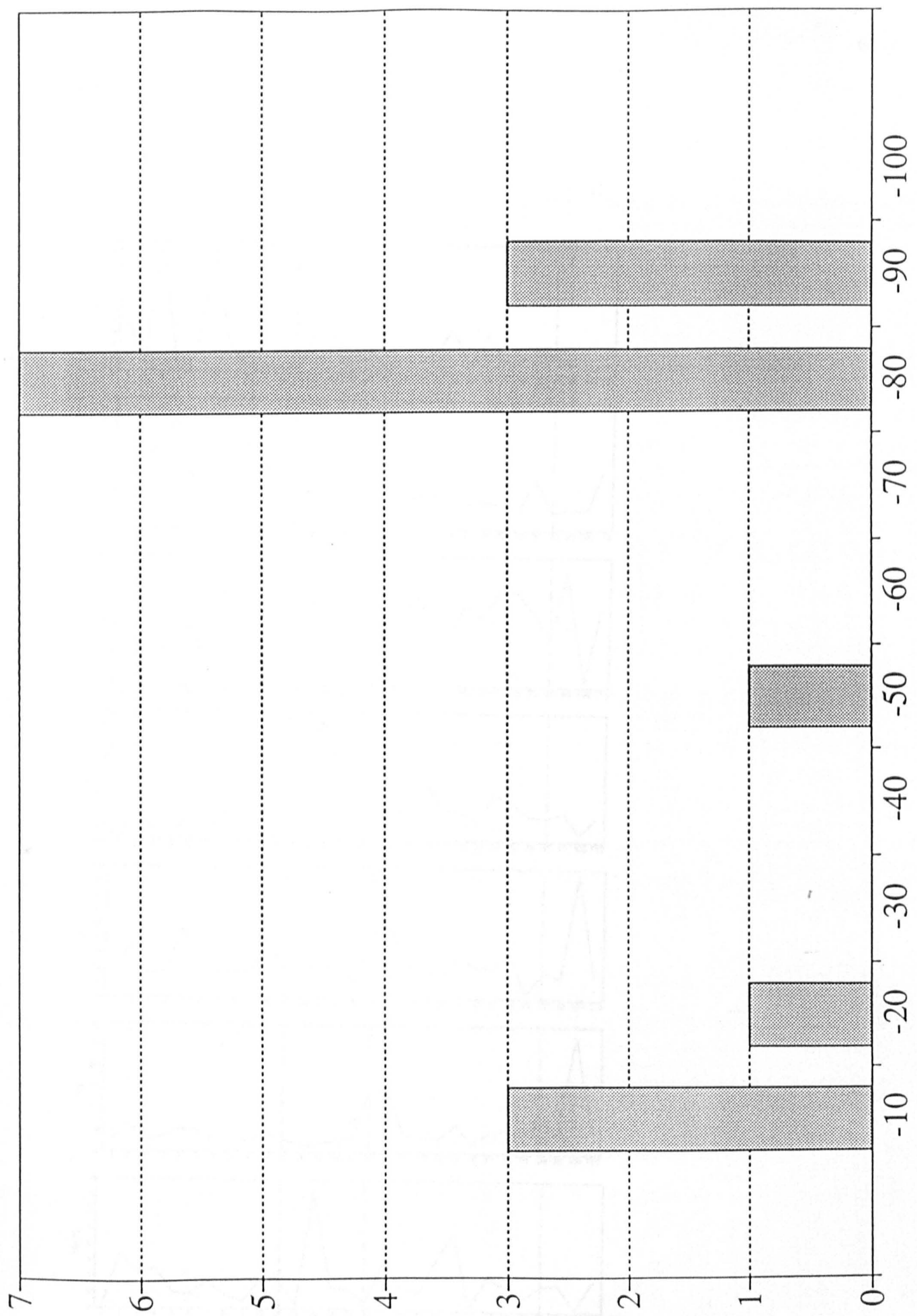


Figure 8.3. Tephra distribution, Loch Obisary.

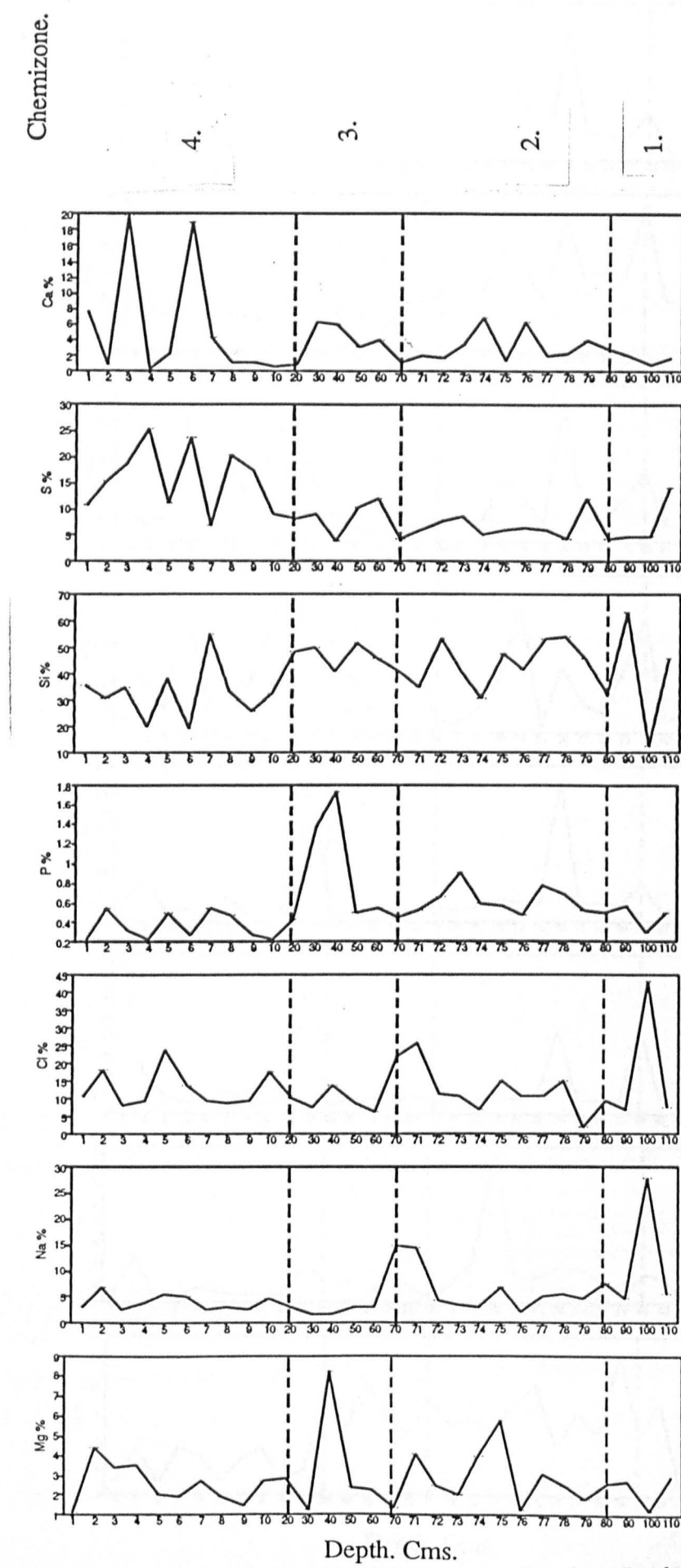


Figure 8.4a. Sediment geochemistry Loch Obisary.

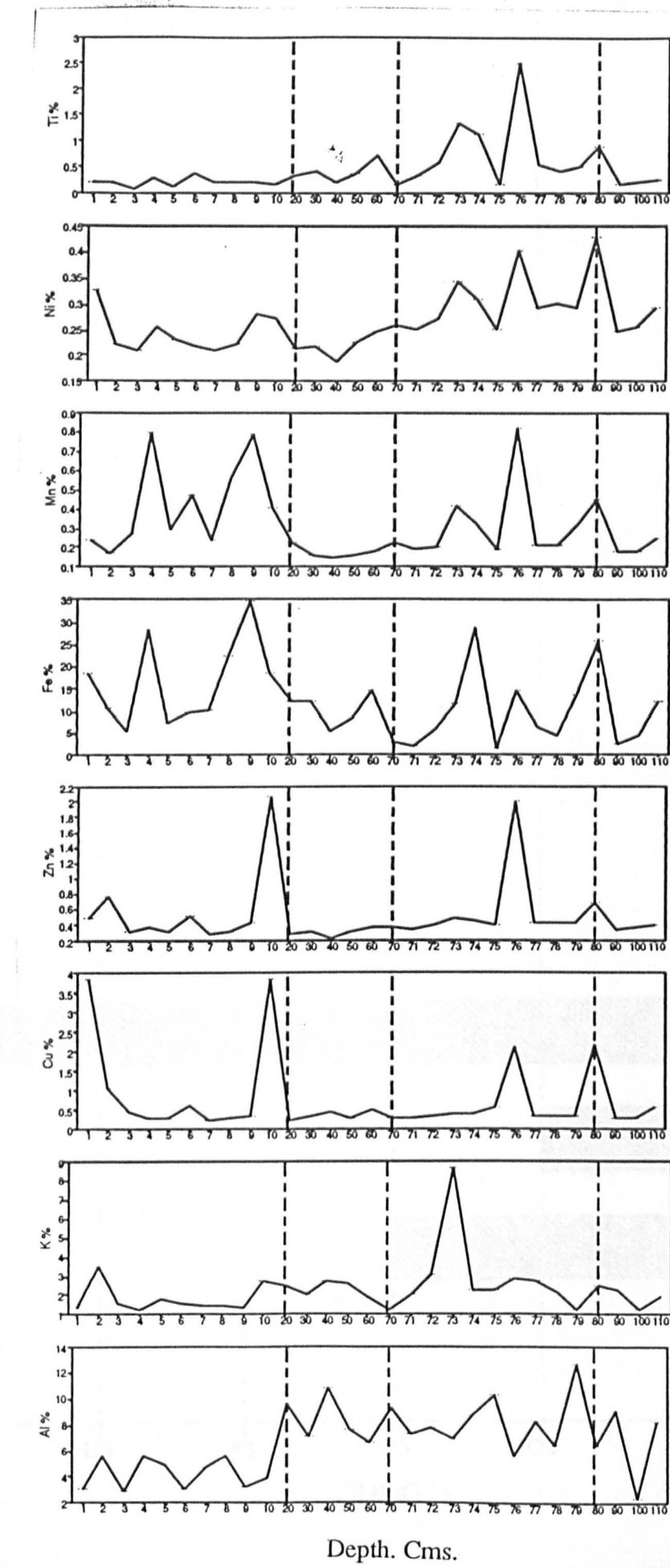


Figure 8.4b. Sediment geochemistry Loch Obisary.

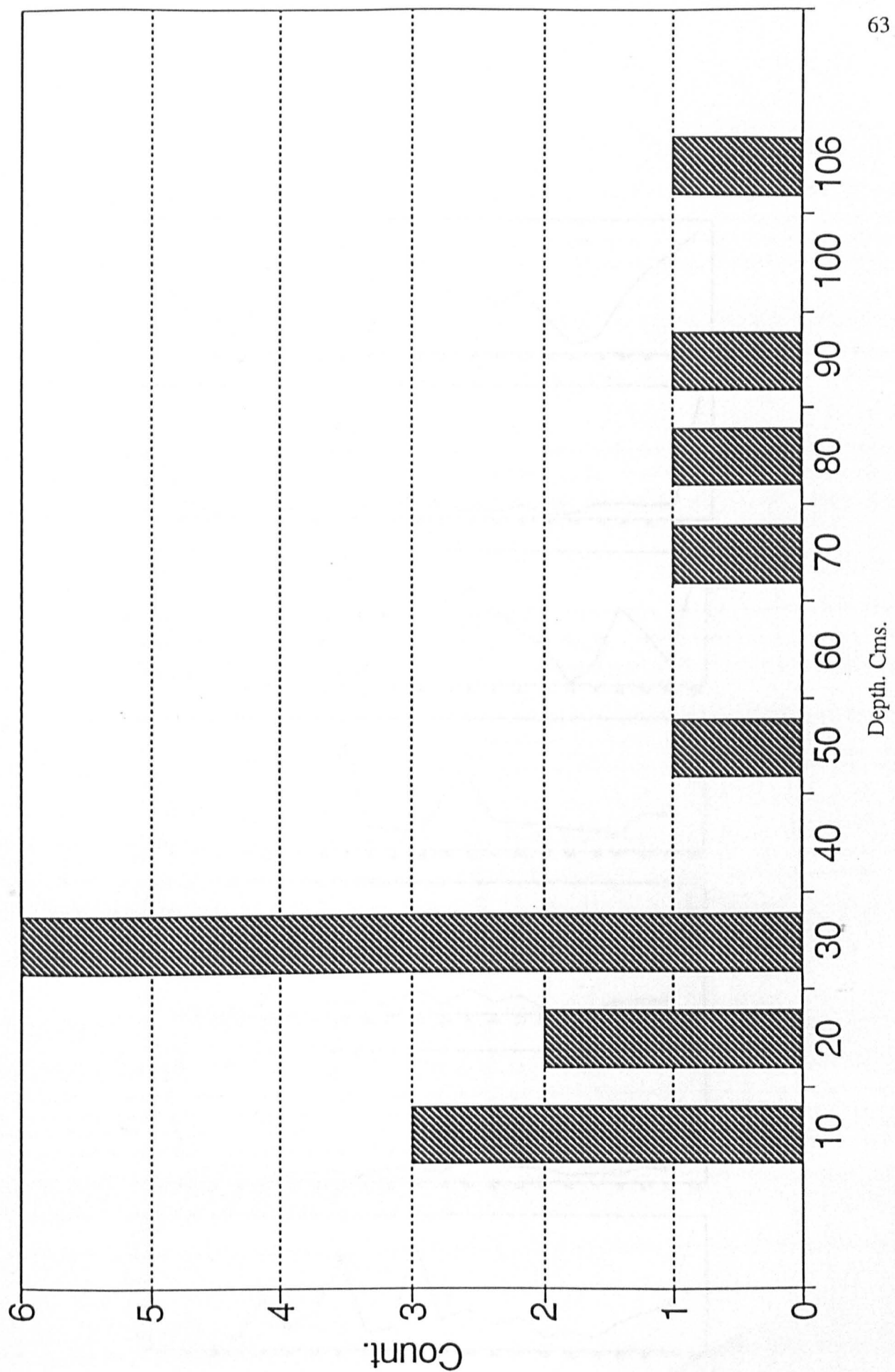


Figure 8.5. Tephra distribution, Loch Druidibeg.

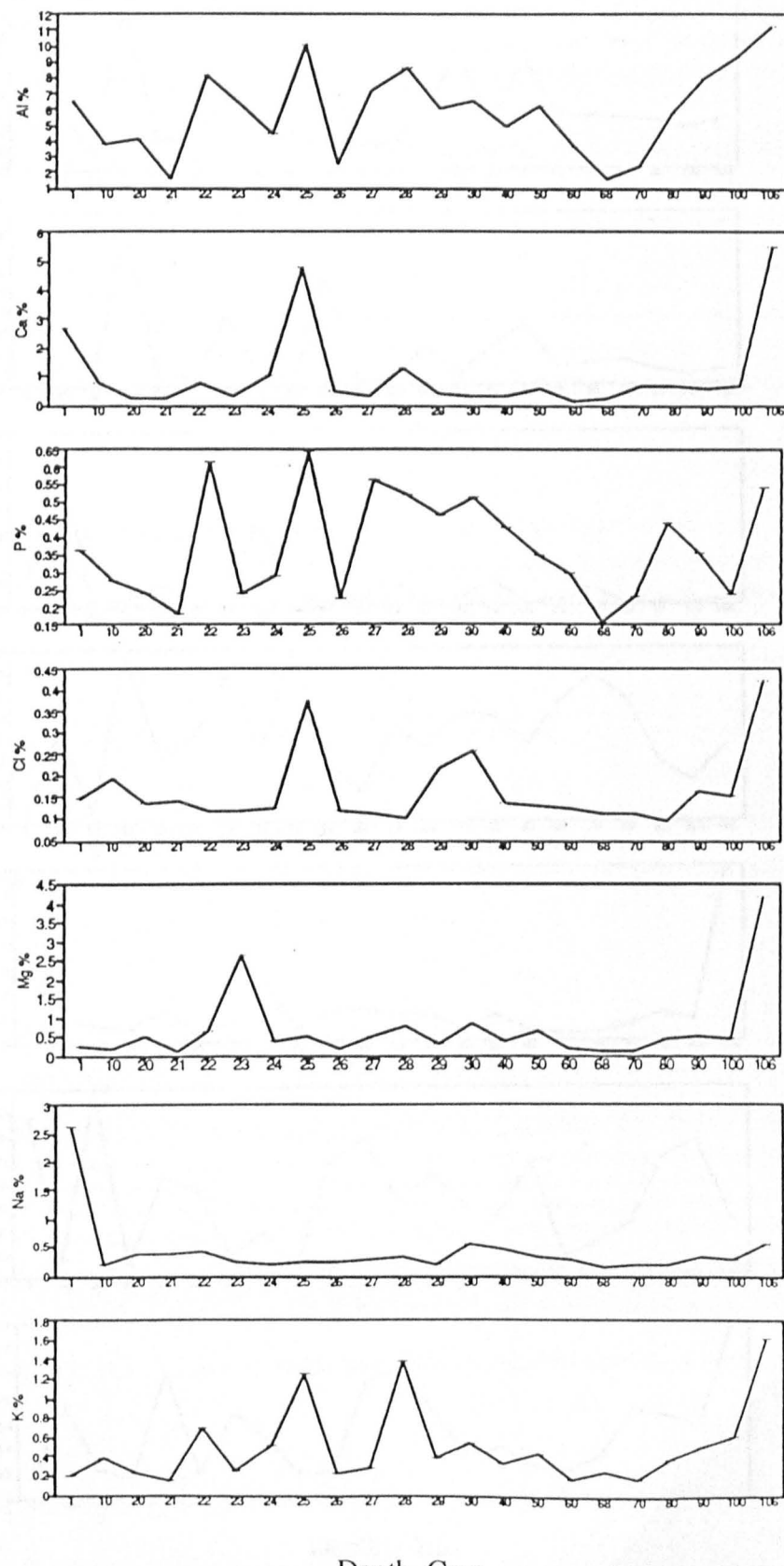


Figure 8.6a. Sediment geochemistry Loch Druidibeg.

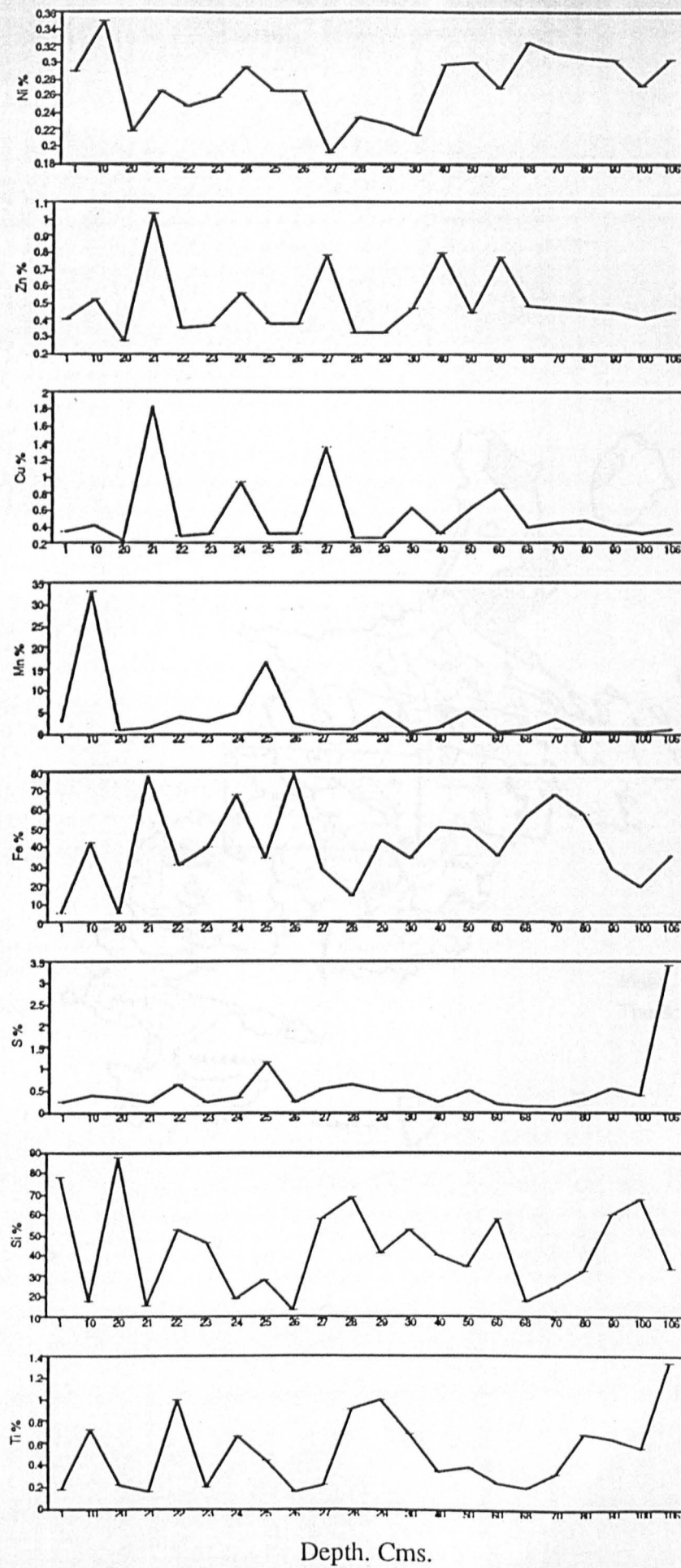


Figure 8.6b. Sediment geochemistry Loch Druidibeg.

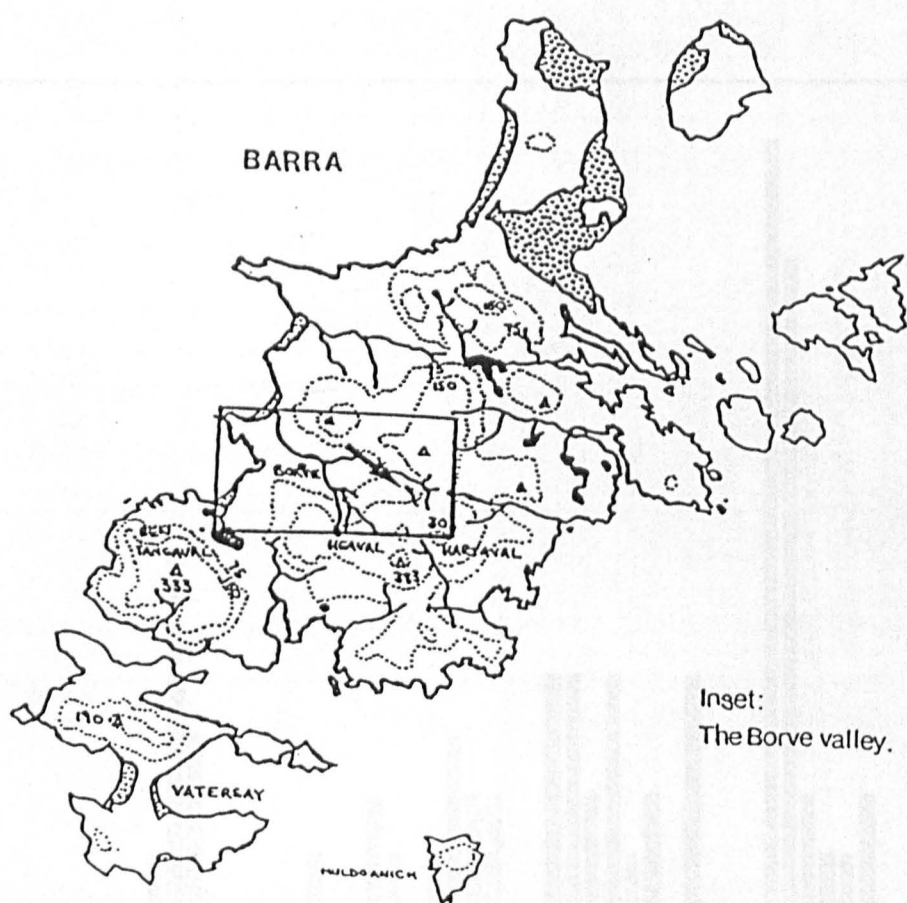


Figure 9.1. Location map, Borve bog. [From Pratt 1992].

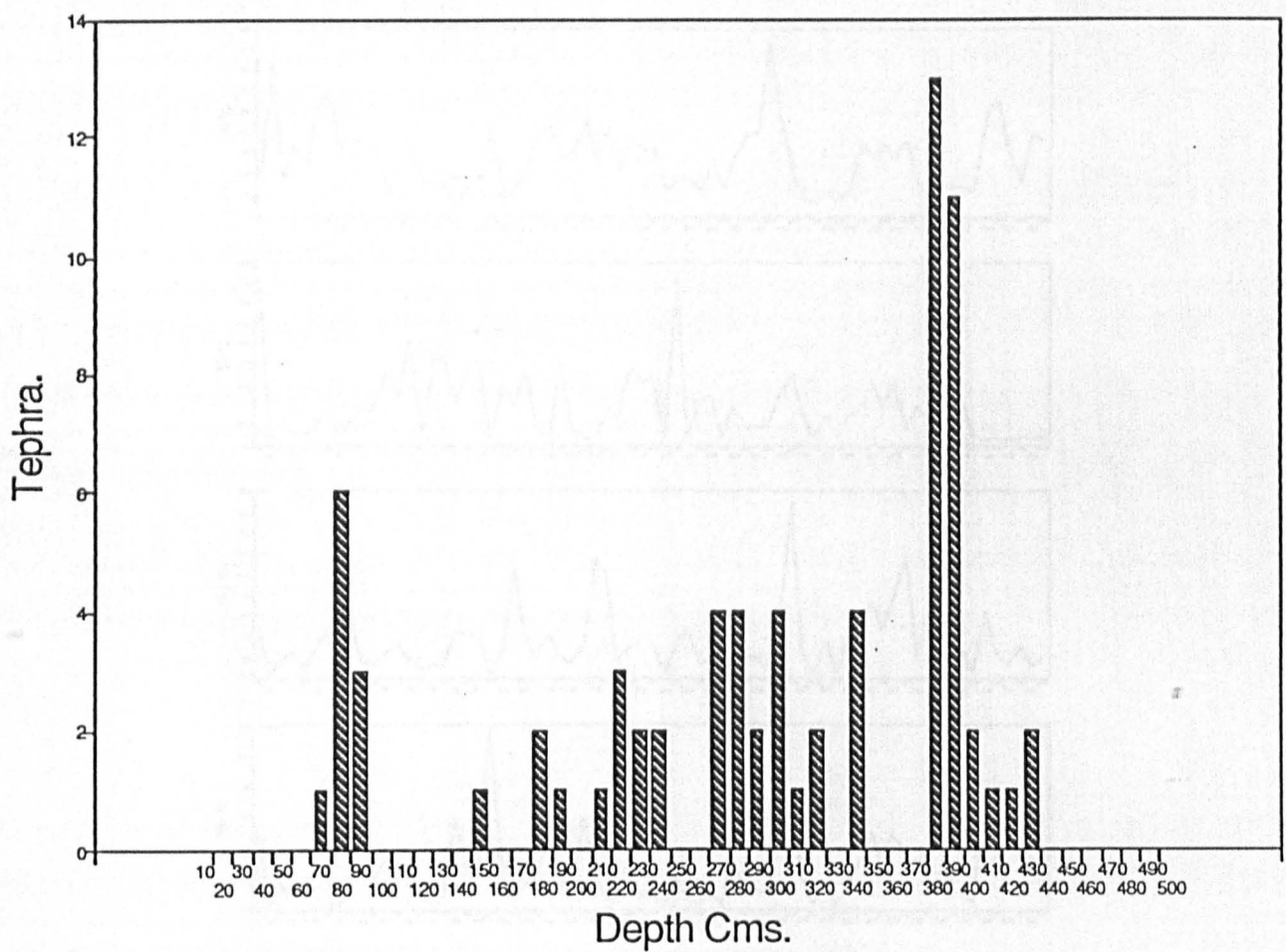


Figure 9.2. Tephra distribution in Borve Bog.

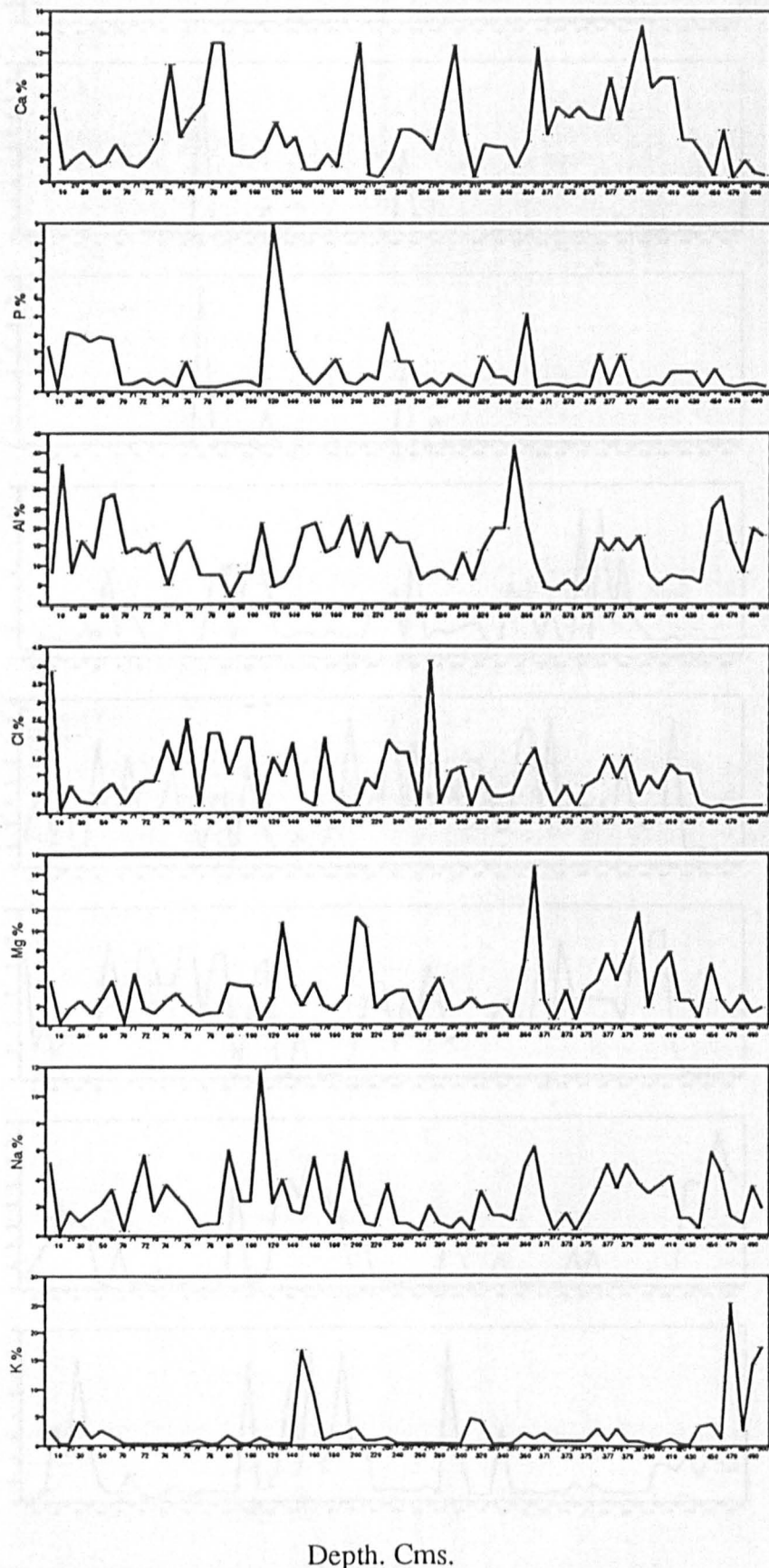


Figure 9.3a. Sediment geochemistry Borve Bog.

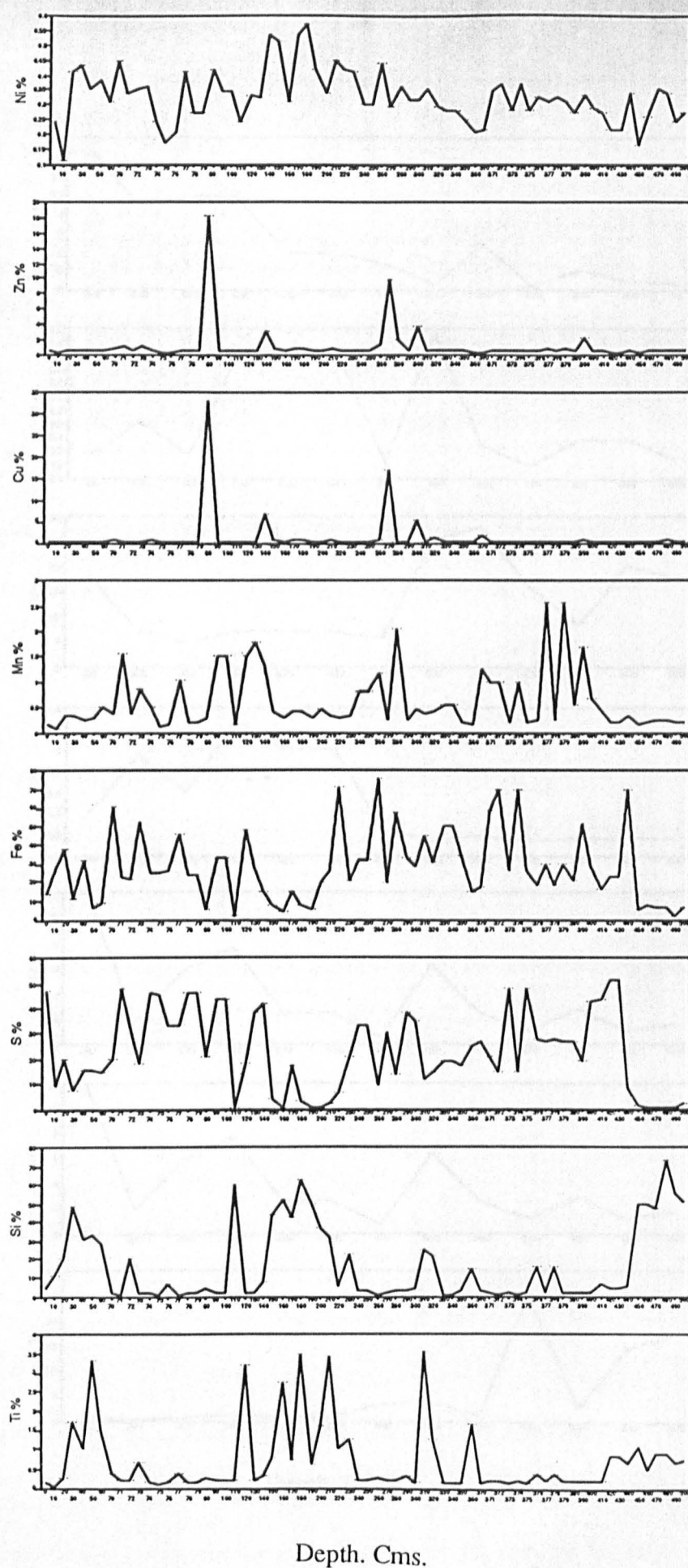


Figure 9.3b. Sediment geochemistry Borve Bog.

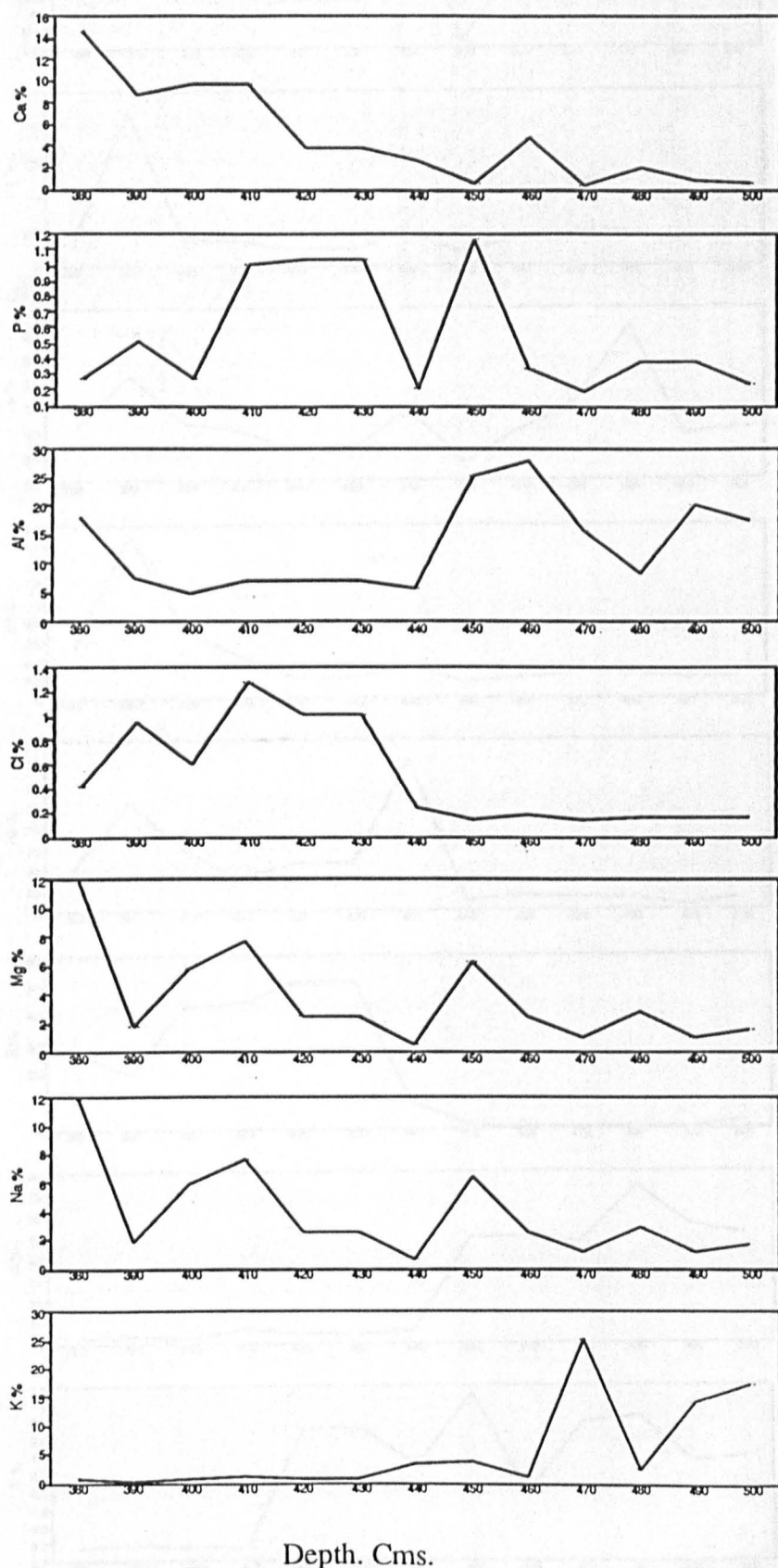


Figure 9.4a. Sediment geochemistry Borve Bog. Chemizone BV1.

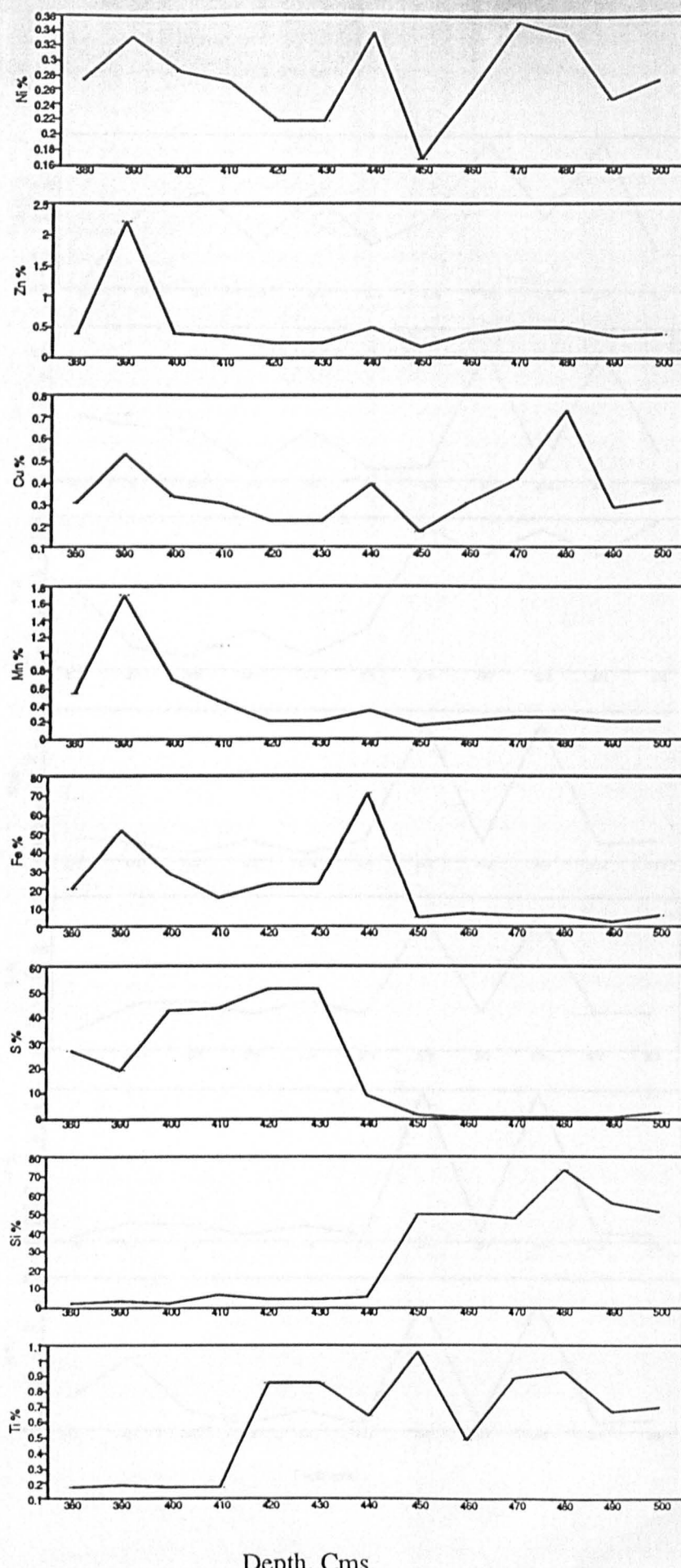


Figure 9.4b. Sediment geochemistry Borve Bog. Chemizone BV1.

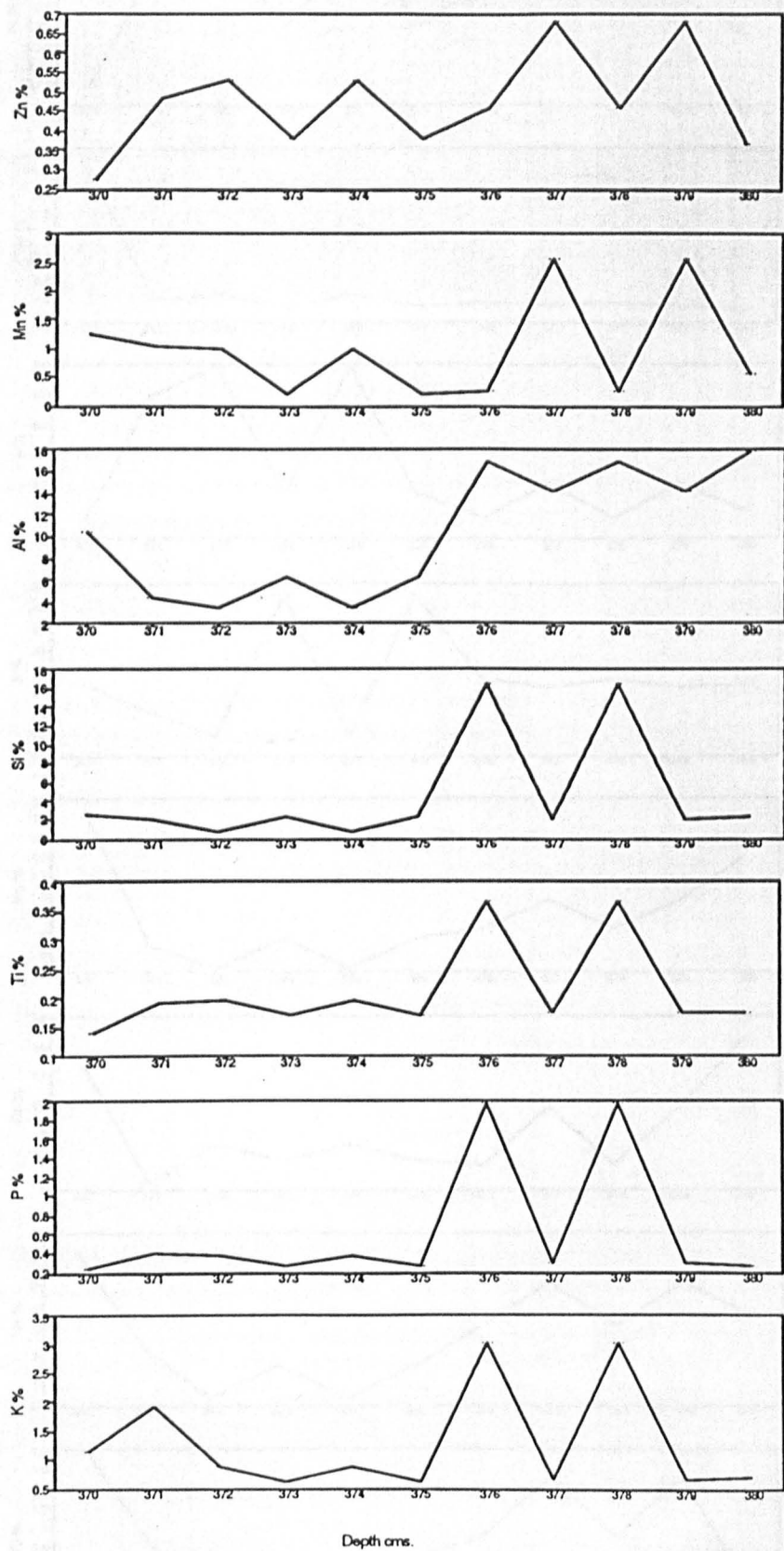


Figure 9.5a. Sediment geochemistry Borve Bog. Chemizone BV2.

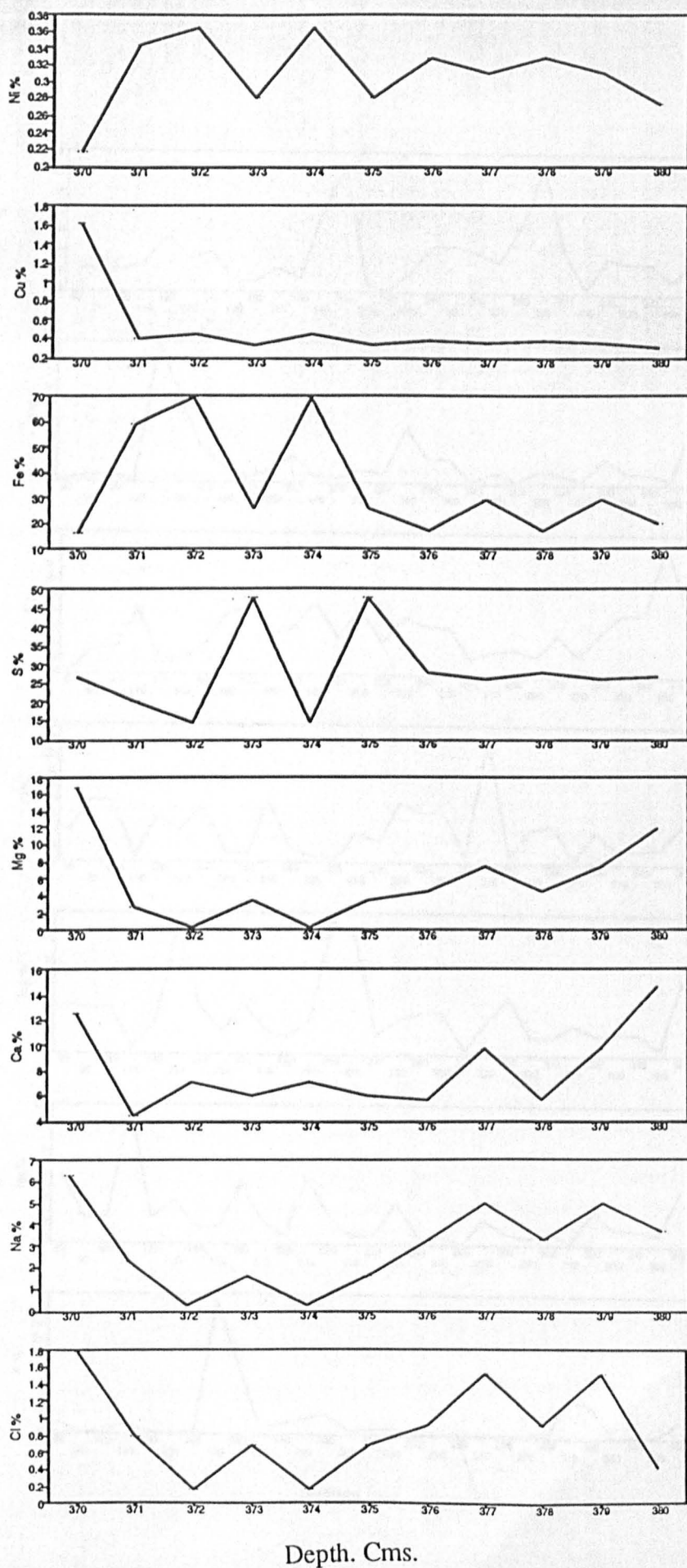


Figure 9.5b. Sediment geochemistry Borve Bog. Chemizone BV2.

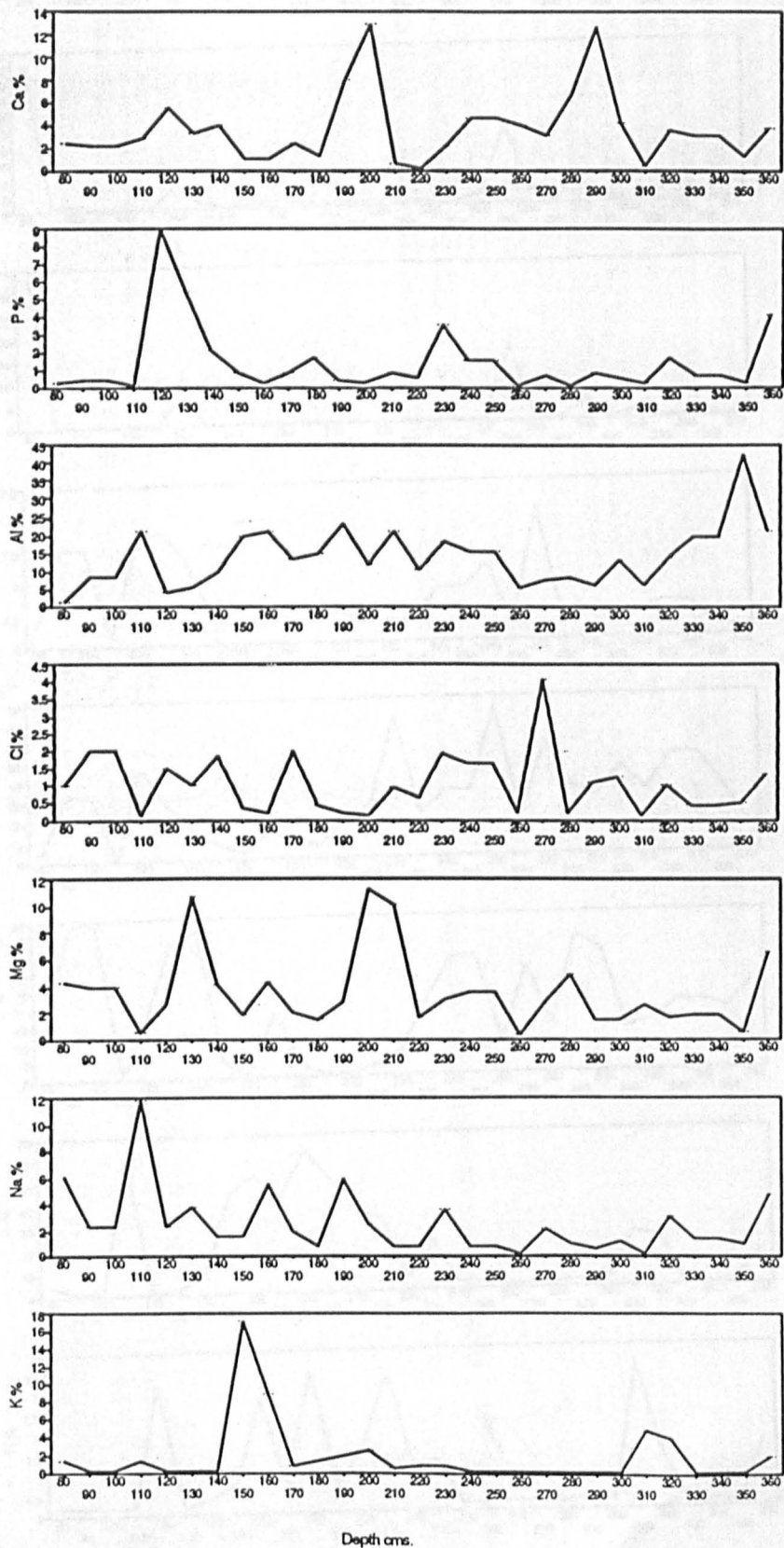


Figure 9.6a. Sediment geochemistry Borve Bog. Chemizone BV3.

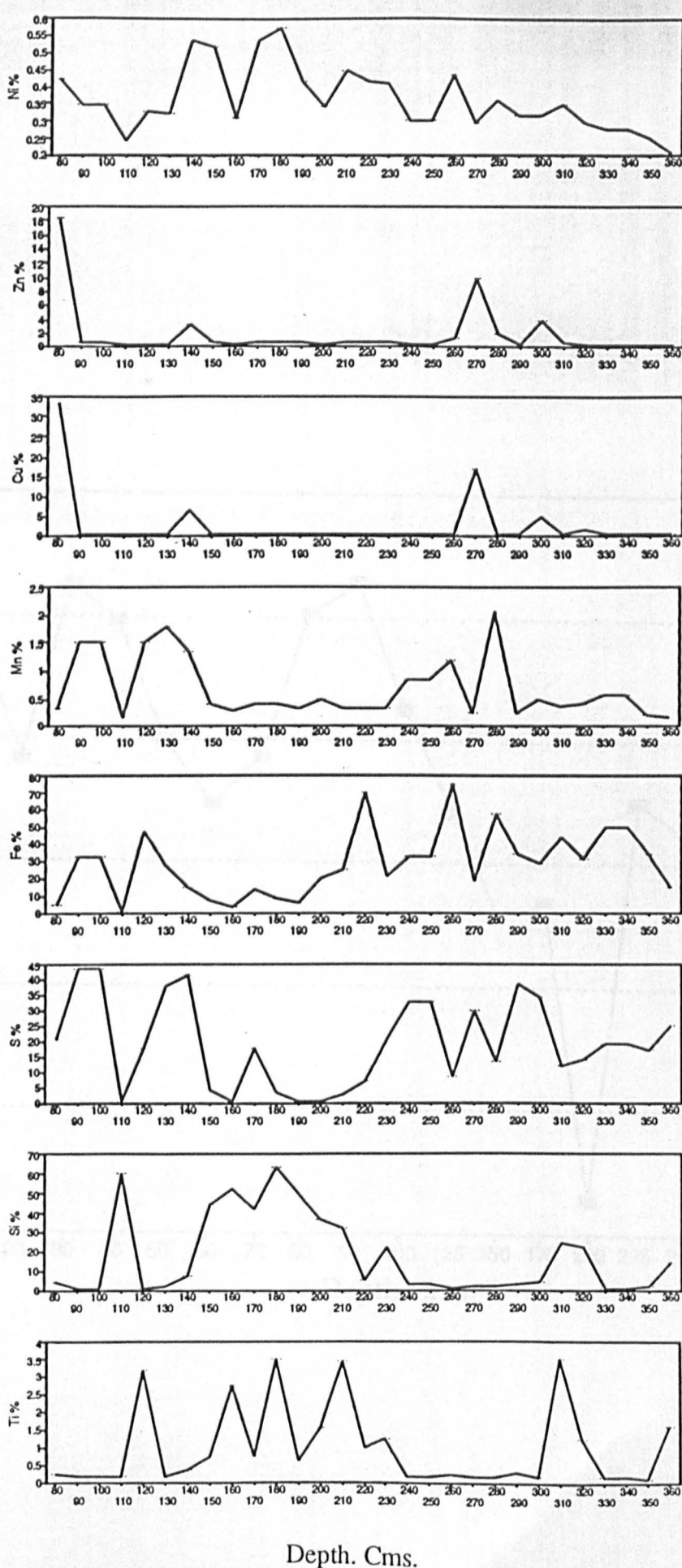


Figure 9.6b. Sediment geochemistry Borve Bog. Chemizone BV3.

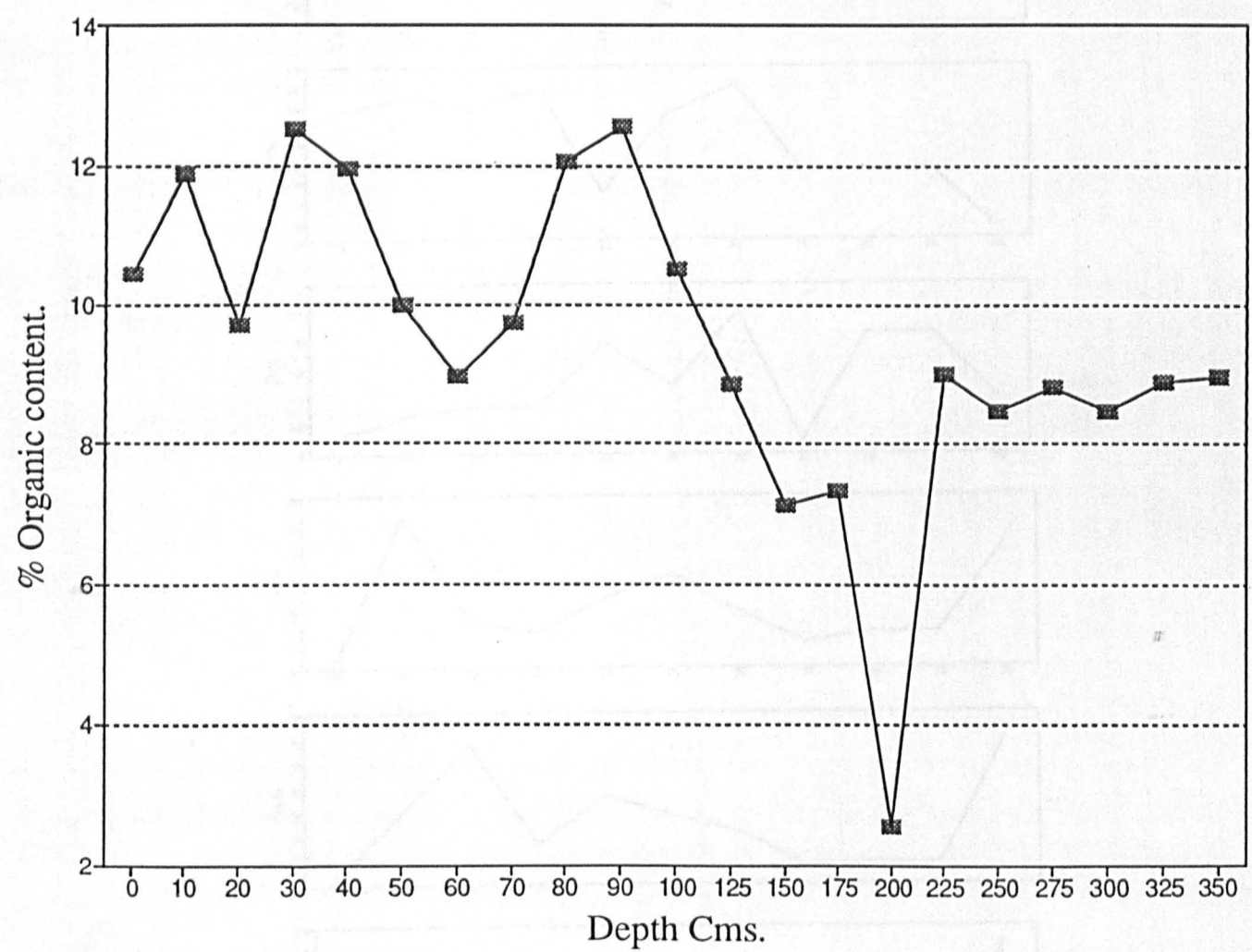


Figure 9.7. Organic content Borve Bog.

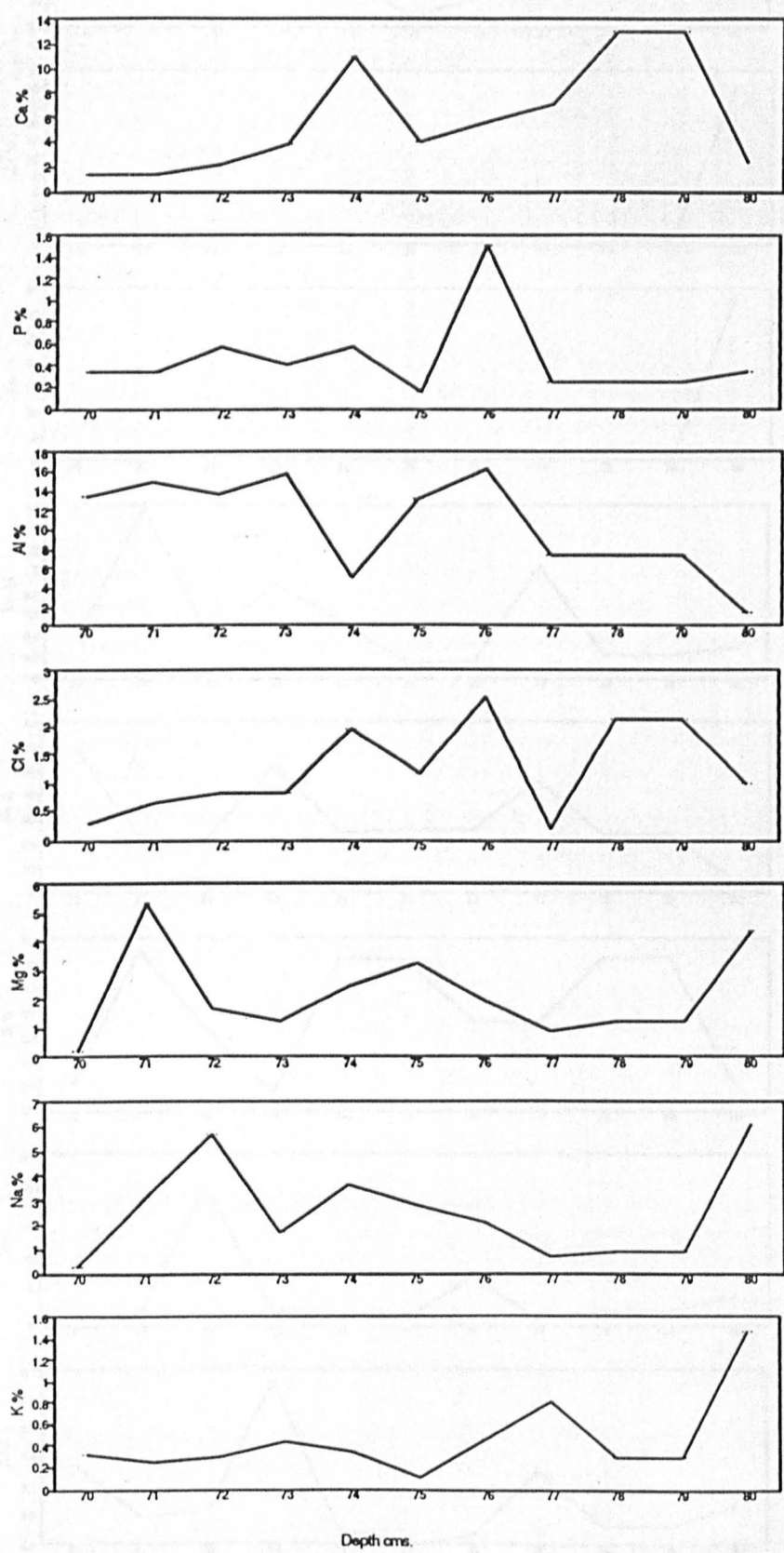


Figure 9.8a. Sediment geochemistry Borve Bog, Chemizone BV4.

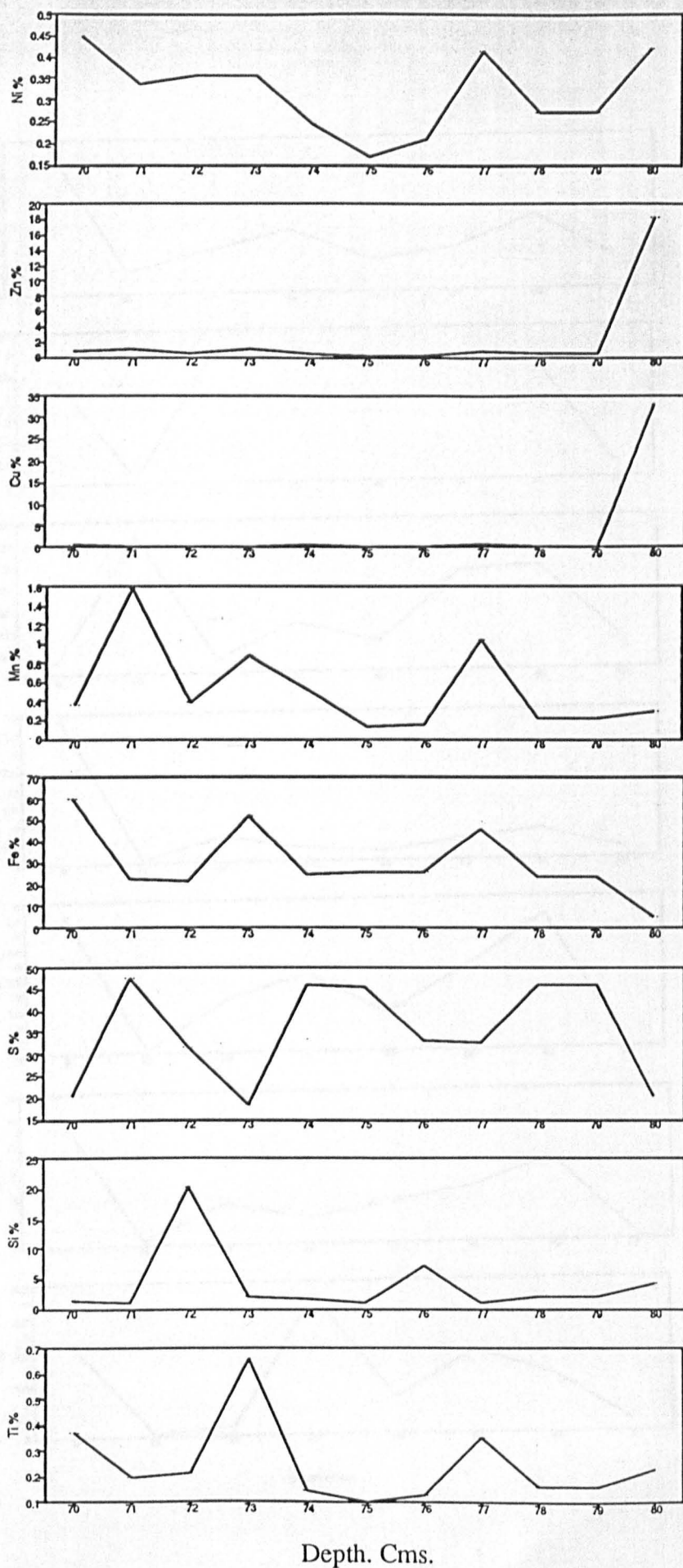


Figure 9.8b. Sediment geochemistry Borve Bog, Chemizone BV4.

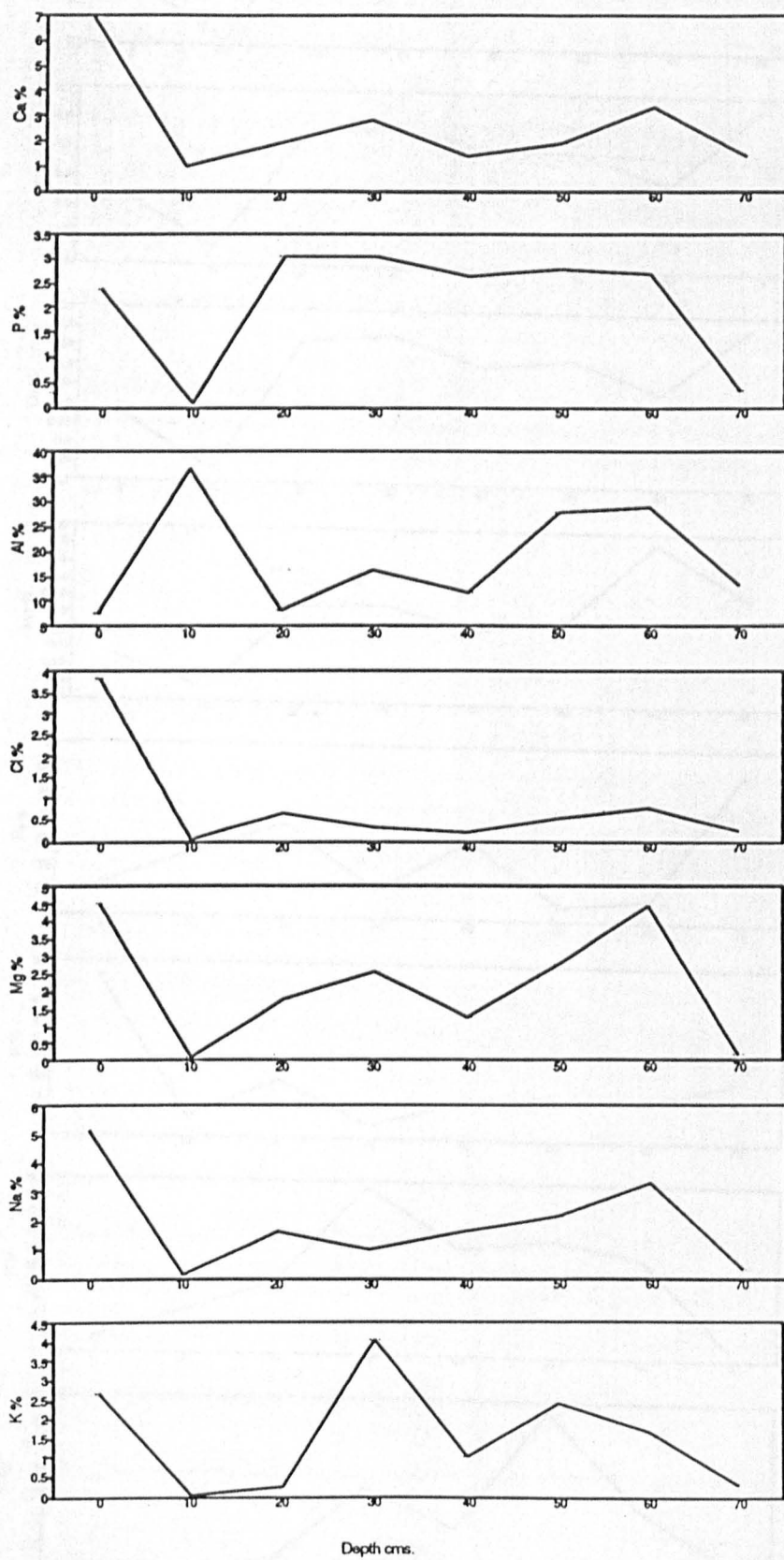


Figure 9.9a. Sediment geochemistry Borve Bog. Chemizone BV5.

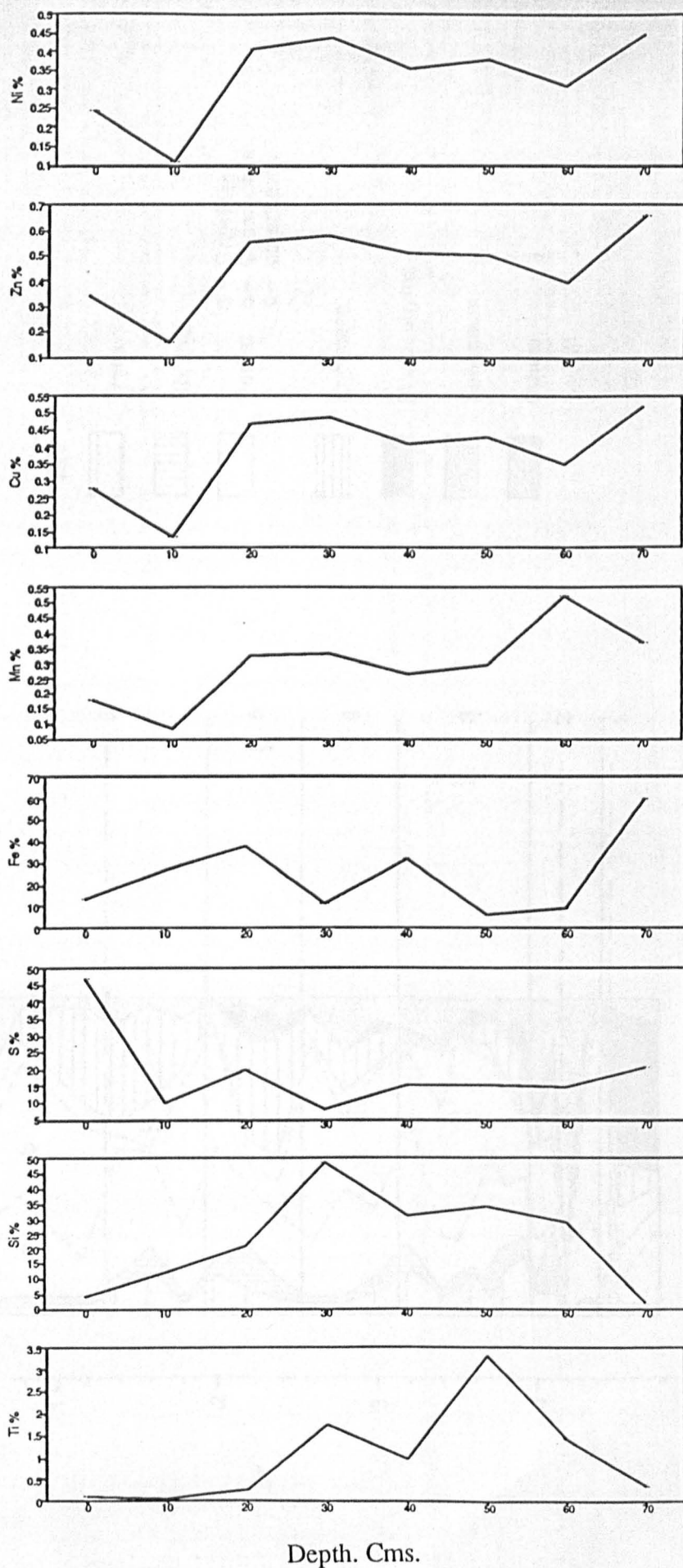


Figure 9.9b. Sediment geochemistry Borve Bog. Chemizone BV5.

Local pollen
assemblage zones.

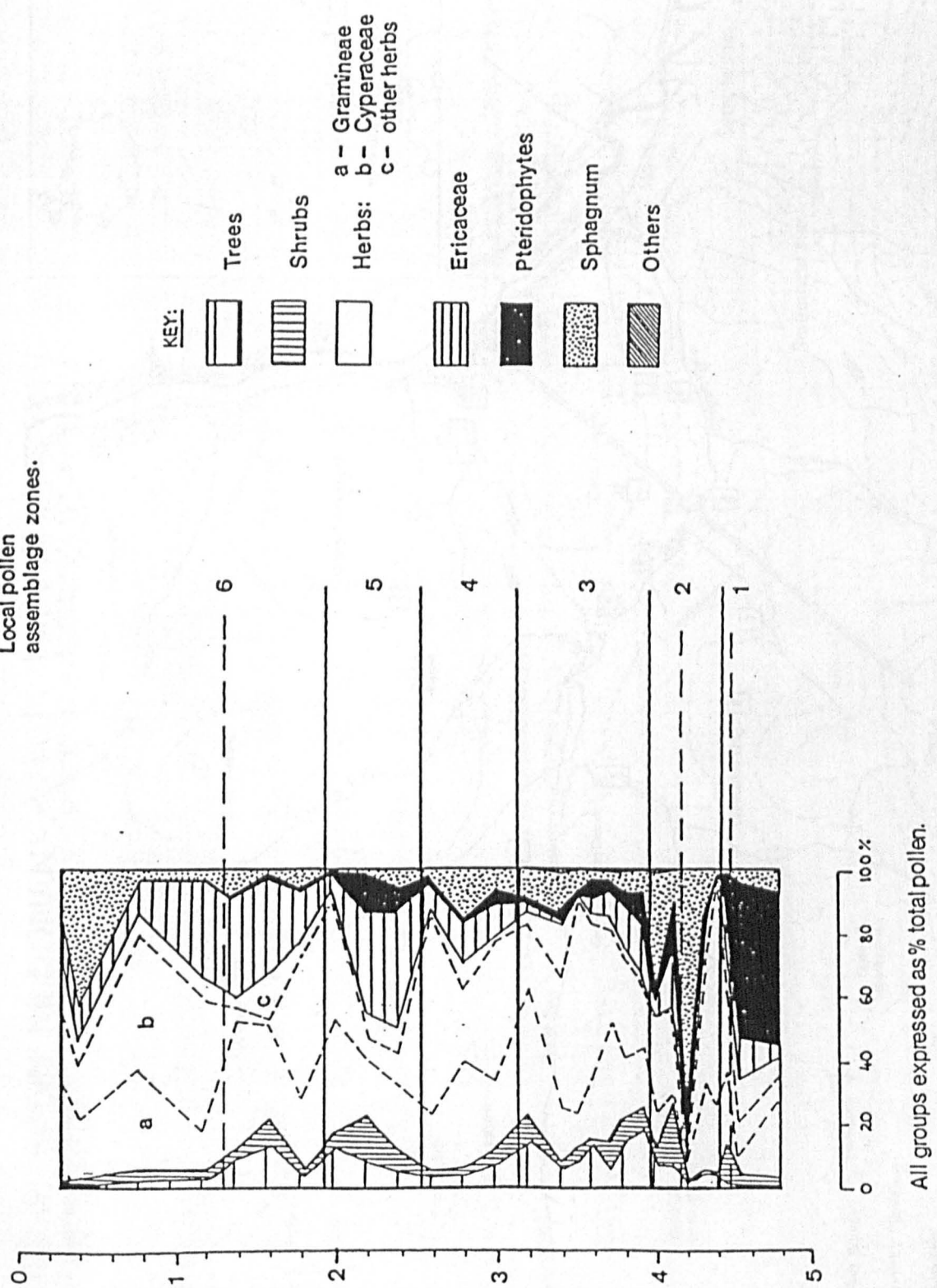
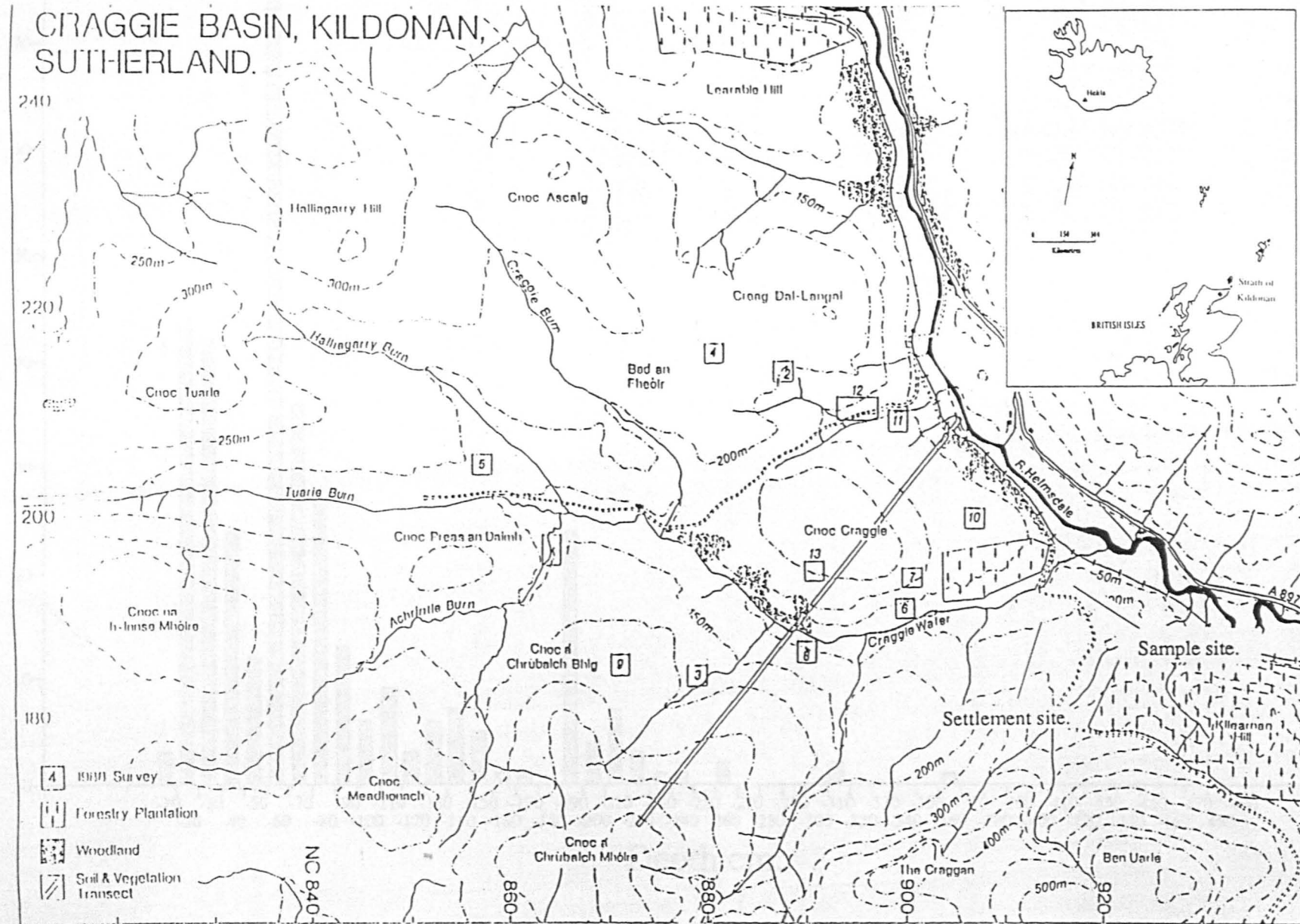


Figure 9.10. Summary pollen diagram Borve Bog. [From Pratt 1992].

Figure 10.1. Site location Strath of Kildonan.



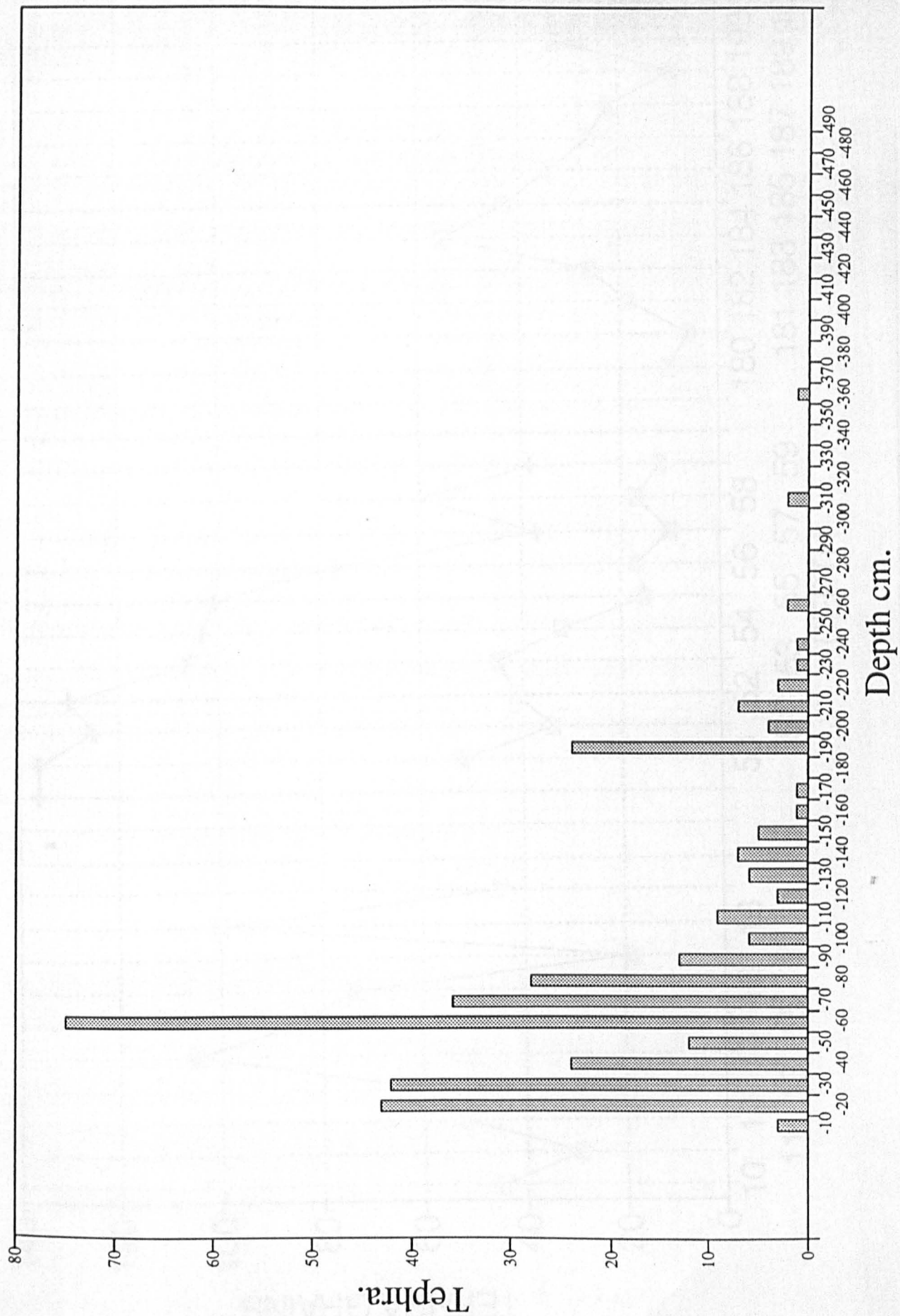


Figure 10.2. General tephra distribution, Strath of Kildonan.

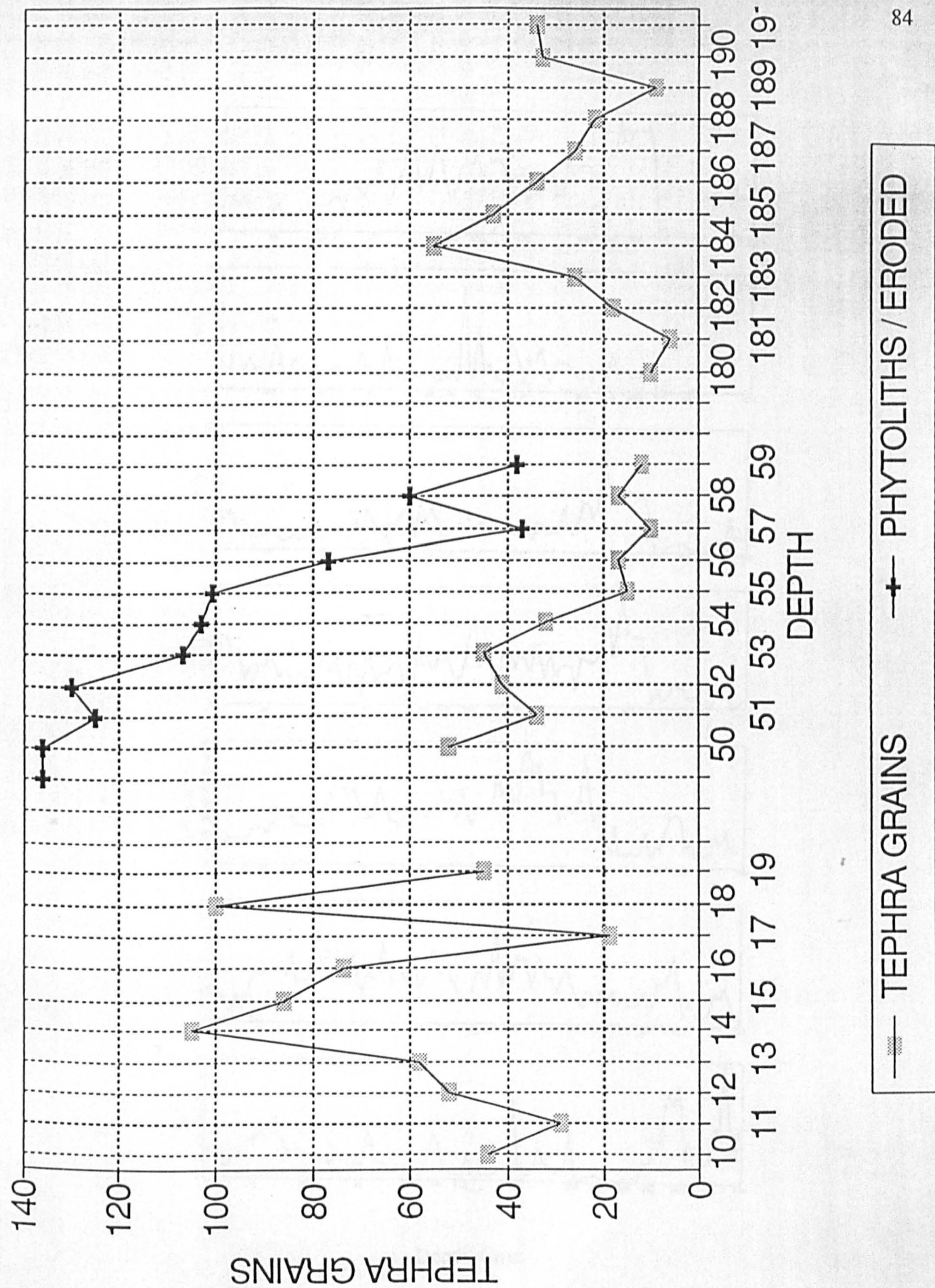
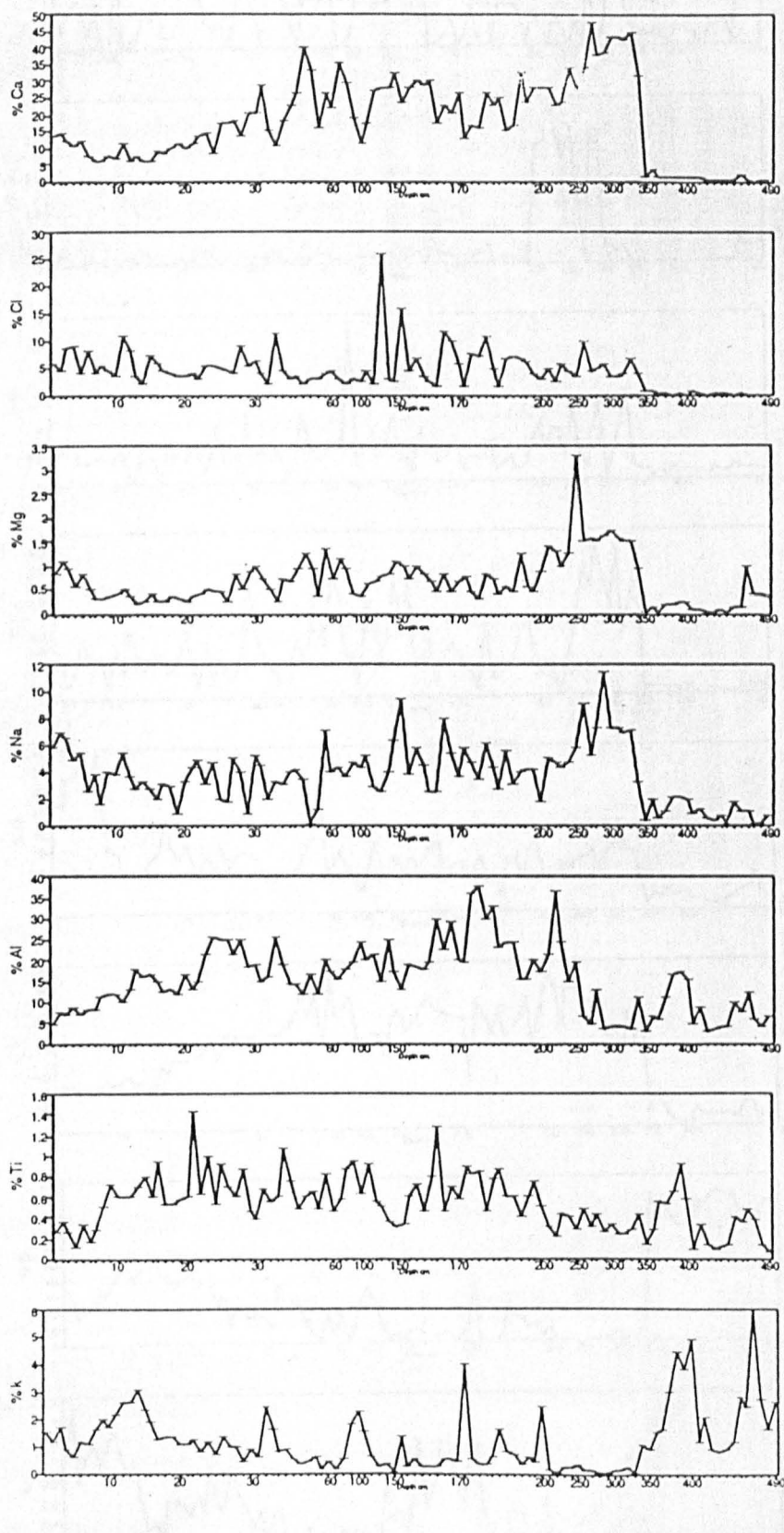


Figure 10.3. Detailed tephra distribution, Strath of Kildonan.



Depth. Cms.

Figure 10.4a. Sediment Geochemistry, Strath of Kildonan.

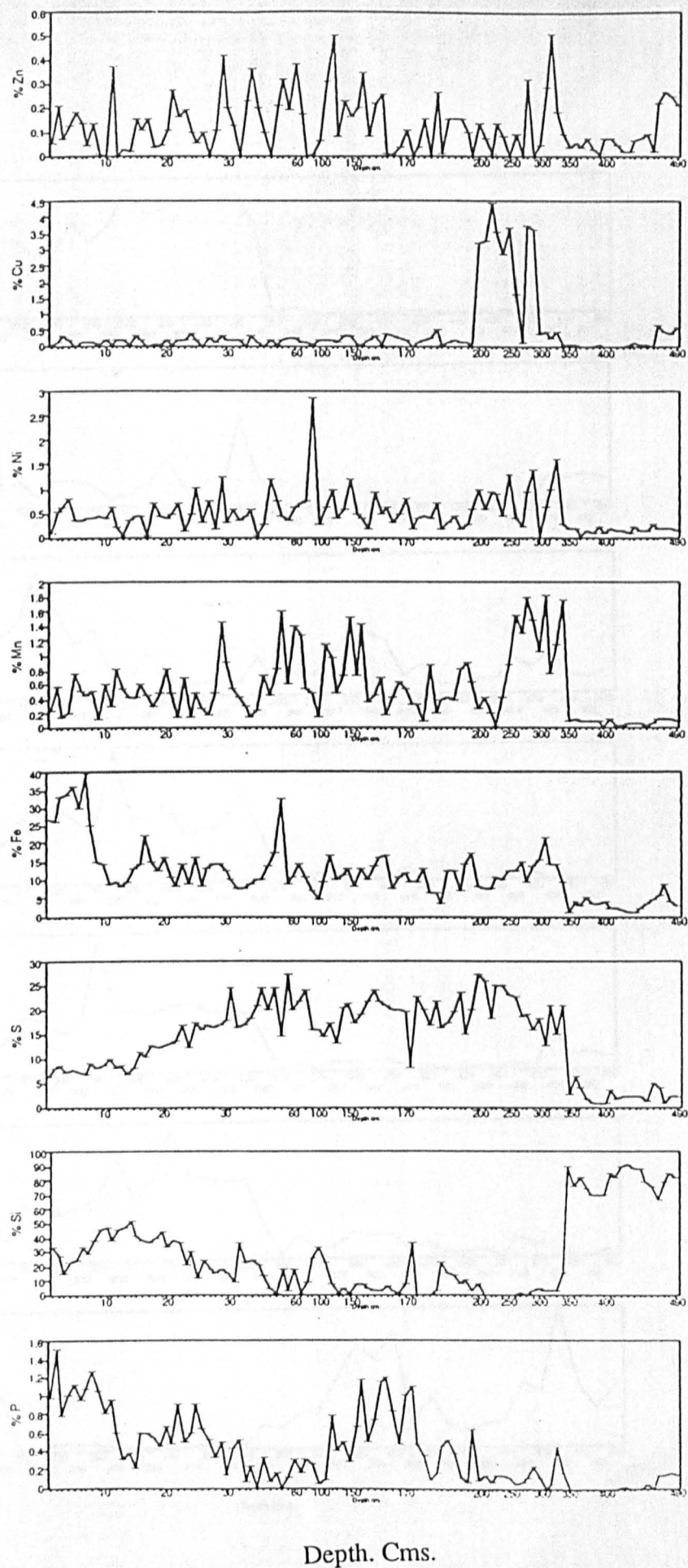


Figure 10.4b. Sediment Geochemistry, Strath of Kildonan.

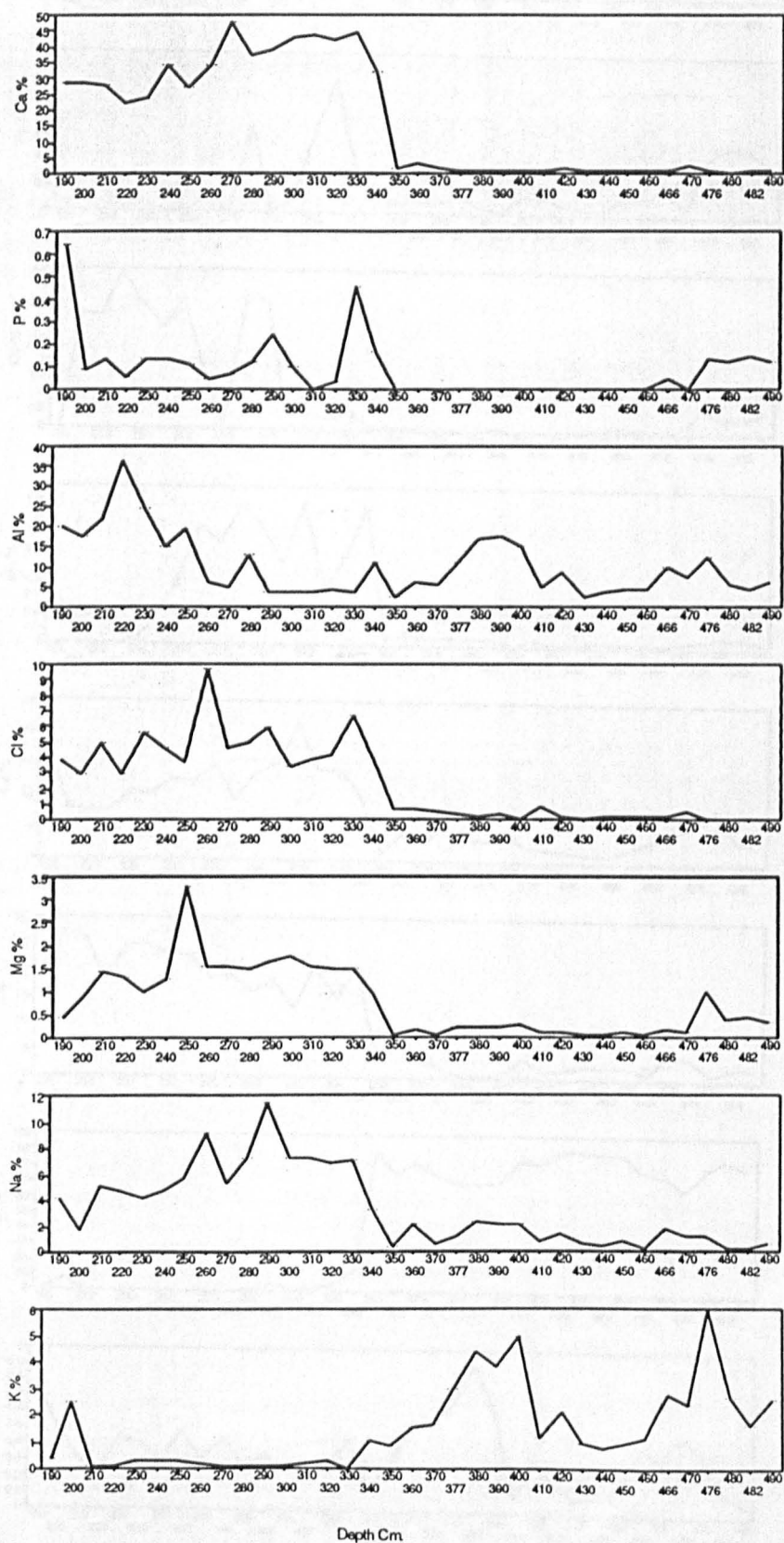


Figure 10.5a. Sediment Geochemistry. Chemizone KL1, Strath of Kildonan.

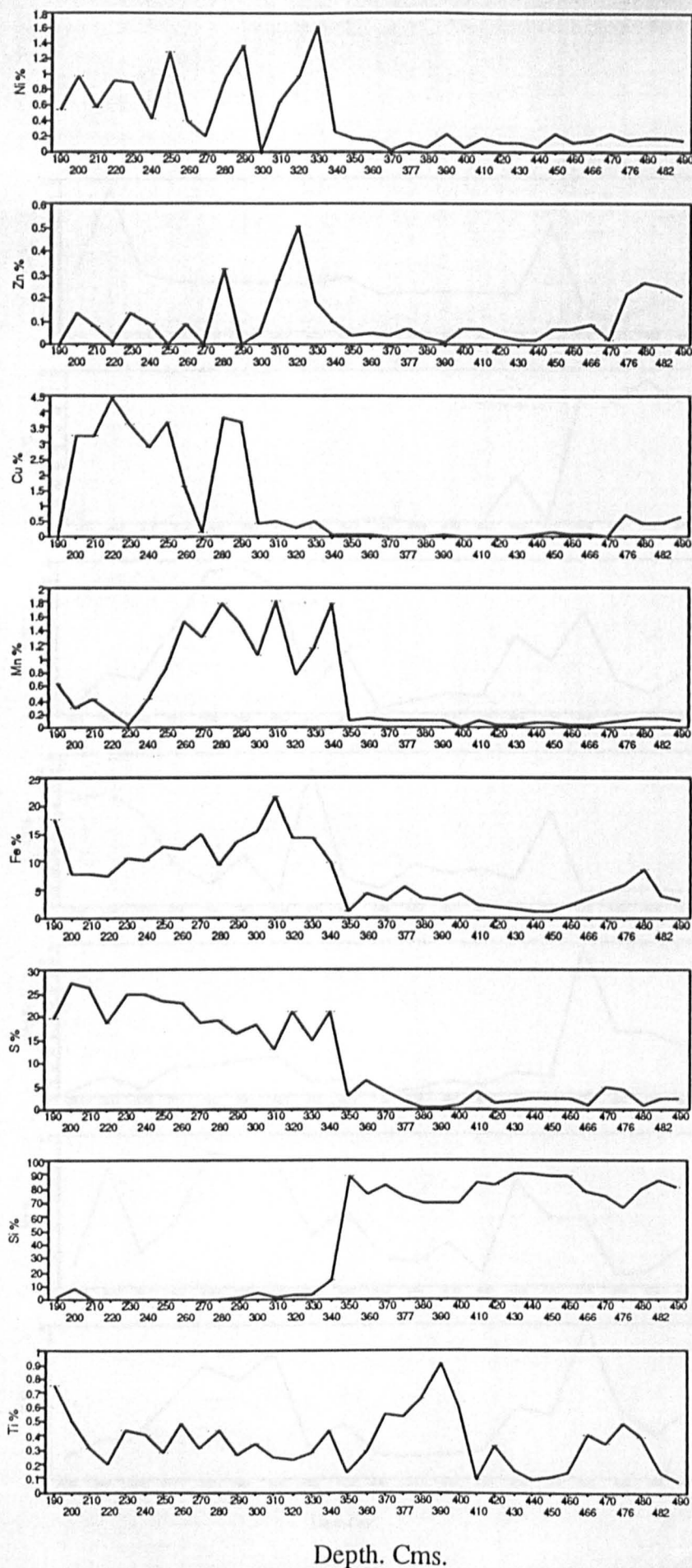


Figure 10.5b. Sediment Geochemistry Chemizone KL1, Strath of Kildonan.

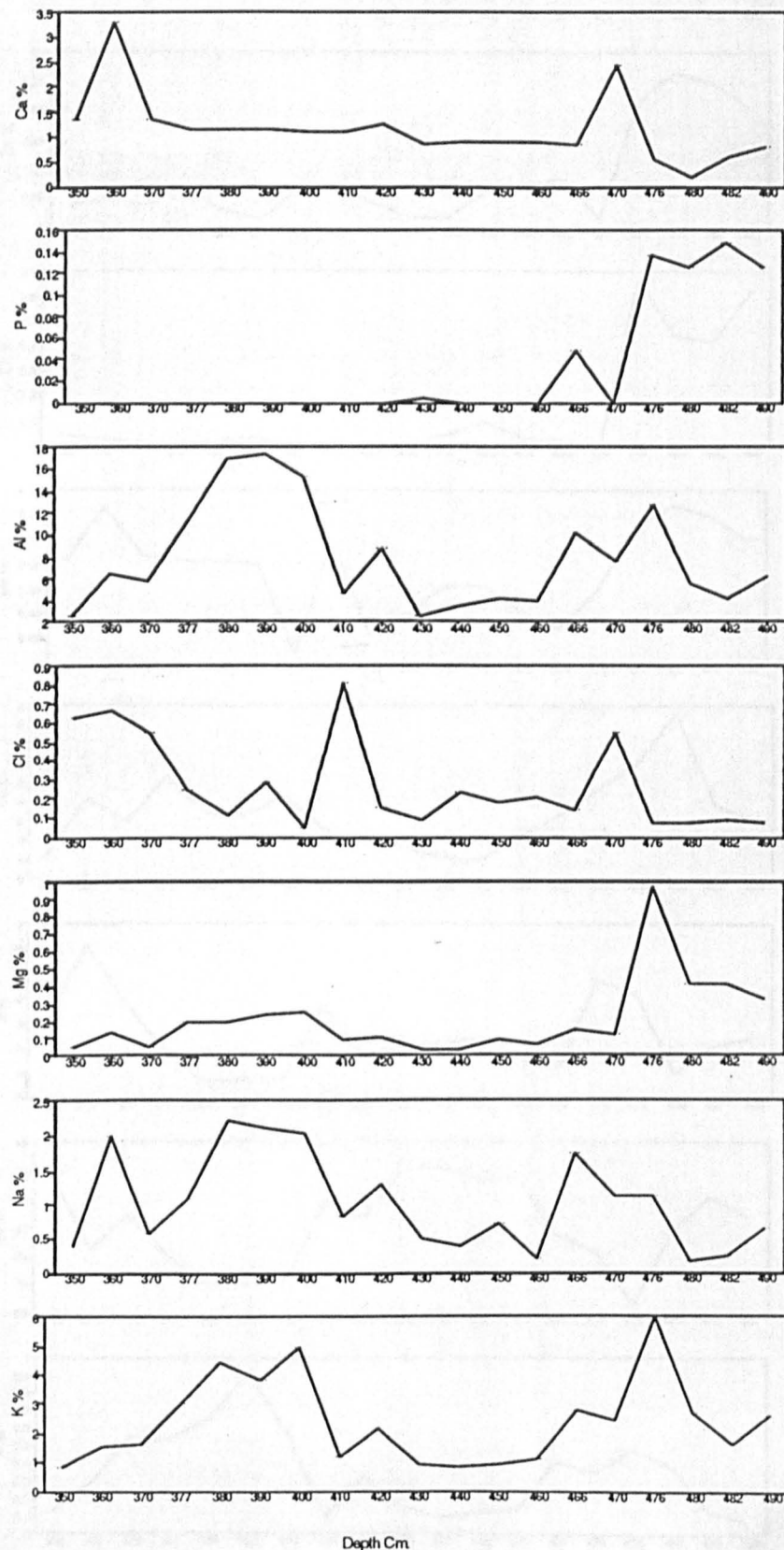


Figure 10.6a. Sediment Geochemistry Chemizone KL1a, Strath of Kildonan.

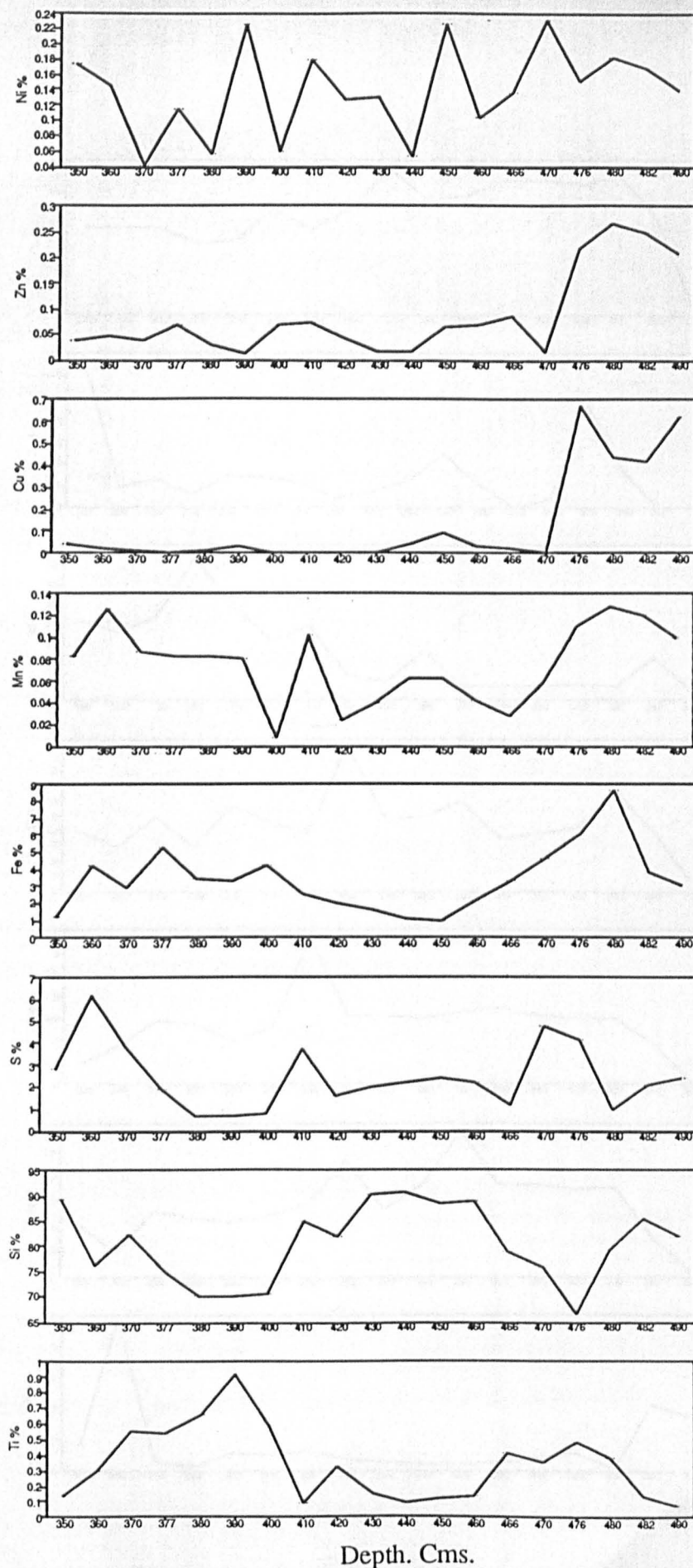


Figure 10.6b. Sediment Geochemistry Chemizone KL1a, Strath of Kildonan.

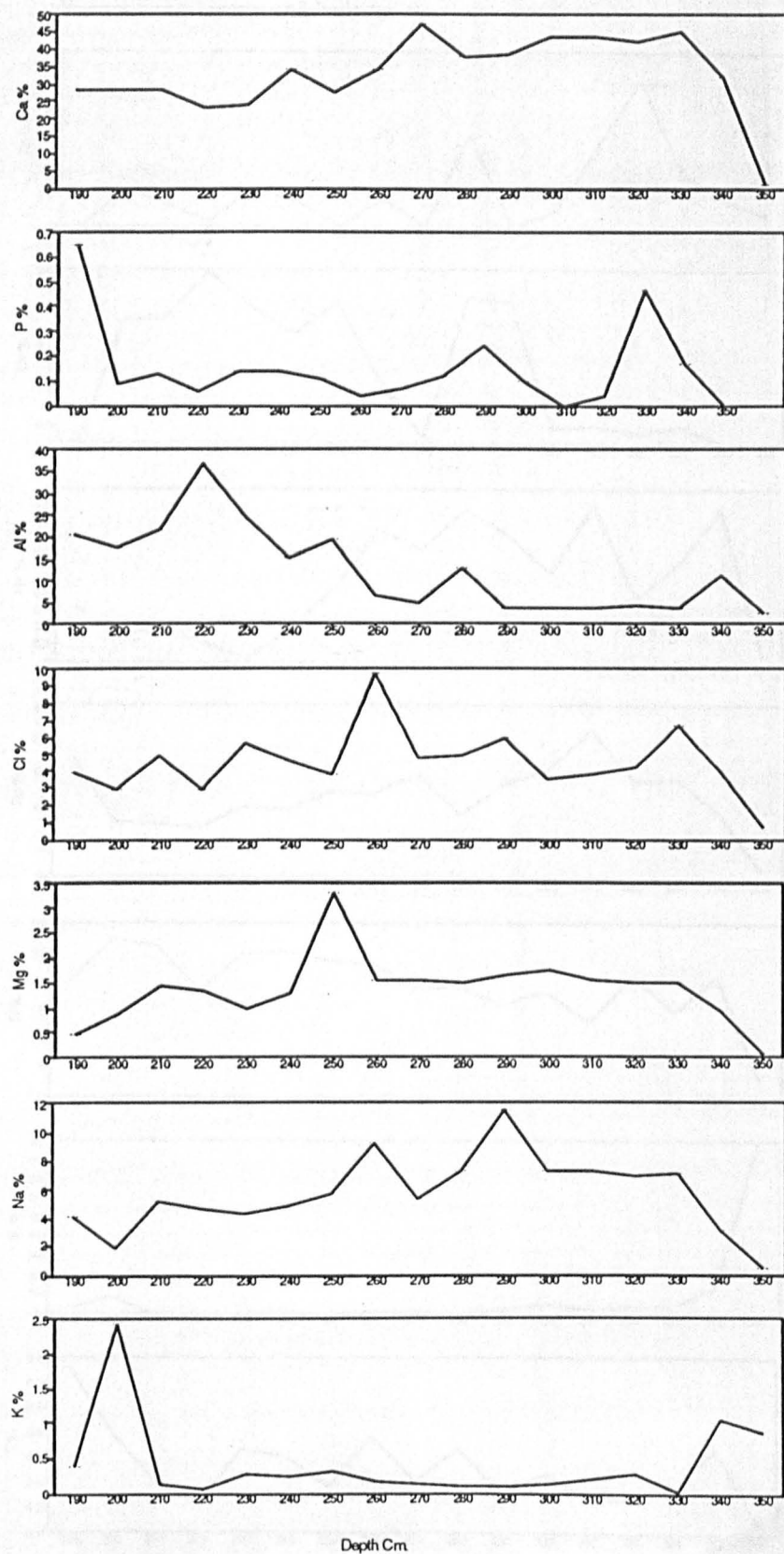


Figure 10.7a. Sediment Geochemistry Chemizone KL1b, Strath of Kildonan.

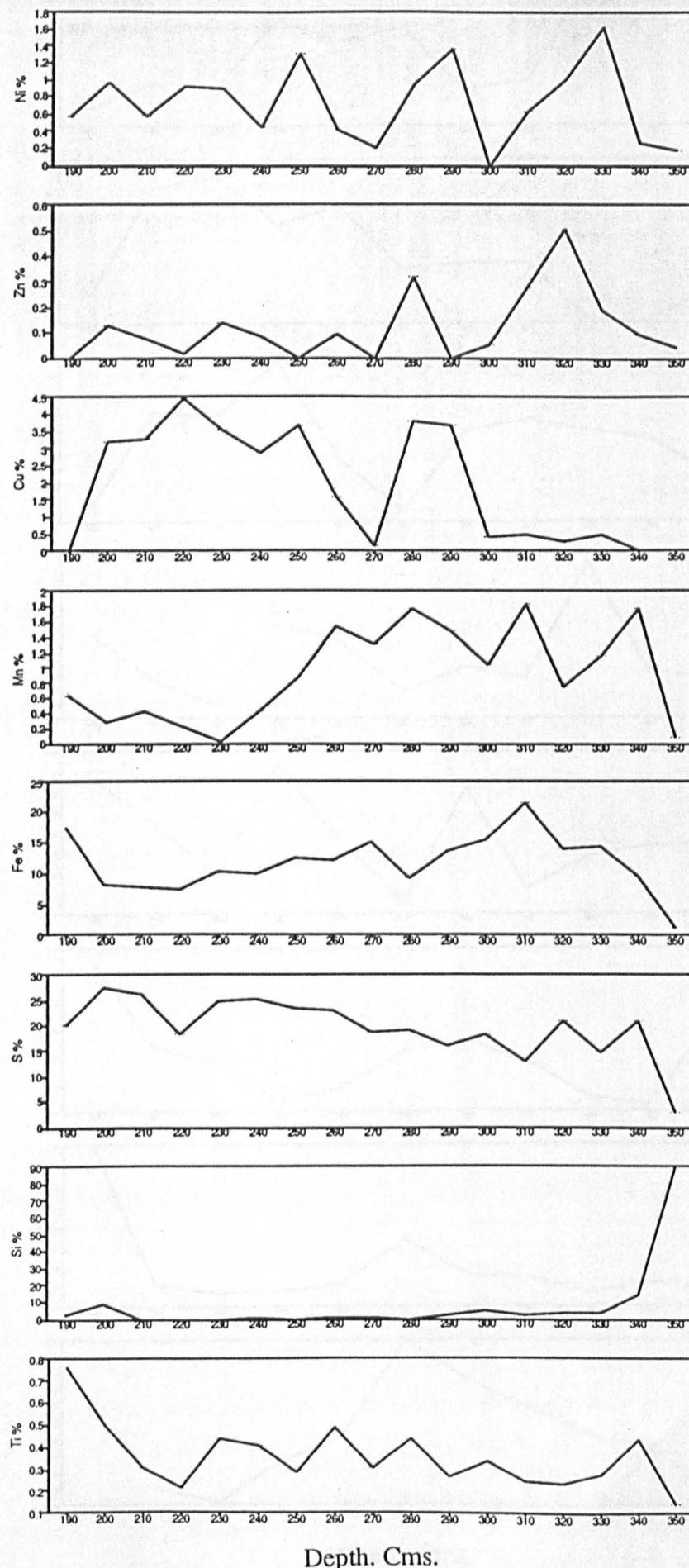
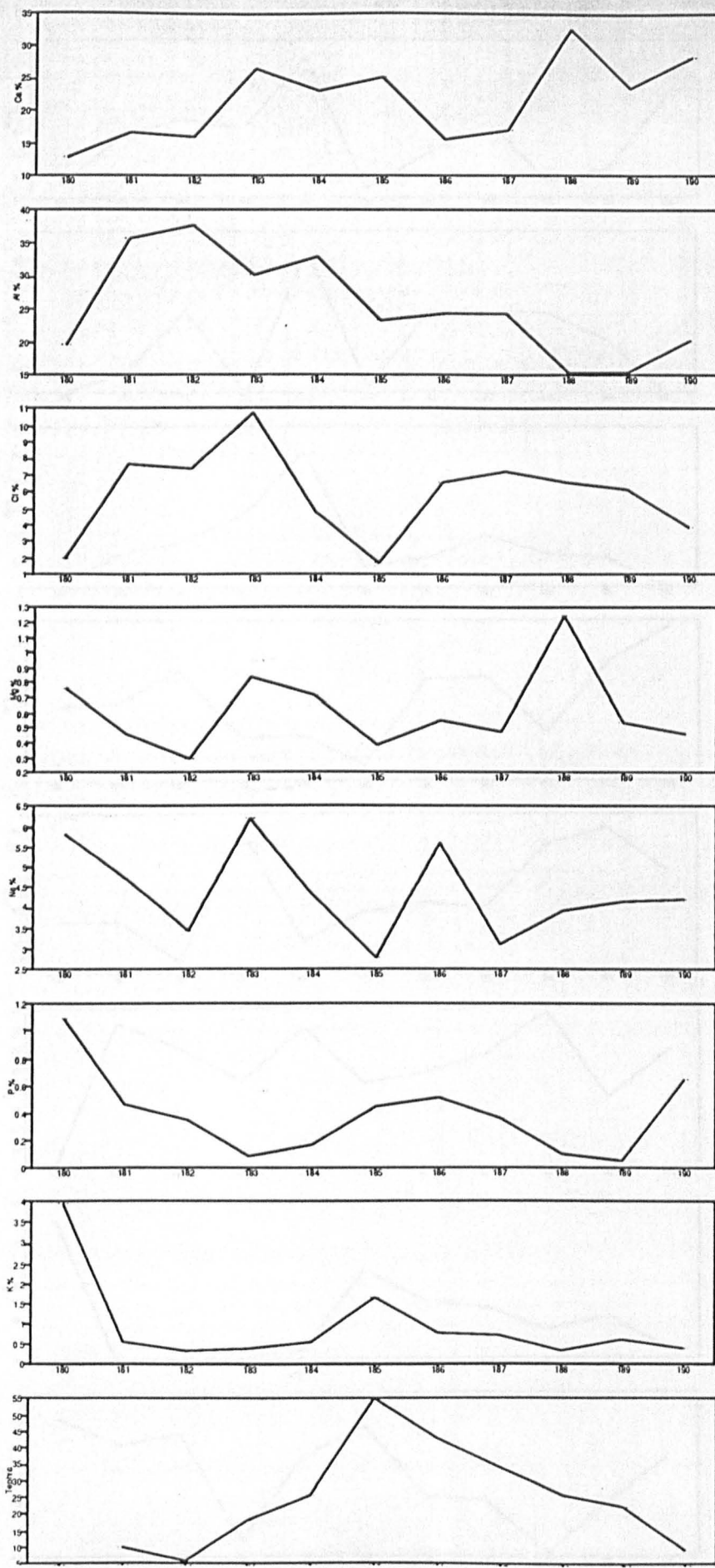
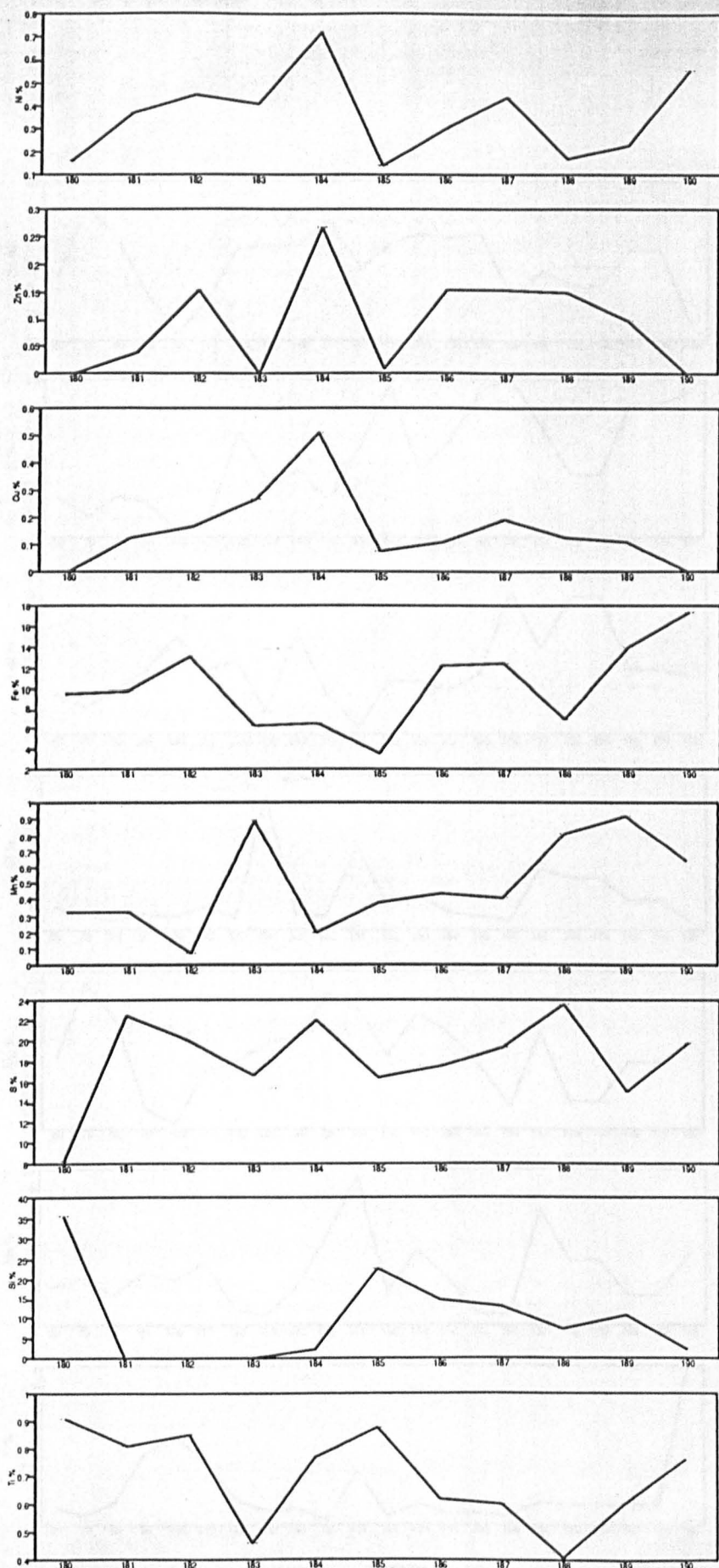


Figure 10.7b. Sediment Geochemistry Chemizone KL1b, Strath of Kildonan.



Depth. Cms.

Figure 10.8a. Sediment Geochemistry Chemizone KL2, Strath of Kildonan.



Depth. Cms.

Figure 10.8b. Sediment Geochemistry Chemizone KL2, Strath of Kildonan.

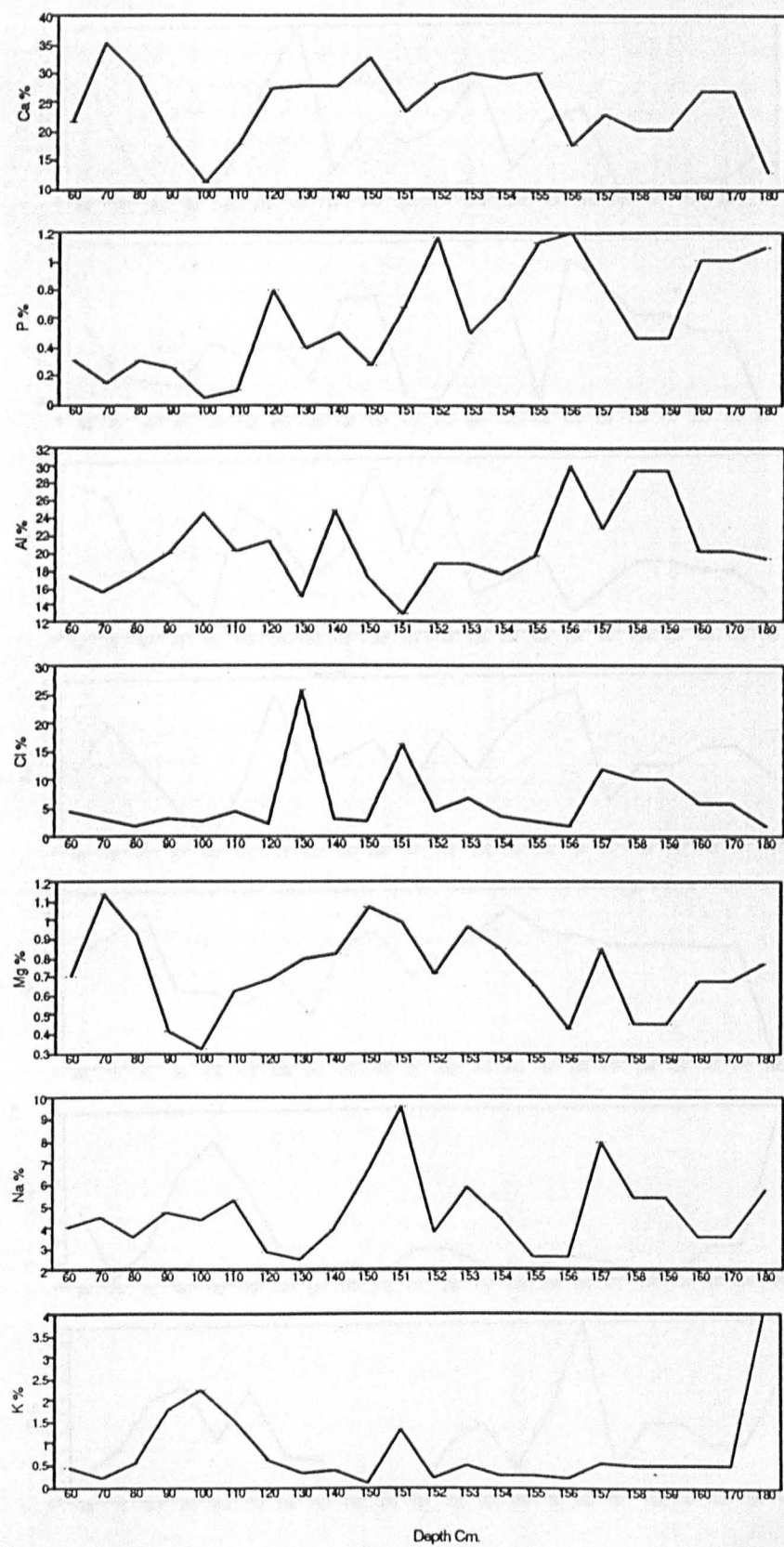


Figure 10.9a. Sediment Geochemistry Chemizone KL3, Strath of Kildonan.

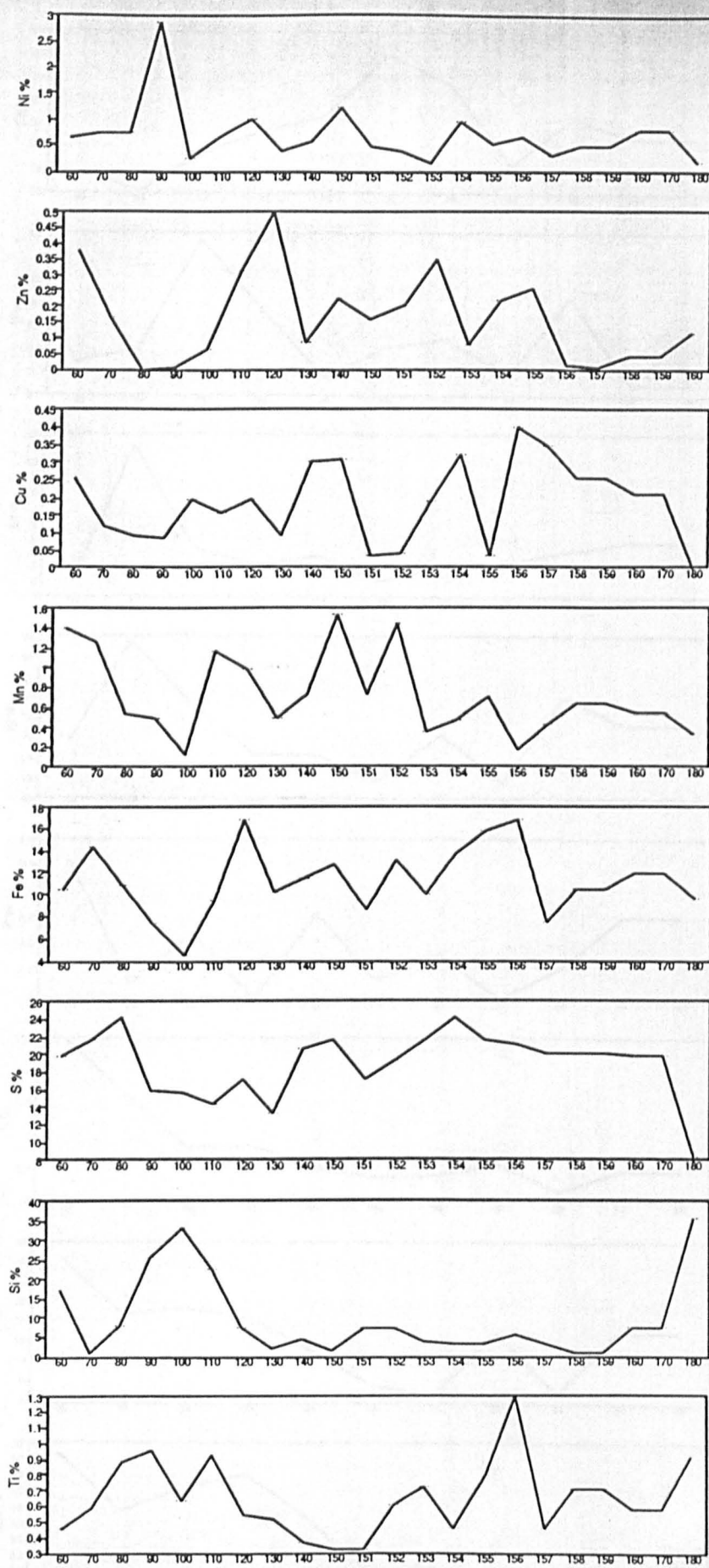


Figure 10.9b. Sediment Geochemistry Chemizone KL3 Strath of Kildonan.

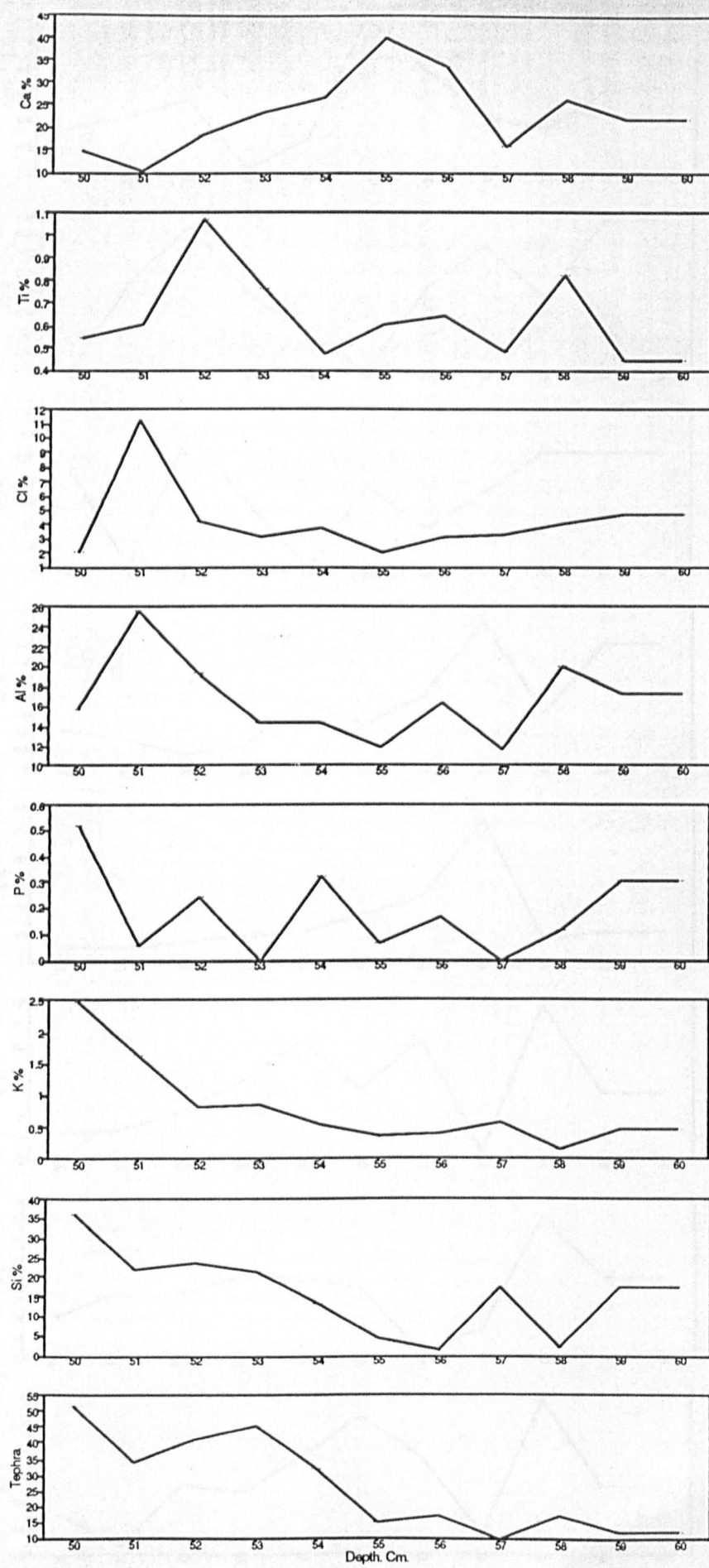


Figure 10.10a. Sediment Geochemistry Chemizone KL4, Strath of Kildonan.

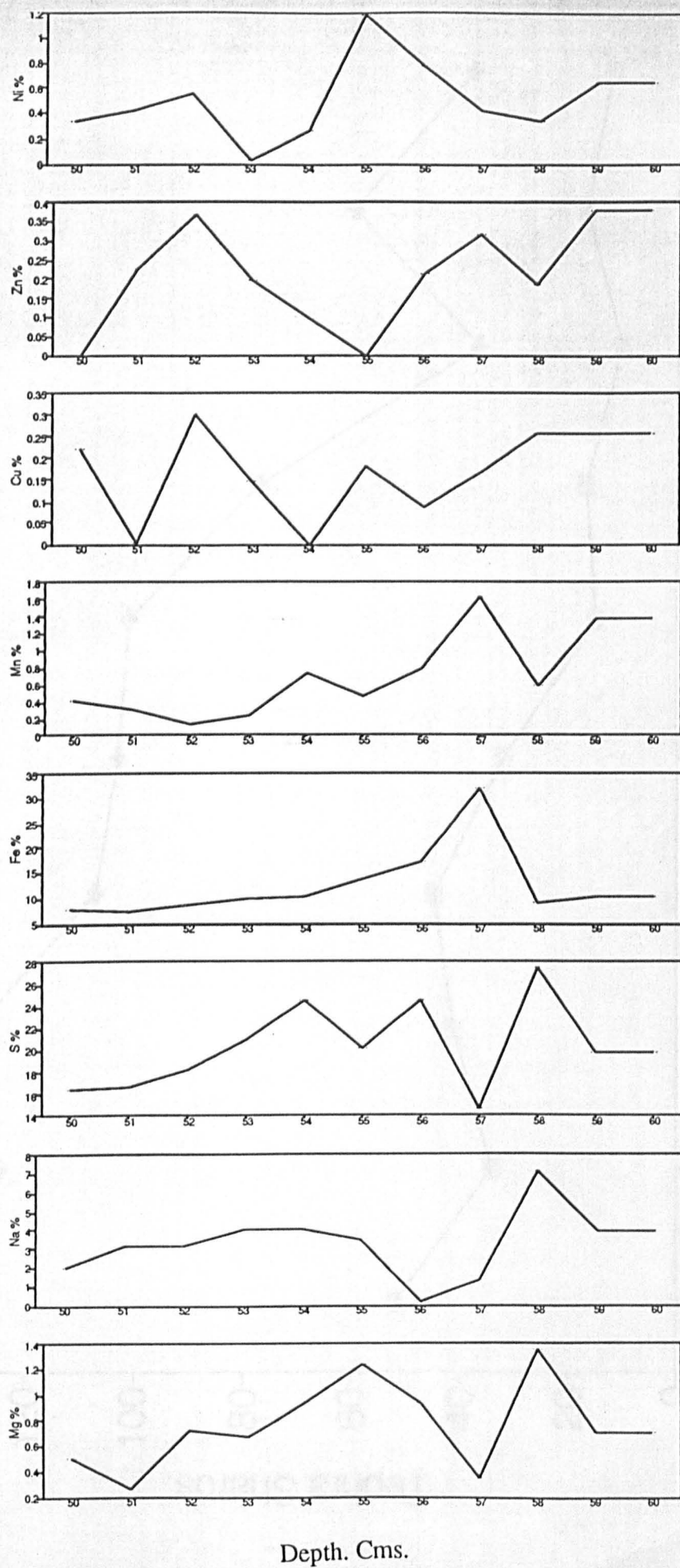


Figure 10.10b. Sediment Geochemistry Chemizone KL4, Strath of Kildonan.

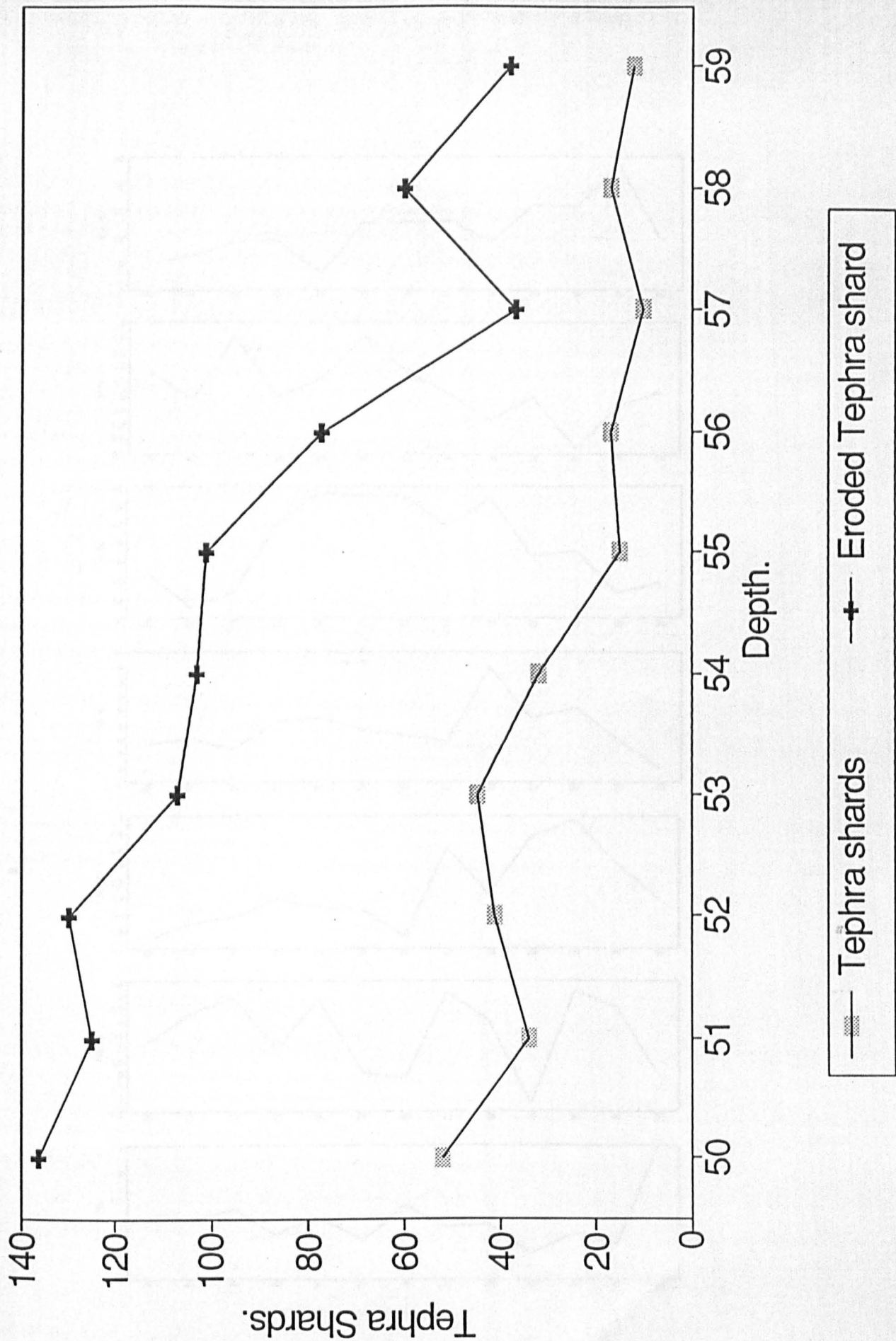


Figure 10.11. Tephra distribution in Chemizone KL4.

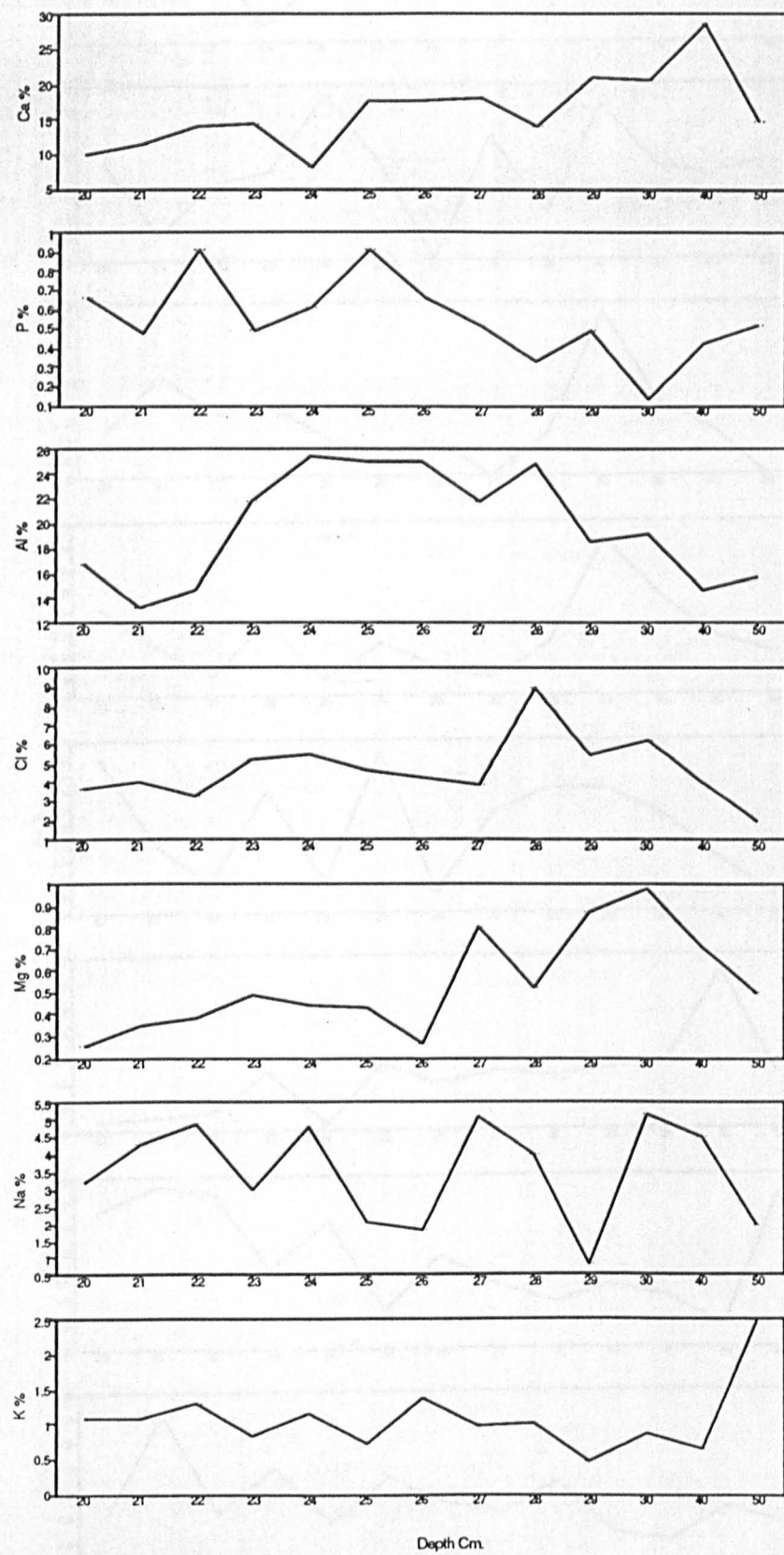


Figure 10.12a. Sediment Geochemistry Chemizone KL5, Strath of Kildonan.

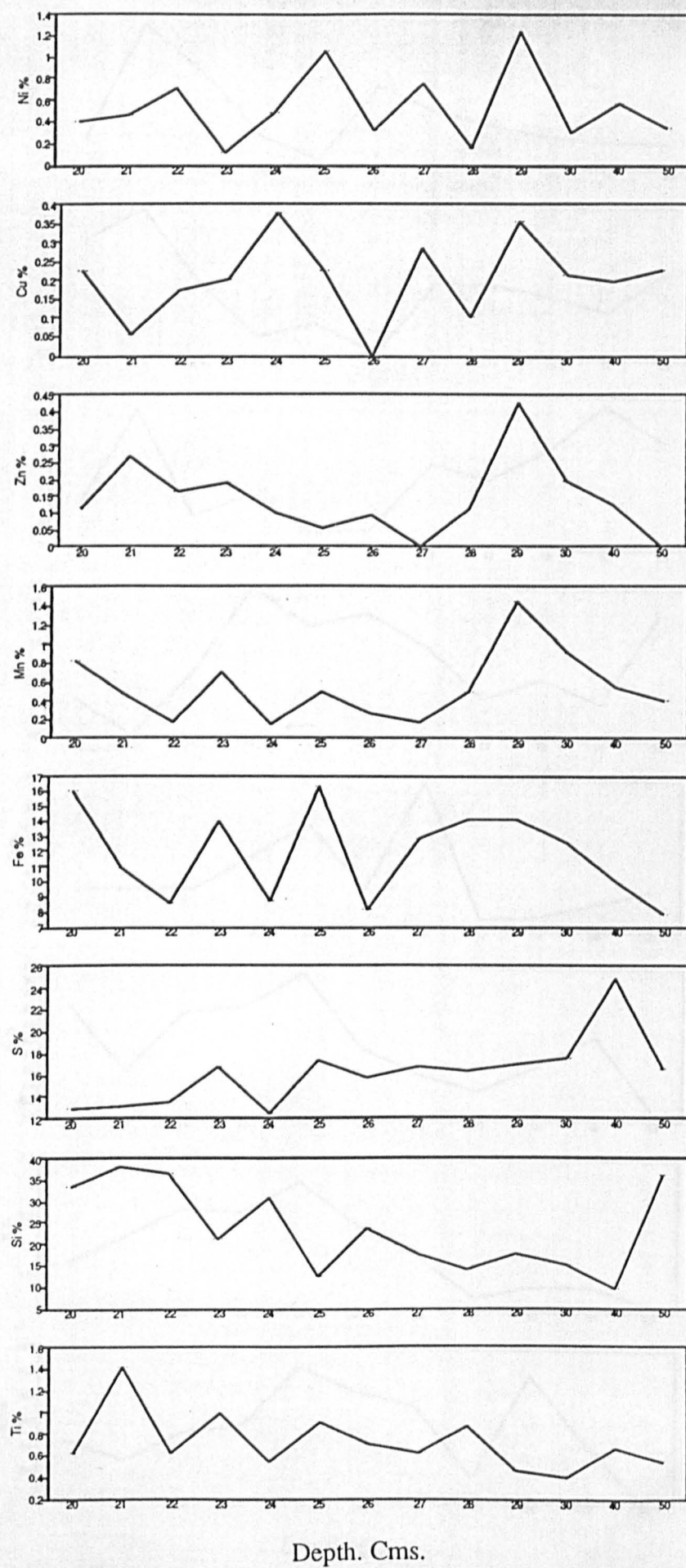


Figure 10.12b. Sediment Geochemistry Chemizone KL5, Strath of Kildonan.

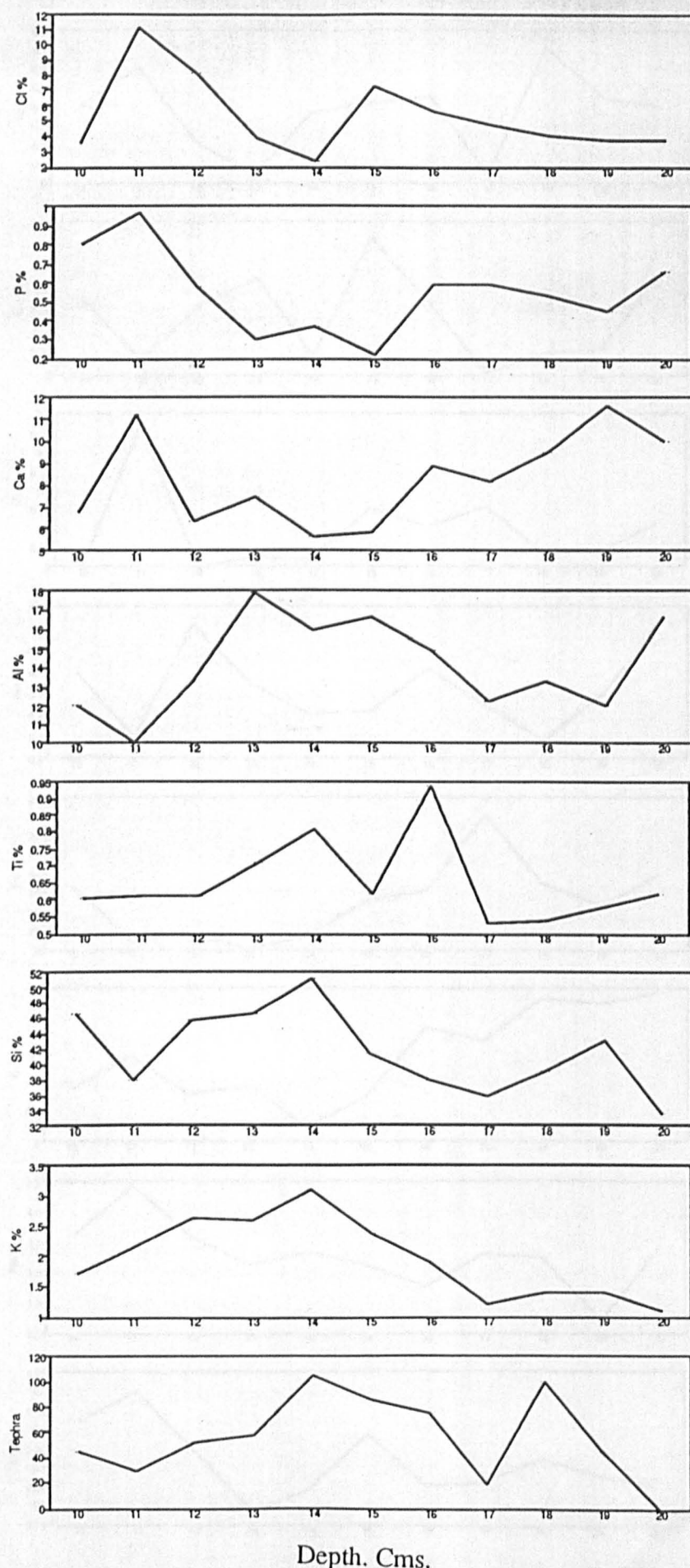


Figure 10.13a. Sediment Geochemistry Chemizone KL6, Strath of Kildonan.

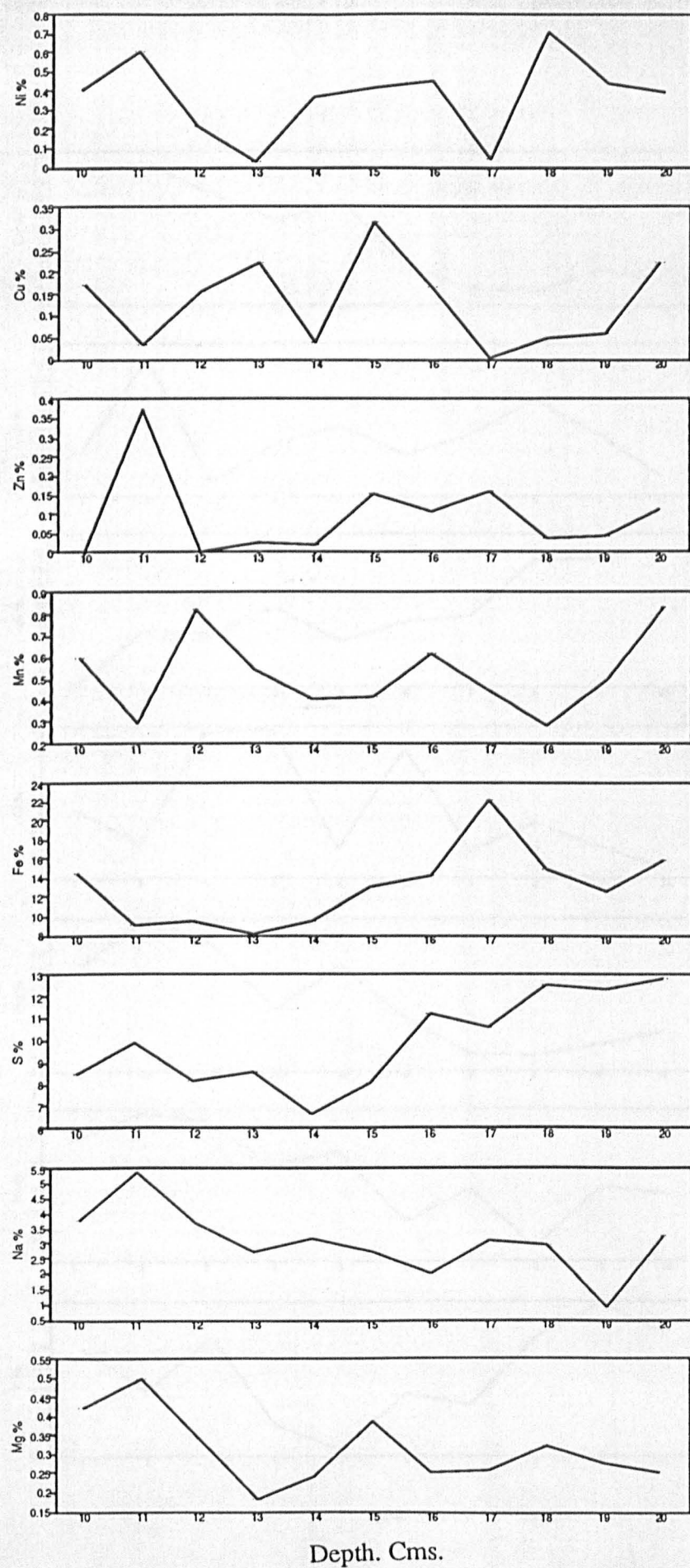


Figure 10.13b. Sediment Geochemistry Chemizone KL6, Strath of Kildonan.

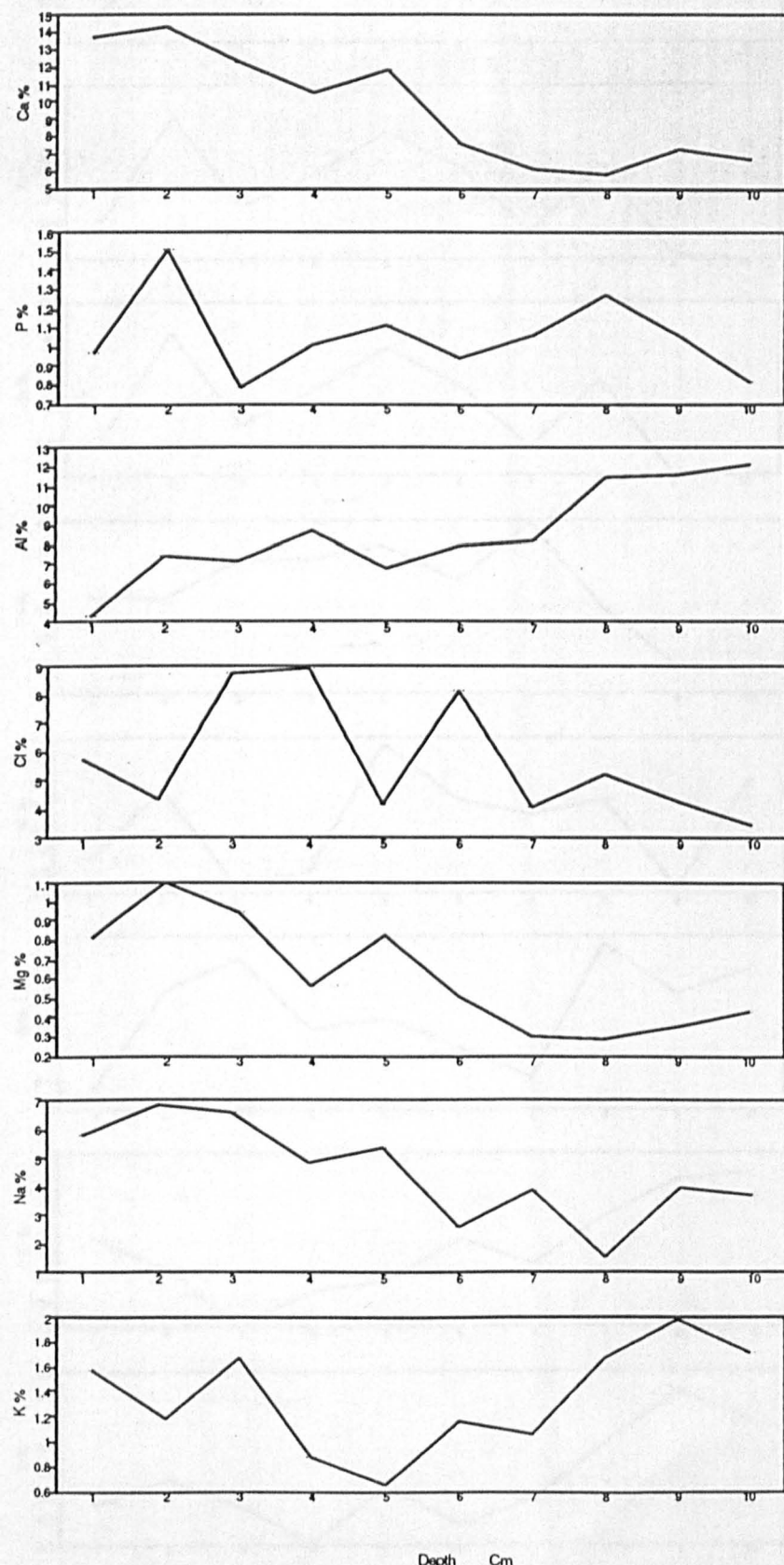


Figure 10.14a. Sediment Geochemistry Chemizone KL7, Strath of Kildonan.

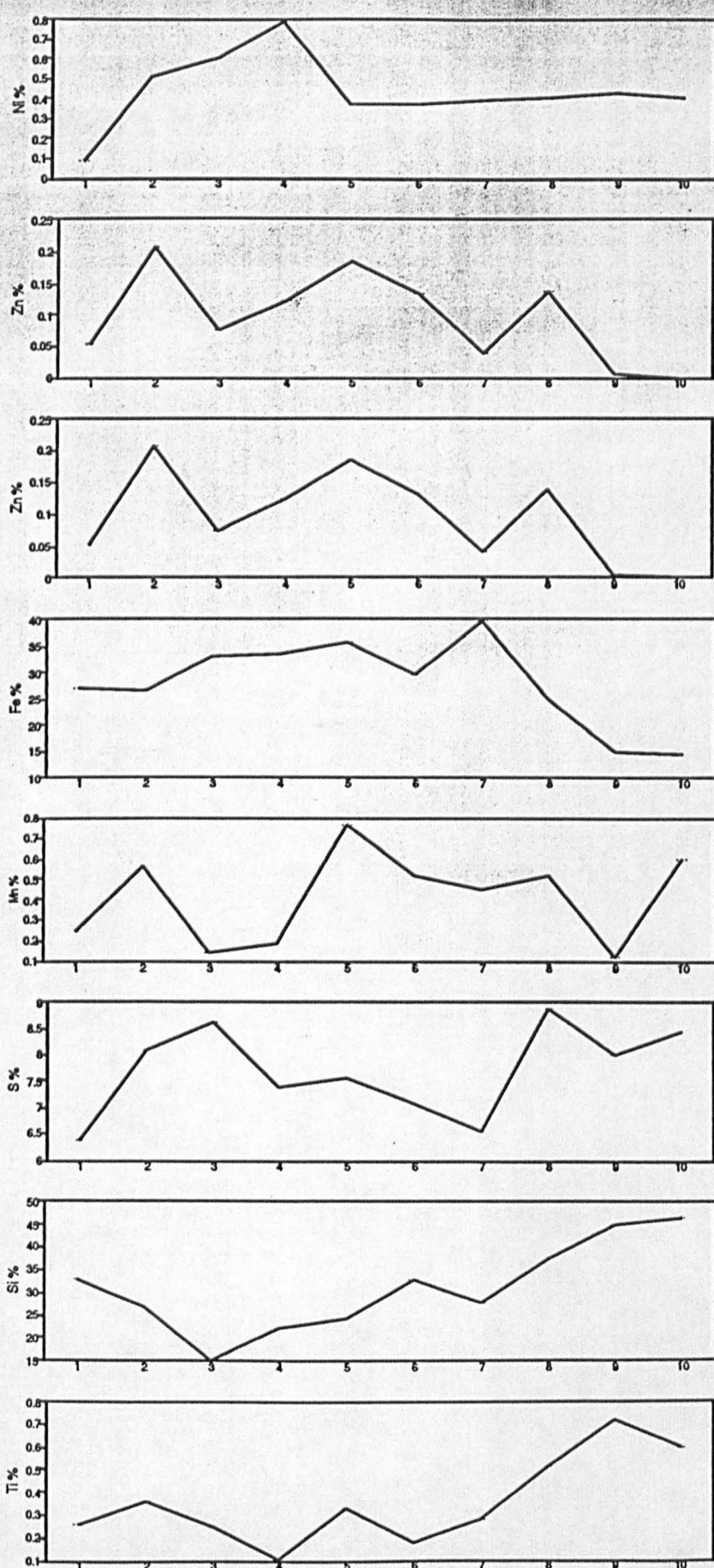


Figure 10.14b. Sediment Geochemistry Chemizone KL7, Strath of Kildonan.